INFORMATION TO USERS

This manuscript has been reproduced from the microfilm master. UMI films the text directly from the original or copy submitted. Thus, some thesis and dissertation copies are in typewriter face, while others may be from any type of computer printer.

The quality of this reproduction is dependent upon the quality of the copy submitted. Broken or indistinct print, colored or poor quality illustrations and photographs, print bleedthrough, substandard margins, and improper alignment can adversely affect reproduction.

In the unlikely event that the author did not send UMI a complete manuscript and there are missing pages, these will be noted. Also, if unauthorized copyright material had to be removed, a note will indicate the deletion.

Oversize materials (e.g., maps, drawings, charts) are reproduced by sectioning the original, beginning at the upper left-hand corner and continuing from left to right in equal sections with small overlaps. Each original is also photographed in one exposure and is included in reduced form at the back of the book.

Photographs included in the original manuscript have been reproduced xerographically in this copy. Higher quality 6" x 9" black and white photographic prints are available for any photographs or illustrations appearing in this copy for an additional charge. Contact UMI directly to order.

UMI

THE FLORIDA STATE UNIVERSITY

FAMU/FSU COLLEGE OF ENGINEERING

INTEGRATED PRODUCT AND PROCESS DESIGN

FOR RESIN TRANSFER MOLDED (RTM) PARTS

By

JULIE KAYE SPOERRE

A Dissertation submitted to the
Department of Mechanical Engineering
in partial fulfillment of the
requirements for the degree of
Doctor of Philosophy

Degree Awarded:
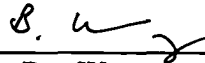Fall Semester, 1995

UMI Number: 9605039

UMI Microform 9605039
Copyright 1995, by UMI Company. All rights reserved.

This microform edition is protected against unauthorized
copying under Title 17, United States Code.

UMI

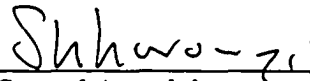300 North Zeeb Road
Ann Arbor, MI 48103

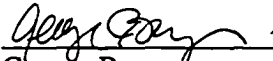The members of the Committee approve the dissertation of Julie Kaye Spoerre defended on July 28, 1995.

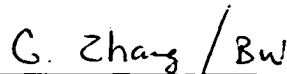_Hsu-Pin Ben Wang_
Professor Directing Dissertation

Srinivas Palanki
Outside Committee Member

Samuel Awoniyi
Committee Member

George Buzyna
Committee Member

Chun Zhang
Committee Member

Approved:

A. Krothapalli, Chairperson, Department of Mechanical Engineering

Ching-Jen Chen, Dean, College of Engineering

With love and gratitude to my husband, Gary

ACKNOWLEDGMENTS

There are many people who have provided me with help and support during the writing of this dissertation. First, I would like to thank Dr. Ben Wang for his guidance, not only during the time of my dissertation work, but through all my years of graduate work. I have been privileged to have had the opportunity to work with an excellent researcher and teacher. In addition, I would like to acknowledge Dr. Chuck Zhang who has played a pivotal role in the completion of this research.

There are several people from the National Institute of Standards and Technology who I would like to recognize. To Dr. Richard Parnas for his technical expertise and for providing me the opportunity to conduct experiments in his lab; without his generosity, it would not have been possible to complete this research. Special recognition goes to Kathy Flynn who was responsible for the completion of the experiments, as well as Dara Woerdeman who provided assistance. I will always feel much gratitude towards them, not only for their technical support and experimental help, but for making this part of my research work so enjoyable. It truly was a pleasure to work with them.

I would also like to thank Dr. Meeter for his statistical support and Dr. Chandra for providing me access to the MTS machine. Also, to Michael Robertson and Jai Rama for their assistance during the mechanical testing.

A special thank you is extended to my parents, Roger and Cynthia McBride, whose selfless love and support have given me the courage to pursue my dreams. They have always been a source of inspiration to me and this achievement is just as much theirs as it is mine.

iv

TABLE OF CONTENTS

vii

viii

LIST OF TABLES

ix

x

xi

LIST OF FIGURES

ABSTRACT

Composite materials have gained increasing attention in the past several years due to their superior mechanical properties and improved strength-to-weight ratio over traditional materials. With this focus on composite materials, a concentration on resin transfer molding (RTM) has followed. RTM is an attractive processing method due to its potential for providing consistently superior parts at a lower cost than other manufacturing techniques.

The resin transfer molding process involves a large number of variables that are linked to the design of the component, the selection and formulation of the constituent materials, such as resin and fiber, and the design of the mold and molding process. These variables are strongly related to the system performance, for example mold filling time, and RTM product quality. In addition to the effect of single variables on product quality and process performance, the interaction of variables may also be significant. The need for understanding the impact of RTM product and process design variables on part quality and process performance is crucial. This is accomplished through an integrated product and process design (IPPD) approach. Genetic algorithms (GA), in conjunction with the cascade correlation neural network architecture (CCA-NN), are utilized for the following purposes: (1) to establish a working model that predicts performance and quality measures in RTM given a set of product and process design parameters, and (2) to determine the optimal settings of the product and process design parameters to enhance the RTM process and improve part quality.

xv

Optimum design of RTM product and process design variables will result in high quality parts and enhance the efficiency and robustness of the RTM process. This, in turn, will lead to longer part life, predictable and reliable performance, lower life cycle costs and improved product yield. An intelligent, adaptive process control procedure yields consistently high quality parts in the presence of interactions and nonlinearities among RTM parameters.

The proposed research outlines two major tasks, (1) the integration of modeling and simulation technologies that support an integrated product and process design (IPPD) approach, and (2) the intelligent, adaptive control of the RTM process. The goal of the proposed research is to achieve optimum design of RTM parts through the development of a robust process and an intelligent, adaptive process control procedure. This is the vision underlying this research.

CHAPTER 1

INTRODUCTION

1.1 Background

In the past decade, engineering materials have gone beyond the traditional structures, such as metals and polymers, and processing of yesterday. Instead, scientists and engineers are continuously searching for new products with improved strength and toughness and with lower density. A need exists for more advanced materials with special combinations of properties, including enhanced corrosion resistance, higher strength-to-weight ratios, high temperature strength, and improved wear and erosion resistance.

Composite materials offer the potential to meet many of the desired properties listed in above. Widespread interest in the manufacture of composite parts has increased research attention on resin transfer molding (RTM) as a fabrication technique for its relatively low equipment and tooling costs, short cycle times and improved control of component shape. RTM is also well-suited for parts requiring tooled surfaces on both sides and for part consolidation. Composite parts exhibit high strength-to-weight ratios, a benefit that is appealing to a variety of industries in both the commercial and defense industries where weight is a crucial factor.

Although RTM is in its early stages of process development, it has tremendous potential to provide consistently superior quality components. The advantages of RTM over more traditional composites manufacturing processes are significant [Advani *et al.*, 1994]. These potential advantages include (1) the ability to acquire excellent control over

1

the mechanical properties of the finished part; the use of a preform, which pre-aligns the fibers into the final part shape, allows for more control of the part's mechanical properties, (2) shorter cycle time compared to other similar processes, such as hand lay-up and filament winding, (3) low mold or tooling costs and lead time; RTM is a comparatively low temperature and low pressure process. In addition, there is no abrasive action of fibers against the mold surface as in compression molding, for example. Tools for medium sized production runs can be made from epoxies, rather than steel, a much less expensive alternative and (4) complex parts with an encapsulated core can be made in one operation. The preform is wrapped around the core and the assembly is placed in the mold. In addition, inserts can be easily included in the part. A reduction in components through part integration is a significant benefit of RTM. The development and testing of an epoxy composite engine block assembly is currently underway in the automotive industries.

A comparison of RTM with other processes is provided in Figure 1.1 [Johnson, 1987]. From the figure, it can be seen that RTM has the greatest potential for producing high-performance part in medium to high volumes. In addition, it is possible to manufacture such components in an economical fashion. Hand lay-up, while providing the capability of producing the desired part properties, requires intensive labor efforts. Due to the cost and time involved in this process, it is an unlikely choice for making a significant number of parts. At the other end of the spectrum are the compression molding and thermoplastic stamping processes. Since the tooling involved is a substantial investment, it is not economically justifiable to use either method for volumes below a certain threshold level. Therefore, RTM is rapidly becoming an emerging technology for replacing other composite processing methods at a significantly lower cost without compromising part performance.

2
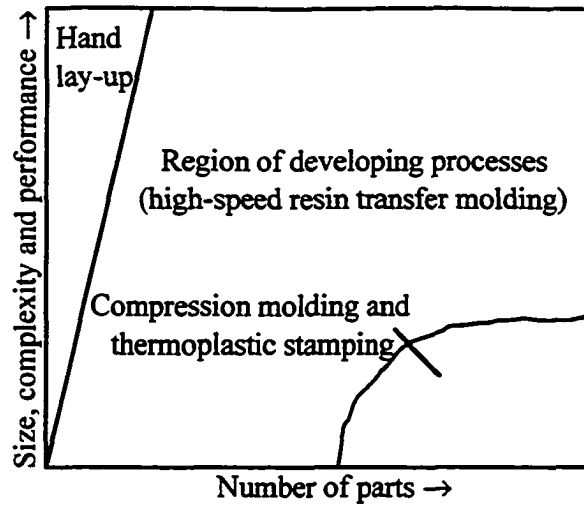
Figure 1.1. Process development for composite parts

1.1.1 Resin Transfer Molding Process

Figure 1.2 depicts the generalized resin transfer molding process. Fiber preforms or mats are placed into the mold. Preforms are layers of fiber mats which are designed and constructed according to the shape of the finished parts. The mold is closed and evacuated after which time the resin mixing and injection system is connected to the mold. A tube connects the closed tool cavity with a supply of liquid resin, which is pumped or transferred into the tool to impregnate the reinforcement. The system is preheated according to the cure kinetics of the resin and when the resin viscosity is sufficiently lowered, the inlet gate to the mold is opened and the resin is forced into the fiber preforms or mats under pressure. Often, the temperature of the resin and mold are different, leading to a nonisothermal process. At this point, heat transfer occurs from the mold walls ad fiber preform to the fluid. Once the mold is filled, pressure is maintained and heat continuously supplied to cure the resin matrix. Cure is initiated due to the heat transfer from the hot mold to the comparatively cold resin; the resin reacts to form a cross-linked

3

polymer network as the resin viscosity increases to infinity and gelling occurs. Because the curing reaction is highly exothermic, the heat transfer is substantially affected by this step. As a final stage, the mold is removed and the finished part retrieved. At this point, some machining may be necessary to cut off sprues and runners.
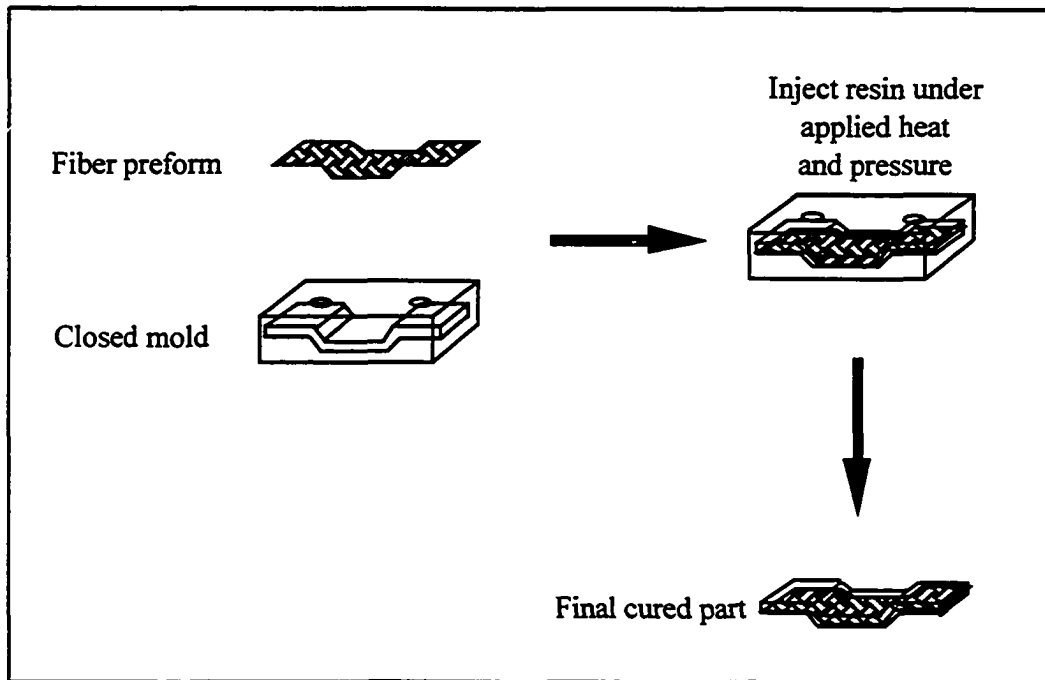
Figure 1.2. Resin transfer molding process

1.1.2 Materials Selection

There are several decisions that must be made prior to part production in resin transfer molding. Initially, a set of design guidelines are addressed; Table 1.1 lists the design guideline issues that must be resolved before materials selection takes place [Stark and Breitigam, 1987]. Material considerations for RTM are provided below:

• tooling

4

- resin pumping/dispensing equipment

- mold releases and cleaner

- resin selection

- reinforcements

Table 1.1. Design guidelines in RTM materials selection

	Issues to address	Specific areas of concern
Mold	Number of parts required/unit time	Primary: Tooling and pumping/dispensing, Secondary: release, cleaners, resin
	Design life considerations	Tooling, pumping/dispensing, cleaners, release agents
	Dimensional requirements	Tooling, cleaners, release agents
	Strength requirements	Tooling, cleaners, release agents
	Surface finish requirements	Tooling, cleaners, release agents, resin system, reinforcement
Part	Performance requirements	Reinforcement, resin system
Prod'n	Shop environmental requirements	Resin system, cleaners, release agents, tooling, pumping/dispensing
	Personnel capabilities	All
	Cost objectives	All

1.1.2.1 Mold design and construction

Components of the mold consist of the injection port(s), air vent(s), guide pins, mold cavity and gasket. Resin is injected through the port(s) and any trapped air or volatiles released can escape through the air vent(s). Ports and vents must be strategically placed in the mold to ensure proper mold filling and to prevent air or volatiles from becoming

5

trapped in the mold. Guide pins are used to align the top and bottom halves of the mold. An adequate seal in the mold is critical for assuring that no resin leaks out during filling and , at the same time, that no additional air enters the mold.

In addition to the above requirements, the mold must maintain its mechanical integrity and dimensional stability under the required temperature and pressure conditions. Metal, ceramic and polymeric composite tooling have been used successfully in RTM, achieving the necessary product volume of three thousand parts for composite tooling and twenty thousand parts for metal tooling.

1.1.2.2 Pumping/dispensing equipment

Resin is transferred into the closed mold through the assistance of pumps, rams and air lines. In most cases, placing the mold under a vacuum prior to injection is desirable to remove air. As was discovered through experiments conducted by Hayward and Harris [1990], significant improvements were found in the mechanical properties and porosity levels of moldings made with vacuum assistance.

1.1.2.3 Resin selection

The resin system is comprised of any combinations of the following: resin, curing agent, catalysts, fillers, pigments, promoters and inhibitors. Selection of the resin is primarily based on the end-use application of the part, but resin systems most compatible with the RTM process have several key characteristics. These include a long pot life - at least 2 hours, low viscosity at resin transfer temperature, short gel time at the cure temperature - less than one hour; and low levels of outgases, volatiles and by-products of cure.

6

1.1.2.4 Reinforcement selection

Similar to the resin selection, the choice of the best reinforcement to use depends heavily on the end-use application. The following is a list of important mechanical, processing and fiber characteristics that determine, to a large degree, which type of reinforcement is selected: physical form of the reinforcement, base fiber material, sizing (if any) and type of stitching.

1.2 Research Needs in RTM

The technical knowledge behind advanced composite materials and composite materials processing alone will not lead to the successful development of a competitive RTM product exhibiting high quality at a lower cost. To achieve these aims, the overall product development cycle must include relevant research tightly linked to design, engineering, manufacturing and marketing within an integrated product and process design (IPPD) framework. It is no longer an acceptable practice to treat these areas as separate and independent entities.

A National Research Council (NRC) publication indicated that the manufacturing of advanced engineered materials is a research priority [1991]. Included within this research area are composites and the resin transfer molding process. As one of the guidelines provided for improving , understanding and promoting the use of advanced engineered materials, the NRC recommends that "an early focus on integration of materials and processing requirements must be part of any manufacturing scheme." In addition, another consideration is that "the effects of processing - both to produce the material and to produce the product - on subsequent properties and performance should be modeled and experimentally verified."

Full exploitation of composite materials will require an effective manufacturing base for producing components and structures more reliably and consistently and at lower costs. In order to achieve these goals, a unified life cycle engineering approach must be adopted for manufacturing. This approach includes integrated product and process design, quality predictions and fatigue tests to determine the long-term effects of immediate design decisions. Costs are reduced since the effect of specific designs can be tested prior to manufacture and costly design changes are avoided late in the development cycle. This unified approach is dependent upon development of the necessary science base for implementation in the next generation of automated manufacturing. This science base would emphasize such aspects as (1) new processing methods which offer unusually strong potential for providing improved quality, reproducibility and yield of product; (2) in-process nondestructive evaluation (NDE) techniques for real-time inspection and closed loop computer control of critical parameters in the manufacturing process; (3) determination of computer integrated manufacturing models incorporating a common data base and compatible software to relate various stages of manufacture, from initial concept and design to prototype production; (4) incorporation of opportunities for process automation and optimized NDE inspection in the field through robotics, sensors, and smart structures; and (5) integrated manufacturing systems concepts. These aspects would comprise a research effort that focuses on reducing the cost of manufacture, improving reliability and extending the useful life of components for commercial and military applications.

Although flow modeling and simulations for the advancement of RTM technology have proven to be useful, the effect of preform architecture on the filling is less understood [Advani, *et al.*, 1994]. It would be very useful and worthwhile, therefore, to investigate the changes in permeability associated with different architectures and the resulting effect on the flow behavior.

8

The resin transfer molding process involves a large number of variables that are linked to the design of the component, the selection and formulation of the constituent materials, resin and fiber, and the design of the mold and molding process. Table 1.2 lists the major variables in RTM product and process design. These variables are strongly related to the system performance, such as mold filling time, and RTM product quality. For example, applying a higher injection pressure can reduce mold filling time, but will increase the possibility of voiding, absence of resin in areas of the fiber matrix, and fiber wash, or the misalignment of fiber tows within the matrix. These phenomena result in a lack of uniformity in strength. Likewise, lowering the injection pressure will decrease the possibility of voiding and fiber wash, but have a negative impact on the mold filling time. In addition to the effect of single variables on product quality and process performance, the interaction of variables may also be significant.

Table 1.2. Major variables in RTM product and process design

• Resin and Fiber Selection
• Mold Temperature
• Injection Pressure
• Fiber Volume
• Location of Resin Injection Gate
• Location of Air Vent
• Resin Viscosity

The need for understanding the impact of RTM product and process design variables on part quality and process performance is critical, since the optimum design of these

9

product and process design variables will result in high quality parts and enhance the efficiency and robustness of the process. This will lead to longer part life, predictable and reliable performance, lower life cycle costs and improved product yield.

1.3 Research Objective

The objective of this research is to incorporate an integrated product and process design optimization approach in the resin transfer molding process in order to determine the crucial product and process design parameters and their settings. By using such an approach, the effect of specific design parameter settings on part quality and process performance can be predicted without actual manufacture of the part. Through this integrated design approach, the resin transfer molding process will be optimized and the quality of the molded parts will be maintained. The primary thrust of the research is the integration of modeling and simulation technologies that make integrated product and process design a viable concept.

A secondary thrust of this research is the intelligent, adaptive control of the RTM process once the optimum design parameters have been determined. A neural network-based control procedure, cascade correlation algorithm (CCA) will be used to monitor the degree of cure within the part and make adjustments to the mold temperature when necessary. In this way, the desired part quality is achieved without compromising on process performance.

In the integrated product and process design optimization stage, the following variables are investigated: mold preheat temperature, mold outlet pressure, driving pressure - outlet pressure minus inlet pressure, and fiber architecture. Through a series of experiments, the effects of these variables on the void content and interlaminar shear

10

strength are determined in order to optimize the RTM process. In addition, the effects of the above mentioned variables on mold filling time are investigated.

Since the mechanical properties of a composite are determined to a large extent by how well a resin is cured [Jang, *et al.*, 1992], cure information collected during processing is the basis for the control procedure. Cure data is collected through fluorescence measurements taken along the length of a centrally-located fiber. Through intelligent, adaptive control of the cascade correlation algorithm, adjustments are made to the cure cycle during processing to maintain quality composite parts.

1.4 Contents of the Research Project

This section highlights the remaining chapters of the research project. Chapter 2 summarizes the previous RTM research performed in the areas of process modeling and simulation, solution of process models, design optimization and intelligent systems for process monitoring and control. Chapter 3 outlines the pilot studies performed earlier in the research project. Methodologies utilized and modified for this research are provided in Chapter 4. The experimental procedure is described in detail, along with the results in Chapter 5. A conclusion of the research is found in Chapter 6, along with the contributions and future research directions.

11

CHAPTER 2

LITERATURE REVIEW

An increasing number of articles have been published on the study of the resin transfer molding process. This chapter will highlight the related work and major contributions to the following areas of resin transfer molding research: (1) process modeling and simulation, (2) design optimization, (3) process monitoring and control, and (4) intelligent systems for optimization and control.

2.1 RTM Process Modeling and Simulation

2.1.1 Process Modeling

Tucker and Dessenberger [1994] developed a set of balance equations specific to RTM processes, derived using a local volume averaging approach. Local volume averaging involves the prediction of an average fluid velocity as opposed to modeling the behavior of the resin around every fiber. The same technique can be applied to temperature and cure. This approach has the advantage that it is possible to precisely define average pressure, average velocity and average temperature.

Fluid flow and heat transfer through a porous medium channel with permeable walls were researched using Kaviany's [1985] momentum and energy transport equations [Lan and Khodadadi, 1993]. The effects of the porous medium shape parameter and the

12

blowing Reynolds number, a function of the permeation velocity at the walls, on the components of velocity were investigated.

A semi-empirical flow model for predicting the filling pattern in multi-cavity transfer molding was developed [Manzione, *et al.*, 1989]. Experimentation was conducted to correlate the pressure drop during flow of thermoset molding compounds through a runner and gates of different geometries and flow resistances. The correlations were used in a one dimensional network flow model which predicts the two-dimensional mold filling pattern as a function of gate resistances and process conditions.

Using Darcy's law for flow through porous media, a simplified RTM process analysis was created based on one-dimensional resin flow [Cai, 1992]. Closed form solutions for the wet length, mold filling time and pressure distributions were derived for various simplified mold shapes. Two design principles were proposed based on results of the simulation: (1) inlets and outlets should be arranged so shorter flow paths can be achieved; (2) the resin flow direction should be arranged from larger sides to smaller sides, or from outside to inside, which guarantees rapid reduction of the unoccupied volume.

Three-dimensional flow phenomena with hydrodynamic interactions around reinforcing fibers during composite manufacturing applications has been defined using a Galerkin boundary element technique with a quadratic approximation of the variables [Chan, *et al.*, 1992]. The second order boundary element technique was found to provide highly accurate results even when coarse meshes were used. Resolution of the two problems of flow of suspension of cylinders and pressure-driven flow through a network of fibers demonstrated the versatility, power and accuracy of the proposed technique in complex fluid mechanics issues.

Two well-established resin flow models for laminate processing, sequential compaction and the squeezed sponge models, were compared [Smith and Poursartip, 1993]. Both models were based on viscous flow through porous media. The fiber bed

13

pressure and compaction curve and the fiber bed permeability were identified as the two key relevant material properties. Results showed that the permeability controls the compaction time and the fiber bed behavior (deformation) controls the shape of the laminate compaction response.

A review of work on steady-state Newtonian fluid flow through isotropic porous media was provided and used as a foundation to explore the validity of extending Darcy's law to flow through aligned fiber beds [Astrom *et al.*, 1992]. The Kozeny-Carman equation was introduced in the flow rate-pressure drop relationship used to describe the flow of Newtonian fluids through beds of spherical particles, where there is a direct relationship between the flow rate and the pressure drop. Theoretical analyses were compared to experimental results obtained from flow through real fiber beds and ideal beds of regularly spaced cylinders. Findings indicated that although the defined flow rate-pressure drop relationship adequately describes the flow of Newtonian fluids through beds of spherical particles, it is much less accurate for beds of aligned fibers in terms of quantitative results. However, it may be used to obtain qualitative results.

A simplified two-dimensional mathematical model was developed to simulate the flow induced fiber mat deformation during liquid composite molding [Han, *et al.*, 1993]. The governing equations, following Darcy's law, were solved using the control volume/finite element method. The numerical results showed reasonable agreement with experimental results obtained by Han, *et al.* [1993].

2.1.2 Solution of RTM Process Models

2.1.2.1 Finite Difference Method

The development of a simple model of the resin transfer molding process was conducted [Wymer and Engel, 1994]. The objective was to study the flow of a thermoset

14

resin parallel to a unidirectional, heated fiber array, where the resin viscosity varies with temperature. By applying a finite differencing scheme to the convective energy equation, the resin temperatures were found. An iterative approach updated the velocity, temperature and viscosity in the flow direction. Near the heated fiber tows, the velocity was found to increase rapidly due to the decrease in viscosity. The study concluded that controlled elevated fiber temperatures have the potential benefit of reducing the total processing time as a result of increased flow rates.

During a squeezing flow of a fiber reinforced material, fiber reorientation occurs. This phenomenon has been simulated using a three-dimensional finite difference scheme [Wheeler, *et al.*, 1992]. A similar two-dimensional scheme is utilized to simulate the fiber reorientation that would occur in other flow geometries. Simulation results were found to agree with experimental observations, demonstrating the success of the continuum model to predict flow behavior.

Two dimensional molds of arbitrary shapes are simulated during the mold filling stage using a boundary-fitted finite difference technique introduced by Gauvin and Trochu [1992, 1993]. The resin pressure distribution and resin front positions were obtained for any time period. Gauvin and Trochu observed an edge effect caused by imperfect installation of the reinforcement along the mold boundary. A second phenomenon, called the capillary effect, was believed to be responsible for discrepancies in pressure between experimental and numerical data.

2.1.2.2 Finite Element Method

Resin transfer molding for automobile manufacture was studied and simulated using a finite element-control volume approach [Owen *et al.*, 1992]. The finite elements were formulated numerically using Gaussian integration and isoparametric Galerkin formulations in pressure. Implementation of the control volume scheme maintained mass

15

conservation by accumulating the fluxes for all control volume edges. The predicted pressure traces and fill patterns were validated using experimental data and the proposed methodology was carried out to determine the flow behavior in the molding of two sample automobile components.

A two-dimensional model was developed for simulating isothermal mold filling during resin transfer molding of polymeric composites under constant pressure during mold filling [Chan and Hwang, 1991]. The model encompasses the anisotropic nature of the fibrous reinforcement and change in viscosity of the polymer resin as a result of chemical reaction. Flow of the resin through the fiber network was described in terms of Darcy's law and the differential equations were solved numerically using the finite element technique. The Galerkin finite element method was used as a tool in obtaining the pressure distribution.

The modeling of polyimide-fiber composites in resin transfer molding has been addressed [Chan and Hwang, 1993] since such composites are important structural components in many high temperature applications requiring high performance, lightweight materials. A simple model was proposed for the resin transfer molding of thin composite parts. The numerical solution of the model was determined through the integration of equations formulated using the finite element method, which accounts for the changing shape of the flow front. Resulting computational schemes were found to be numerically stable and efficient.

A computer program based on nonconforming finite elements was developed to simulate the resin transfer molding process [Trochu et al., 1993, Trochu et al., 1992]. The use of nonconforming finite elements ensured the conservation of the flow rate across inter-element boundaries when approximating the pressure field. Advancement of the resin front through orthotropic preforms and inside molds of arbitrary shapes are handled by the program. Evaluation of the filling time and positioning of the injection ports and air

16

vents were clarified. Good agreement was observed between calculated and experimental flow fronts and program results compared well with those obtained by other simulation techniques.

Finite element methods were utilized in the development of a software system, the composite materials analysis program, which implemented the homogenization methodology for evaluation of macroscopic effective thermal and elastic moduli of continuous and short fiber reinforced composites [Blankenship *et al.*, 1992]. The system treated composites with various fiber shapes and packing arrangements. Data was imported to the system from a standard database of material properties and computational results were evaluated to analyze the structural behavior of materials formed from composites.

Work was presented on the simulation of the mold filling stage for nonisothermal molds in thin mold cavities preplaced with fibrous reinforcement [Chan and Hwang, 1992]. Resin flow through the fibers was modeled using two-dimensional flow based on Darcy's law. Resin reaction and heat transfer among resin, mold walls and fibers were considered simultaneously. The proposed technique emphasized the use of the least squares finite element method to solve the convection dominated mass and energy equations for the resin. Simulation results from example case studies of polyurethane-glass fiber composites demonstrated the potential of the model.

A two-dimensional finite element model for the simulation of the advancing front in reaction injection molding was developed [Hayes *et al.*, 1991]. Model creation was based on the solution of the full Navier-Stokes equation for the computation of the velocity and pressure; the Lagrange-Euler method was used for the moving front; and the method of characteristics was used for the solution of the mass and energy equations. In addition, employment of an automatic remeshing algorithm prevented element distortion and optimized element size and number.

17

2.1.2.3 Boundary Element Method

Numerical simulation of the mold filling process during resin transfer molding was performed using the boundary element method [Um and Lee, 1991]. Darcy's law for anisotropic porous media was employed, in conjunction with mass conservation, to construct the governing differential equation and this system of equations was solved with the boundary element technique. The agreement between the numerical calculations and the experimental results was good. In the simulation presented, the boundary element method analysis gave accurate numerical results in relatively short computing time, compared with the control volume methods, due to the simplification in node generation.

The development of the boundary element equations for the compression molding process of isothermal Newtonian fluids was pursued by Osswald and Tucker [1988]. Simulation results indicated that this technique was useful when analyzing flat parts with otherwise complex geometries. Osswald and Tucker concluded in their paper that simulation based on the boundary element technique required less input and gave more accurate results for higher order derivatives than the finite element method under the following limitations: simple geometry parts (slightly curved) and isothermal Newtonian problems.

2.1.3 Permeability

In-plane flow of fluids through various fiber reinforcements was studied by Parnas and Salem [1993]. One-dimensional and radial flow experiments were conducted using several glass fabrics with Newtonian fluids. Results indicated that the radial and one-dimensional measurement techniques produce similar permeability tensors. In addition, the crimp angle correlated with the orientation of the permeability tensors.

The finite element-modified control volume approach has been used to calculate the flow pattern (velocities and flow front movement) for the mold filling of Newtonian fluids

18

in an anisotropic porous media [Bruschke et al., 1992, Bruschke and Advani, 1990]. In the simulation model, the heat transfer between the heated mold, resin and fiber preform were taken into account, as well as resin cure during all stages of resin transfer molding. The effective in-plane permeability of generalized multi-layered preforms was approximated by considering the transverse flow across layers, in addition to the in-plane permeabilities of each layer.

Permeability experiments were conducted and permeability measured by imposing a pressure differential across a test fiber bed [Lam and Kardos, 1991]. The experimental fiber bed permeabilities were determined for flow perpendicular to unidirectionally aligned fibers and fitted to the Kozeny-Carman relation for permeability. The same procedure was used to determine the permeability for flow along the fiber direction in unidirectionally aligned fiber beds by changing the Kozeny constant. Finally, the effect of off-axis fiber orientations (fiber bed anisotropy) on axial permeability was studied and the axial permeability equation rewritten to reflect this phenomenon.

A method has been presented for obtaining components of the second order anisotropic permeability tensor from in-plane radial flow experiments and the two-dimensional form of Darcy's law [Chan et al., 1993]. Experimental data on changes in flow front position and inlet pressure with mold filling time were utilized to determine the in-plane permeability tensor. The proposed method described the case of constant flow rate mold filling for three preform types: isotropic, orthotropic and anisotropic. The findings from the study resulted in the conclusion that the proposed procedure provided a means of detecting changes in permeability as a result of preform deformation.

The dependence of the flow permeability of highly compressible porous media on the degree of compression (deformation of pore structure) was studied [Kataja et al., 1992]. Investigations were conducted into the simple capillary theory by Kozeny and Kozeny-Carman. The research was extended to include a case where the pore size is statistically

19

distributed. Variants of the basic model were considered through the introduction of constraints, such as constant pore surface area, that exist during the deformation of the porous structure under compression.

A review of resin flow through the fiber beds in composite material manufacturing processes was presented [Skartsis *et al.*, 1992]. The Blake-Kozeny-Carman equation, describing the permeability, was found to be valid for slow Newtonian flow through porous media over limited porosity ranges. Theoretical models, based on aligned arrays of cylinders, adequately described the transverse permeability of ideal fiber beds in the high-porosity range (0.6 and higher).

2.1.4 Void Formation

The formation and growth of voids in polymeric materials is related to the phenomenon of bubble nucleation and growth. Nucleation of bubbles in polymers has been studied by several researchers. One approach used classical nucleation theory to model heterogeneous nucleation of bubbles in a polymer melt [Colton and Suh, 1987]. A similar model of the nucleation of bubbles incorporated the presence of long chain molecules and the supersaturation requirement for nucleation in the polymer, and their effect on the free energy formation of bubble nuclei.

A predictive model for void formation and growth during the processing of thermoplastic polymers and composites was presented [Roychowdhury, *et al.*, 1992]. The model incorporated the effect of heating rate on the residual moisture profile that contributes to void formation and growth, the variation of moisture diffusivity with temperature and the limited availability of moisture for growth. Process parameters that were varied in the study were the heating rate and the applied pressure. Material properties considered included the polymer surface tension and the diffusion coefficient of moisture in the polymer. Conclusions resulting from the investigation were that a

20

higher initial moisture content, high heating rates, low applied pressures, low surface tension and a low diffusion coefficient of the moisture in the polymer enhance void formation and growth.

A model for fluid flow in RTM was developed by Parnas and Phelan [1991] that takes into account both macroscopic resin flow through the preform and microscopic flow of resin through the individual fiber bundles. This approach led to the prediction of transient flow phenomena, increased effective permeabilities and the formation of voids in the fiber bundles.

Tow impregnation during resin transfer molding of bi-directional nonwoven fabrics was modeled based on the existence of two main regions of resin flow: the macropore space formed among fiber tows and the micropore space formed among individual fiber filaments within a tow [Chan and Morgan, 1992, Chan and Morgan, 1993]. Formulation of the model included provisions for constant flow rate and constant pressure mold filling. Predictions on void formation were provided under the conditions of ambient pressure mold filling and vacuum-imposed mold filling. The flow model provided a basis for the study of the relationship between resin transfer molding parameters and the resin impregnation process.

To enhance the rate of mold filling in the RTM process, Chan and Morgan [1992] proposed a scheme referred to as the sequential multiple port method. Simulations were based on a model for resin impregnation of non-woven bi-directional fabrics, with global resin flow along one spatial direction. A simple void formation model was used in conjunction with the simulation and results from a numerical study showed a reduction in mold filling time without an increase in void content.

21

2.2 Design Optimization

Han, *et al.* [1993] studied the effect of gate design on fiber mat deformation. Experimental results indicated that the effect of fiber mat deformation is limited to a small region near the injection gate. The deformation of the fiber bed depends on the characteristics of the fiber mat, the stacking sequence of the fiber mat, the flow rate and the resin viscosity. It was concluded that modifying the gate design will reduce the maximum pressure, thereby reducing the fiber mat deformation.

An algorithm for the optimization of the resin fraction at the completion of a fiber reinforced composites manufacturing process was developed for two-step press processing [Dementyev *et al.*, 1992]. The temperature-time dependence in each layer was measured, which allowed the calculation of the optimal process parameters which give minimal quadratic dispersion of the layer resin fraction values from the optimal fraction. Optimal parameters were defined to be the initial pressure value and the time moment when the pressure changes to a second value.

Flow visualization experiments and mathematical model development were used to characterize the heating and flow behavior of a thermoset molding compounding in the pot of a transfer molding process [Manzione *et al.*, 1988]. Variations in pot diameter, preheat temperature and pot temperature were examined. The most effective way of altering the material properties was through changes in the preheat temperature. Conclusions were that chemical conversion of the extrudate is well below the conversion to gel and that cure time was strongly affected by the pot temperature and insensitive to preheat temperature. This research provides motivation and background for future work on the optimization of productivity and yield of resin transfer molding.

A simplified mold filling simulation was developed to estimate the process variables for resin transfer molding of structural composite parts [Cai, 1992]. The input variables provided for the simulation were the permeability of the preform, the viscosity of the

22

resin, flow rate and pressure limit; the outputs were the filling time for each section and the total filling time. An example was used to verify the simplified approach with a more sophisticated simulation program.

Application of the Taguchi method to experimental design methodology resulted in an improved engineered plastic part in terms of increased endurance under dynamic loads [Warner and O'Connor, 1989]. A 16-run experimental design was developed to test seven factors and six interactions of interest using an orthogonal design. The results of experimentation confirmed the most significant variables (bottom mold temperature, top mold temperature and pressure) and the best settings for each.

Process modeling and design issues for resin transfer molding were addressed [Rudd *et al.*, 1993]. Models used to describe reinforcement deformation and resin flow can be applied to RTM in the development of a prototype component. Initial results were presented for reinforcement drape, compaction and in-plane permeability. Mold filling prediction was also included. Finally, the implications for mold design were discussed and the techniques presented were identified as key elements in an integrated design approach.

Work on reducing the minimum cycle times in resin transfer molding was addressed by Rudd, *et al.* [1990]. The fundamental study was conducted to determine the importance of several process variables regarding the individual process times and the overall cycle time. Experimental results indicated that the process is particularly sensitive to those variables that affect the heating rate in the laminate. A series of predictions were made using a simple finite difference model and compared with the experiments under standard conditions. Except where a significant degree of mold cooling or through thickness gradient occurred, the two methods were in good agreement.

The effect of variations in process variables on the quality of RTM moldings was discussed [Hayward and Harris, 1990]. Four major process variables were selected: resin injection pressure, mold temperature, resin viscosity and vacuum assistance. Several

23

conclusions were drawn from the experimental studies. First, significant improvements were found in the mechanical properties and porosity levels of moldings made with vacuum assistance. Second, variations in resin injection pressure appeared to have no affect on the quality of the molded parts. Finally, mold temperature variations, over a moderate range, do not appear to affect part quality other than through resin cure differences.

Design strategies for the RTM process were presented [Gonzalez-Romero and Macosko, 1990]. The approach used moldability diagrams to define a set of conditions necessary to meet the process requirements. Diagrams were depicted for both the filling and curing steps. The criterion for selecting the amount of fiber reinforcement, injection time, catalyst level and process temperatures in order to optimize properties and demold time was discussed.

The influence that process parameter exhibit on void formation in resin transfer molding has been studied by Lundstrom and Gebart [1994]. The experiments were conducted using a flat mold with unidirectional flow. A significant conclusion from the study was that the void content was strongly reduced by an applied vacuum and, furthermore, can be almost completely eliminated. These results agree with those found by Hayward and Harris [1990]. Similar effects were obtained with an increased pressure during cure.

2.3 Intelligent Systems for Process Monitoring and Control

Viscoelastic properties of a resin undergo continuous change during the cure cycle and can be useful for cure cycle design and monitoring. A technique called mechanical impedance analysis (MIA) has been applied to real-time in-process cure monitoring of composite fabrication [Jang, et al., 1992, Jang and Zhu, 1986]. By modeling a transfer

24

function, the relationship between the sensor output and material properties was known. The MIA technique was concluded to be a versatile tool for evaluating the dynamic mechanical properties of a composite as a function of the material's physical and chemical state.

Resin transfer molding processes require that a large number of material processing parameters be observed, known and/or controlled during the processing. Viscosity during impregnation and cure is one such parameter. For this reason, work has been done on the use of frequency dependent electromagnetic sensing (FDMS) techniques to monitor properties in the RTM tool [Kranbuehl et al., 1991]. The objective of the research was to use FDMS techniques to address problems of RTM for large complex parts and to develop a closed loop, intelligent, sensor controlled RTM fabrication process. The sensors were found to provide an in-situ method for measuring impregnation rate and uniformity of cure at various positions during processing.

Control and optimization of the autoclave production of high performance composites was studied by Kenny [1992]. The intelligent system allowed the computation, in real time, of heat transfer coefficients for each selected tool, the prediction of temperature changes inside the laminate as a function of air temperature and the optimization of the cure cycle. The optimization phase was developed to determine the optimum air temperature that minimizes processing times, while considering specification constraints and part relevance. The intelligent system was applied to optimize and control the processing conditions when different raw materials, geometries or autoclave tools were used.

A rule-based expert system was developed for controlling the autoclave temperature and pressure during the curing of fiber reinforced thermosetting matrix composites [Ciriscioli et al., 1992]. Rules were established to ensure that the temperatures and pressures remained within the required limits, the laminate was fully compacted and

25

cured, the void content was minimized and the residual stresses were low. Inputs to the expert system included the measured instantaneous temperature and pressure, composite midpoint and surface temperatures, composite thickness and ionic conductivity. Tests proved that the control system resulted in reduced cure times and laminates that exhibited good mechanical properties.

The results of finite element simulation for a cold-forging process was utilized as experience for expert system development [Osakada *et al.*, 1990]. The researchers transformed data, collected from hundreds of simulations, into rules through the aid of statistical techniques and neural networks. The researchers discovered that the combination of an expert system with FEM simulation and neural networks is an effective method for knowledge acquisition.

Karbhari [1992] presented a scheme in which decisions concerning the materials transformation process were aided through a deselection process resident on a decision support system. This was accomplished through the use of a hierarchical system that incorporated major part discriminators, such as shape, material and form. The scheme emphasized the use of simulation and intelligent deselection to obtain the optimum design space for a process. The decision support system acted as a tool towards the facilitation of concurrent engineering by ensuring that the knowledge necessary for a successful product realization process was made available in the most accessible format. As importantly, the integration of the decision support system with an expert system for process control provided the ability to closely monitor the manufacturing process.

Joseph and Hanratty [1993] presented an architecture for a predictive control model of batch processes using artificial neural network models. The application studied was that of a simulated autoclave curing process for composite manufacturing. Intermediate measurements taken during batch processing provided feedback correction to compensate for modeling errors and unmeasured disturbances. The neural network model was used to

26

generate models of batch processes relating product quality to process input variables and processing conditions.

2.4 Summary

An extensive amount of work has been done in the simulation of the RTM process: models have evolved from single phase, two dimensional types to those that characterize all three phases of processing for three-dimensional parts. This progress has been useful in allowing researchers to gain a clearer picture of the phenomena that occur during RTM processing. In addition, these simulation models have provided insight into the formation of voids during the resin flow stage, which affect the overall quality of RTM parts.

Although the processing of RTM parts is better understood and more accurately characterized, there are several key issues that must be resolved: (1) What are the significant factors that affect the quality of RTM parts? (2) Given the significant factors, can we define a relationship between these factors and the resulting product and process characteristics; for instance, is it possible to develop a model that accurately predicts the mold filling time in terms of the injection pressure, mold temperature and other significant factors? (3) Given a set of product and process constraints, as well as the defining relationships, how can we optimize the RTM process; i.e., determine the settings of the product and process variables such that in-process changes have little or no effect on the desired characteristics of the part? (4) Due to the existence of nonlinearities and interactions among RTM product and process variables, there is a need for an effective technique to ensure that the final components maintain the desired properties. What technique(s) are appropriate for process control in RTM?

There is a great need for work in the area of design optimization in the RTM process, beginning with identifying the relationship among the significant variables and their

27

combined effect on the resulting composite part. It is necessary that an integrated product and process design approach be taken if the achievements of a robust design, and the desired part properties and performance are to be realized. In addition, due to the nonlinearities and interactions among variables, there is a need for an intelligent control system to ensure that the final RTM components remain within their specifications.

28

CHAPTER 3

RESEARCH INVESTIGATIONS

An extensive amount of work has been done in the simulation of the RTM process, as described in Chapter 2. Models have evolved from single phase, two dimensional types to those that characterize all phases of processing in three-dimensions. This progress has been useful in allowing researchers to gain a clearer picture of the phenomena that occur during RTM processing. In addition, these simulation models have provided insight into the formation of voids during the resin flow stage, which affect the overall quality of RTM components.

Despite these advances, little work has been done in the area of design optimization. Although the processing of RTM parts is better understood and more accurately characterized, the relationship among the variables and their effect on the resulting composite part is not well known. It is crucial that these process models be utilized in the design of the mold and optimization of material and process parameters to achieve desired part properties and performance.

Two main areas are addressed in the research studies to validate the feasibility of the proposed methodology for resin transfer molding: (1) development of a product and process design optimization model and (2) application of the cascade correlation algorithm in process control.

29

3.1 Design Optimization

This section defines the experimental design method used in the design optimization pilot studies. The purpose of this approach is to identify the critical product and process design parameters in resin transfer molding. A procedure for regression model fitting is defined, as well as the diagnostic checks for validating the fit of the regression model. In addition, a cascade correlation neural network model was investigated as a replacement for the regression analysis technique using identical experimental data.

3.1.1 Experimental Design

Initially, a list of product and process design parameters must be identified. The process parameters are those factors adjusted during the RTM process, while the product design parameters are determined prior to processing and remain fixed thereafter. Through a well-constructed design of experiments, optimal design parameters can be identified.

As in the case of resin transfer molding, a large number of factors are of interest. For this reason, a factorial experimental design should be used to define the critical design parameters. In a factorial experiment, all possible combinations of the levels of the factors are investigated in each complete trial or replicate of the experiment [Montgomery and Runger, 1994]. For example, suppose that the factors that are expected to have an effect on mold filling time in the RTM process are injection pressure, mold temperature and fiber volume, denoted as factor A, factor B and factor C, respectively. In addition, let each factor be assigned three different levels: a levels of factor A, b levels of factor B and c levels of factor C. An example of all combinations of factors and levels would be represented by the data shown in Table 3.1.

In this table, there are three factors at three levels each, for a total of 27 treatment combinations. This is a 3^3 factorial design. In other words, a minimum of twenty seven experiments, as in the single replicate case, are needed for a complete factorial design. The

30

response to each treatment combination is the mold filling time. The y_{ijk} values in Table 3.1 represent the response associated with the ith level of factor A, the jth level of factor B and the kth level of factor C, where i,j,k varies from 1 to 3.

Table 3.1. A factorial experiment with three factors

Factor A	Factor B								
	B_1			B_2			B_3		
	Factor C								
	C_1	C_2	C_3	C_1	C_2	C_3	C_1	C_2	C_3
A_1	y_{111}	y_{112}	y_{113}	y_{121}	y_{122}	y_{123}	y_{131}	y_{132}	y_{133}
A_2	y_{211}	y_{212}	y_{213}	y_{221}	y_{222}	y_{223}	y_{231}	y_{232}	y_{233}
A_3	y_{311}	y_{312}	y_{313}	y_{321}	y_{322}	y_{323}	y_{331}	y_{332}	y_{333}

There are several advantages of using factorial designs: (1) they are more efficient than experiments that observe one factor at a time; (2) they are necessary when interactions exist and (3) they provide an estimation of the effects of a factor at several levels of the other factors, yielding conclusions that are valid over a range of experimental conditions.

The effect of a factor is defined as the change in response produced by a change in the level of the factor. This is frequently called a main effect because it refers to the primary factors of interest in the experiment [Montgomery, 1984]. In some experiments, however, the difference in response between the levels of one factor is not the same at all levels of the other factors. When this occurs, there is an interaction between the factors. In a 3^3 factorial design, there are three main effects, three two-factor interactions and one three-

31

factor interaction. By calculating the sum of squares, typically compiled in an analysis of variance table, the significance of each main factor and all interactions are determined.

With the expertise of an RTM engineer at Brunswick Defense, several parameters were identified as the most critical in their effect on mold filling time, void frequency and void size. Table 3.2 lists these critical factors and the three levels of each. Voiding is of particular interest in the resin transfer molding process since an increase in void content by 5% results in a decrease in the inter-laminar shear strength by greater than 20% [Bowles and Frimpong, 1992].

Table 3.2. Factors that affect mold filling time and voids in RTM processing

	Factor	Level 1	Level 2	Level 3
1	Mold temperature (°F)	150	175	200
2	Injection pressure (psi)	50	100	150
3	Fiber volume (% volume)	45	52.5	60

From the simulation model, it was only possible to obtain information on the mold filling time; therefore, the phenomenon of voids was ignored in the pilot investigations. However, the issue of voids is addressed through experimentation on the actual RTM process.

In the above case, injection pressure, mold temperature and fiber volume are the main effects. Each is represented at three levels. All combinations of factors and levels are represented by the data shown in Table 3.3, where the y_{ijk} values represent the mold filling time associated with the ith level of injection pressure, the jth level of mold temperature and the kth level of fiber volume.

32

Table 3.3. A 3^3 factorial design for RTM

Injection pressure (psi)	Mold temperature (°F)								
	150			175			200		
	Fiber volume (% volume)								
	45	52.5	60	45	52.5	60	45	52.5	60
50	y_{111}	y_{112}	y_{113}	y_{121}	y_{122}	y_{123}	y_{131}	y_{132}	y_{133}
100	y_{211}	y_{212}	y_{213}	y_{221}	y_{222}	y_{223}	y_{231}	y_{232}	y_{233}
150	y_{311}	y_{312}	y_{313}	y_{321}	y_{322}	y_{323}	y_{331}	y_{332}	y_{333}

3.1.2 Simulation Experiments

For each of the factor-level combinations in Table 3.3, a simulation experiment was performed to estimate the mold filling time, in minutes. The mold filling times, or y_{ijk} values, for the 27 trials are shown in Table 3.4. The simulation model was validated using mold filling time data provided by Brunswick Defense. In the experiments in Table 3.4, the part molded was a flat panel, 20" x 20" in dimension.

The results of the design of experiments procedure, or mold filling times, are analyzed through a technique called analysis of variance (ANOVA). This provides information on the significance of each factor and of each factor interation on the response. For example, using the analysis of variance technique, it can be determined which of the factors have a significant effect on the mold filling time in the resin transfer molding process; in addition, if there are any interactions among factors that influence the mold filling time, these are identified as well.

33

Table 3.4. Mold filling times in RTM using a 3^3 factorial design

Injection pressure (psi)	Mold temperature (°F)								
	150			175			200		
	Fiber volume (% volume)								
	45	52.5	60	45	52.5	60	45	52.5	60
50	0.8062	1.7254	3.5685	0.4312	0.9647	2.1023	0.5230	1.1063	2.4386
100	0.3928	0.7955	1.7826	0.2141	0.4587	1.0611	0.2722	0.5544	1.1903
150	0.2680	0.5251	1.1902	0.1427	0.3109	0.6951	0.1787	0.3671	0.7934

3.1.3 Analysis of Variance

Consider the three-factor case, where the analysis of variance model is defined as:

$$y_{ijkl} = \mu + \tau_i + \beta_j + \gamma_k + (\tau\beta)_{ij} + (\tau\gamma)_{ik} + (\beta\gamma)_{jk} + (\tau\beta\gamma)_{ijk} + \varepsilon_{ijkl}$$

where

$i = 1,2,...,a$

$j = 1,2,...,b$

$k = 1,2,...,c$

$l = 1,2,...,n$ (replicates)

(3.1)

Then, the formulas for the sum of squares are given by the following equations:

$$SS_T = \sum_{i=1}^{a}\sum_{j=1}^{b}\sum_{k=1}^{c}\sum_{l=1}^{n} y_{ijkl}^2 - \frac{y_{....}^2}{abcn}$$

(3.2)

$$SS_A = \sum_{i=1}^{a}\frac{y_{i...}^2}{bcn} - \frac{y_{....}^2}{abcn}$$

(3.3)

$$SS_B = \sum_{j=1}^{b}\frac{y_{.j..}^2}{acn} - \frac{y_{....}^2}{abcn}$$

(3.4)

34

$$SS_C = \sum_{k=1}^{c} \frac{y_{..k}^2}{abn} - \frac{y_{...}^2}{abcn} \tag{3.5}$$

$$SS_{AB} = \sum_{i=1}^{a}\sum_{j=1}^{b} \frac{y_{ij.}^2}{cn} - \frac{y_{...}^2}{abcn} - SS_A - SS_B \tag{3.6}$$

$$SS_{AC} = \sum_{i=1}^{a}\sum_{k=1}^{c} \frac{y_{i.k.}^2}{bn} - \frac{y_{...}^2}{abcn} - SS_A - SS_C \tag{3.7}$$

$$SS_{BC} = \sum_{j=1}^{b}\sum_{k=1}^{c} \frac{y_{.jk.}^2}{an} - \frac{y_{...}^2}{abcn} - SS_B - SS_C \tag{3.8}$$

$$SS_{ABC} = \sum_{i=1}^{a}\sum_{j=1}^{b}\sum_{k=1}^{c} \frac{y_{ijk.}^2}{n} - \frac{y_{...}^2}{abcn} - SS_A - SS_B - SS_C - SS_{AB} - SS_{AC} - SS_{BC} \tag{3.9}$$

$$SS_E = SS_T - SS_A - SS_B - SS_C - SS_{AB} - SS_{AC} - SS_{BC} - SS_{ABC} \tag{3.10}$$

Using Equations (3.2)-(3.10), the analysis of variance table is completed as shown in Table 3.5.

Table 3.5. Analysis of variance table for three-factor model

Factor	Sum of Squares	D.O.F.	Mean Square	F_0
A	SS_A	a-1	$MS_A = SS_A/SS_T$	MS_A/MS_E
B	SS_B	b-1	$MS_B = SS_B/SS_T$	MS_B/MS_E
C	SS_C	c-1	$MS_C = SS_C/SS_T$	MS_C/MS_E
AB	SS_{AB}	(a-1)(b-1)	$MS_{AB} = SS_{AB}/SS_T$	MS_{AB}/MS_E
AC	SS_{AC}	(a-1)(c-1)	$MS_{AC} = SS_{AC}/SS_T$	MS_{AC}/MS_E
BC	SS_{BC}	(b-1)(c-1)	$MS_{BC} = SS_{BC}/SS_T$	MS_{BC}/MS_E
ABC	SS_{ABC}	(a-1)(b-1)(c-1)	$MS_{ABC} = SS_{ABC}/SS_T$	MS_{ABC}/MS_E
Error	SS_E	abc(n-1)	$MS_E = SS_E/SS_T$	
Total	SS_T	abcn-1		

35

If the following assumptions are made: (1) the model in Equation (3.1) is adequate and (2) the error terms ε_{ijk} are normally and independently distributed with constant variance σ^2, the ratios of mean squares MS_A/MS_E, MS_B/MS_E, MS_C/MS_E, MS_{AB}/MS_E, MS_{AC}/MS_E, MS_{BC}/MS_E, MS_{ABC}/MS_E are distributed as F with a-1, b-1, c-1, (a-1)(b-1), (a-1)(c-1), (b-1)(c-1), (a-1)(b-1)(c-1), and abc(n-1) denominator degrees of freedom, respectively. The critical region is defined by the upper tail of the F distribution. For example, F_0 for factor A is MS_A/MS_E, which is distributed as $F_{\alpha,a-1,abc(n-1)}$. If $F_0 > F_{\alpha,a-1,abc(n-1)}$, it is concluded that factor A is significant. This means that varying the level of factor A results in a substantial change in the value of the response. Similar calculations are performed for the remaining main effects, as well as the interaction effects.

The analysis of variance table for the 3^3 factorial design in Table 3.5 is shown in Table 3.6. The final column, F_0, is the column of interest. To determine the significant factors, the F statistic is calculated for each factor and interaction. For all main effects factors, at $\alpha = 0.01$, $F_{0.01,1,8} = 11.26$ and for all interaction effects factors, $F_{0.01,3,8} = 7.59$. Therefore, using the condition that the factor is significant if $F_0 > F_{\alpha,j,abc(n-1)}$, where j is equivalent to the degrees of freedom of the factor of interest, all factors and interactions are significant at $\alpha = 0.01$. However, the F-test is more significant for the main effects compared to the interaction effects. Therefore, the conclusion is that temperature, pressure and fiber volume have a significant effect on the mold filling time and will be included in the regression analysis. The interaction effects have relatively little significance and will be ignored in further analyses.

Table 3.6. Analysis of variance table for experimental results in Table 3.4

Factor	Sum of Squares	D.O.F.	Mean Square	F_0
temp	1.33737	2	0.66868	68.95
press	5.10514	2	2.55257	263.22
fiber	7.83101	2	3.91550	403.77
temp*press	0.31734	4	0.07933	8.18
temp*fiber	0.39459	4	0.09865	10.17
press*fiber	1.69633	4	0.42408	43.73
Error	0.07758	8	0.00970	
Total	16.75936	26		

3.1.4 Regression Analysis

Once the significant factors are identified through analysis of variance, regression analysis techniques are used to build a quantitative model relating the significant factors to the response. Since many regression problems involve more than one regressor variable, a multiple linear regression model is used to define the response in terms of the significant variables. The general model is defined by the following equation:

$$y = \beta_0 + \beta_1 x_1 + \beta_2 x_2 + \ldots + \beta_k x_k + \varepsilon \tag{3.11}$$

where y is the response, β_i is the regression coefficient associated with the independent variable, x_i, and ε is the error term.

Equation (3.11) can be rewritten in terms of the observations as

$$
\begin{aligned}
y_j &= \beta_0 + \beta_1 x_{1j} + \beta_2 x_{2j} + \ldots + \beta_k x_{kj} + \varepsilon_j \\
&= \beta_0 + \sum_{i=1}^{k} \beta_j x_{ij} + \varepsilon_j \qquad j = 1,2,\ldots,n
\end{aligned}
\tag{3.12}
$$

37

where y_j is the response at observation j, $j = 1, 2, ..., n$.; β_i is the regression coefficient for independent variable, x_i and x_{ij} is the level of independent variable x_i at observation j.

The regression coefficients, or $\beta_i's$, are estimated using the method of least squares. Assuming that $n > k$ observations are available, the least squares function is written as:

$$L = \sum_{j=1}^{n} \left[y_j - \beta_0' - \sum_{i=1}^{k} \beta_i (x_{ij} - \bar{x}_i) \right]^2 \tag{3.13}$$

and the least squares estimators of $\beta_0', \beta_1, ... , \beta_k$ must satisfy

$$\frac{\partial L}{\partial \beta_0'} \bigg|_{\hat{\beta}_0', \hat{\beta}_1, ..., \hat{\beta}_k} = -2 \left[\sum_{j=1}^{n} y_j - \hat{\beta}_0' - \sum_{u=1}^{k} \hat{\beta}_u (x_{uj} - \bar{x}_u) \right] = 0 \tag{3.14}$$

and

$$\frac{\partial L}{\partial \beta_i} \bigg|_{\hat{\beta}_0', \hat{\beta}_1, ..., \hat{\beta}_k} = -2 \left[\sum_{j=1}^{n} y_j - \hat{\beta}_0' - \sum_{u=1}^{k} \hat{\beta}_u (x_{uj} - \bar{x}_u) \right] (x_{ij} - \bar{x}_i) = 0, \quad i = 1, 2, ..., k \tag{3.15}$$

To simplify the procedure, the model in Equation (3.12) can be written in matrix notation as

$$y = X\beta + \varepsilon \tag{3.16}$$

where

$$y = \begin{bmatrix} y_1 \\ y_2 \\ \cdot \\ \cdot \\ \cdot \\ y_n \end{bmatrix} \quad X = \begin{bmatrix} 1 & (x_{11} - \bar{x}_1) & (x_{21} - \bar{x}_2) & ... & (x_{k1} - \bar{x}_k) \\ 1 & (x_{12} - \bar{x}_1) & (x_{22} - \bar{x}_2) & ... & (x_{k2} - \bar{x}_k) \\ \cdot & \cdot & \cdot & & \cdot \\ \cdot & \cdot & \cdot & & \cdot \\ \cdot & \cdot & \cdot & & \cdot \\ 1 & (x_{1n} - \bar{x}_1) & (x_{2n} - \bar{x}_2) & ... & (x_{kn} - \bar{x}_k) \end{bmatrix}$$

38

$$\beta = \begin{bmatrix} \beta_0' \\ \beta_1 \\ \cdot \\ \cdot \\ \cdot \\ \cdot \\ \beta_k \end{bmatrix} \quad and \quad \varepsilon = \begin{bmatrix} \varepsilon_1 \\ \varepsilon_2 \\ \cdot \\ \cdot \\ \cdot \\ \cdot \\ \varepsilon_n \end{bmatrix}$$

Then, L may be expressed by the equation:

$$L = y'y - \beta'X'y - y'X\beta + \beta'X'X\beta$$
$$= y'y - 2\beta'X'y + \beta'X'X\beta \tag{3.17}$$

The least squares estimators must satisfy

$$\left. \frac{\partial L}{\partial \beta} \right|_{\hat{\beta}} = -2X'y + 2X'X\hat{\beta} = 0 \tag{3.18}$$

Thus, the least squares estimator of β is

$$\hat{\beta} = (X'X)^{-1}X'y \tag{3.19}$$

After conducting the experiments in Table 3.1 and obtaining the response values shown in Table 3.4, regression analysis is used to hypothesize a model that predicts the behavior of the response given a set of predictors [Weisberg, 1985]. Using the data in Table 3.4, the mold filling time is predicted for varying levels of injection pressure, mold temperature and fiber volume. The regression equation that best fit the set of data was determined to be:

$$logfill = 74.952 + 0.404temp + 0.0118press + 0.191fiber - 10.9\sqrt{temp} \tag{3.20}$$
$$- 0.443\sqrt{press} - 1.29\sqrt{fiber}$$

The above regression model seemed reasonable since, according to the experience of an RTM engineer at Brunswick Defense, all three variables - temperature, pressure and fiber volume - are known to have an effect on the mold filling time. Intuitively, an increase in

39

temperature or pressure, or a decrease in fiber volume would be expected to cause a decrease in the mold filling time.

The plot of the actual versus fitted values shows that the regression equation did well in predicting the mold filling times (see Figure 3.1).
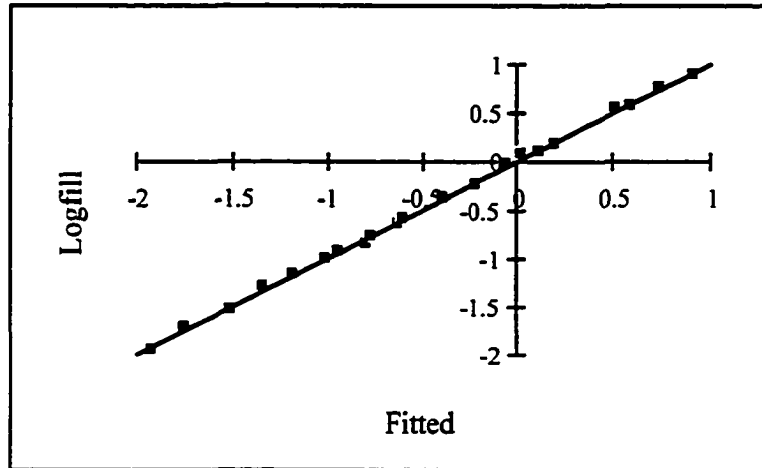
Figure 3.1. Plot of actual filling times versus predicted fillling times

3.1.5 Model Adequacy Checking

In order to validate the regression model, Equation (3.20), a series of diagnostics were performed. The following is an explanation of each validation test.

3.1.5.1 Residual Analysis

Analysis of the residuals from a regression model is necessary to determine the adequacy of the least squares fit. A plot of the residuals versus the fitted values can reveal potential problems in the model, depending on the shape of the plot. Under the normality assumption, there should be no correlation between the residuals, e_j, and the fitted

40

values, $\hat{y}_j$. Therefore, the plot of residuals versus fitted values should not reveal any apparent pattern or trending.

In addition, it is helpful to plot the residuals versus each of the regressor variables. As in the case of the residuals versus fitted values plot, the behavior of the plotted points should be fairly random. If so, it is concluded that the regression model is an adequate fit to the experimental data.

Figures 3.2-3.6 display the residuals plot and the residuals versus fitted values, mold temperature, injection pressure and fiber volume, respectively. In each of the plots, there is no evidence of patterns since the points appear fairly random. Therefore, it is concluded that equation (3.20) is adequate.
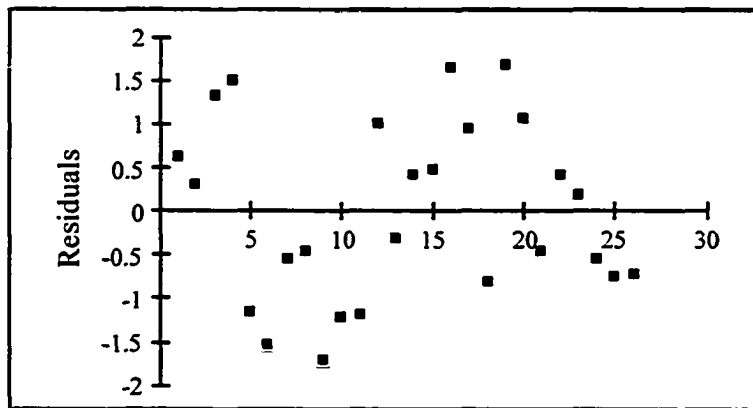
Figure 3.2. Residuals plot for mold filling time
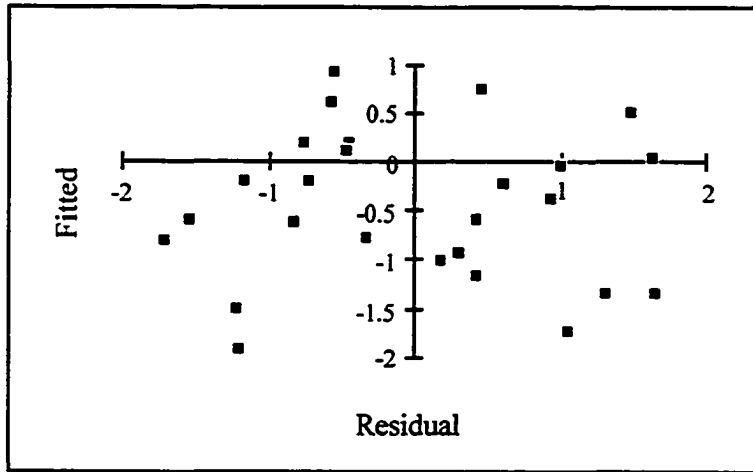
Figure 3.3. Plot of predicted filling times versus residuals
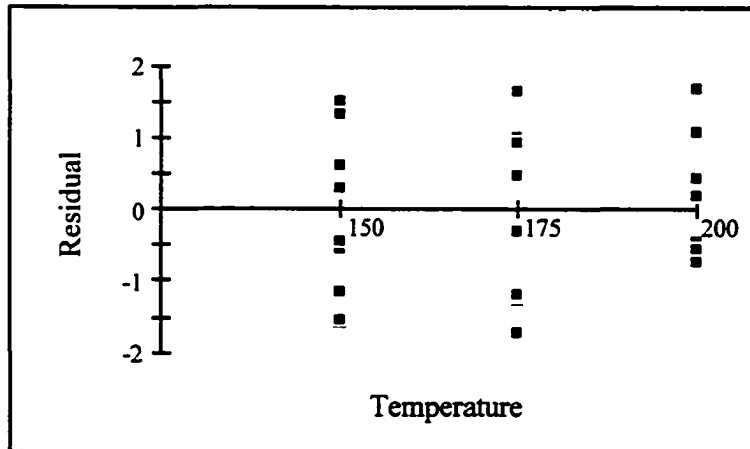
Figure 3.4. Plot of residuals versus mold temperature

42
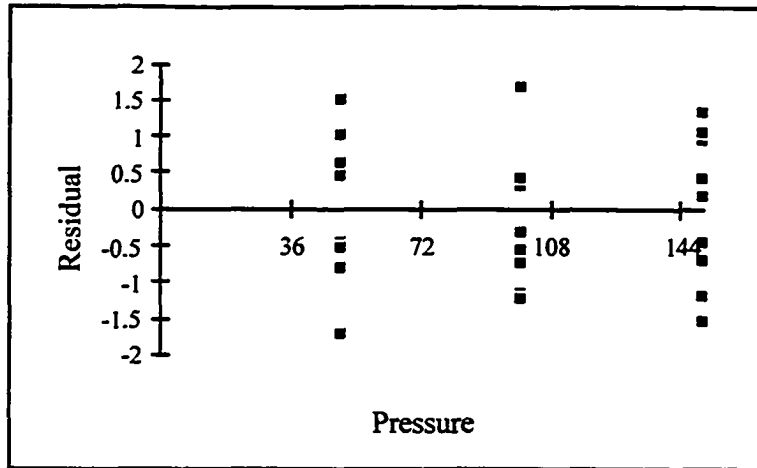
Figure 3.5. Plot of residuals versus injection pressure
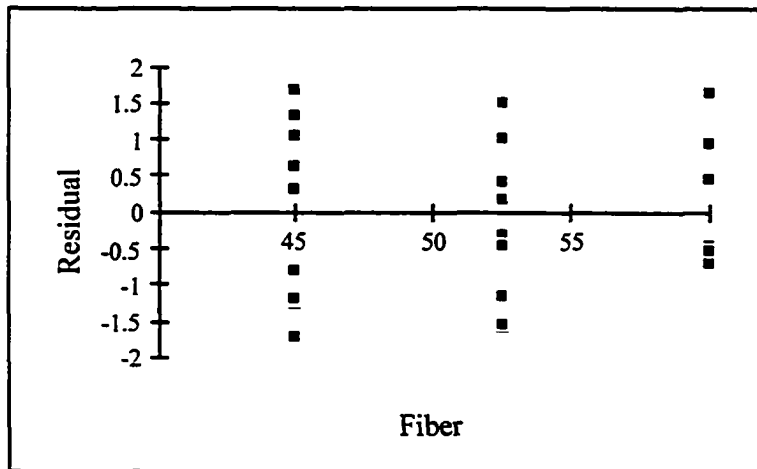
Figure 3.6. Plot of residuals versus fiber volume

43

3.1.5.2 Lack-of-Fit Test

The lack-of-fit test will validate the order of the model that was selected to represent the approximating function of the data. A test for the "goodness of fit" of the regression model begins with the hypotheses:

H_0: The regression model is correct.

H_1: The regression model is not correct.

In order to test the hypotheses, the residual sum of squares is partitioned into the sum of squares as a result of pure error and the sum of squares characterized by the lack of fit of the model. In equation form, the sum of squares of the error is written as:

$$SS_E = SS_{PE} + SS_{LOF} \tag{3.21}$$

Assume that there are n total observations, with repeated observations on the response Y for at least one level of x, such as

$$
\begin{aligned}
&y_{11}, y_{12}, \dots, y_{1n_1} && \textit{repeated observations at } x_1 \\
&y_{21}, y_{22}, \dots, y_{2n_2} && \textit{repeated observations at } x_2 \\
&\qquad\quad \vdots \\
&y_{m1}, y_{m2}, \dots, y_{m1n_m} && \textit{repeated observations at } x_m
\end{aligned}
$$

The total sum of squares for pure error is obtained by the summation equation:

$$SS_{PE} = \sum_{i=1}^{m} \sum_{u=1}^{n_i} (y_{iu} - \bar{y}_i)^2 \tag{3.22}$$

where $\bar{y}_i$ represents the average of all n_i repeat observations on the response y at x_i.

After calculating Equation (3.22), the sum of squares for the lack of fit is easily obtained by the following equation:

44

$$SS_{LOF} = SS_E - SS_{PE} \qquad (3.23)$$

The test statistic for lack of fit is defined by

$$F_0 = \frac{SS_{LOF} / (m-2)}{SS_{PE} / (n-m)} = \frac{MS_{LOF}}{MS_{PE}} \qquad (3.24)$$

and the hypothesis that the model is adequate is rejected if $F_0 > F_{\alpha,m-2,n-m}$. Otherwise, there is no apparent reason to doubt the adequacy of the model.

The lack of fit test described above requires that more than one replication exist for each factor-level combination. However, a single replicate was used in the experiments conducted in Table 3.4. The lack of fit test is modified to handle the single replicate case.

First, the model is fit to the original data. Then, a separate test is performed for each predictor variable, x_i. The data is split into two parts, based on the mean of x_i, and each part is modeled. If a large difference exists between the two-part model and the original model, this indicates a lack of fit in the original model. In the model described by Equation (3.20), there was no indication of a lack of fit in the original model.

3.1.5.3 Coefficient of Determination

The coefficient of determination is defined by

$$R^2 = \frac{SS_R}{SS_T} = \frac{\sum\limits_{j=1}^{n} (\hat{y}_j - \bar{y})^2}{\sum\limits_{j=1}^{n} (y_j - \bar{y})^2} \qquad (3.25)$$

and represents the proportion of variability in the data that is accounted for by the regression model, where $0 < R^2 \leq 1$. Obviously, the higher the value of R^2 the better. The R^2 statistic, however, should be used cautiously since it is always possible to obtain a value of 1 for R^2 by adding additional terms to the model; a higher R^2 value does not

45

necessarily mean that the model is better. The effect of additional variables on the error term should be monitored closely.

After fitting the data in Table 3.4 to a regression model, the overall R^2 value was calculated to be 99.9%.

3.1.6 Validation of Regression Model

The regression equation in (3.20) is assumed to be valid over the range under which the predictor variables were modeled. In the original experiment, defined in section 3.1.2, the predictor variables were defined by three levels each. Therefore, it is of interest to verify that Equation (3.20) holds for other values of the predictor variables within the specified range. For example, the mold temperature was set at 150, 175 and 200 degrees Fahrenheit; the injection pressure levels were 50, 100 and 150 psi; and the fiber volume was assigned a value of 45, 52.5 and 60 percent, by weight. Intermediate settings for the predictor variables are, for example, mold temperature equals 180 degrees Fahrenheit; injection pressure equals 120 psi and fiber volume equals 50 percent. Table 3.6 lists the experimental settings for all three predictor variables in the validation of the regression model defined by Equation (3.20). The mold filling times associated with each combination of predictor variables, defined in Table 3.7, are shown in Table 3.8.

Table 3.8 gives the actual mold filling times based on simulation experiments. By plugging the settings of the predictor variables into Equation (3.20), the predicted values for the mold filling time can be obtained. Table 3.9 displays the actual and fitted values for the mold filling time.

In Figure 3.7, the actual versus fitted values are plotted from Table 3.9. If the regression model is a good fit, the predicted values will be very close to the actual values. Therefore, the points on the plot should lie approximately on a 45° line drawn through

46

the graph. From Figure 3.7, it is seen that this is the case and it is concluded that the regression model in Equation (3.20) accurately represents the data.

Table 3.7. Predictor variable settings for validation procedure

Experiment #	Mold Temperature, ° F	Injection Pressure, psi	Fiber Volume, % by wt
1	150	50	45
2	175	150	60
3	200	100	52.5
4	155	50	45
5	160	75	50
6	165	80	55
7	180	120	50
8	185	90	60
9	190	60	45
10	195	100	55
11	170	70	60

Table 3.8 Mold filling times for validation procedure.

Experiment #	Mold Temperature, ° F	Injection Pressure, psi	Fiber Volume, % by wt	Mold filling time, min
1	150	50	45	0.78697
2	175	150	60	0.66755
3	200	100	52.5	0.64040
4	155	50	45	0.61208
5	160	75	50	0.61994
6	165	80	55	0.74090
7	180	120	50	0.26631
8	185	90	60	1.11403
9	190	60	45	0.41797
10	195	100	55	0.70861
11	170	70	60	1.39591

47

Table 3.9. Predicted mold filling times from regression analysis

Actual mold fillling time, min	Predicted mold filling time, min
0.78697	0.79000
0.66755	0.67812
0.64040	0.54934
0.61208	0.65934
0.61994	0.61655
0.74090	0.85929
0.26631	0.29218
1.11403	1.12309
0.41797	0.38286
0.70861	0.65226
1.39591	1.54846
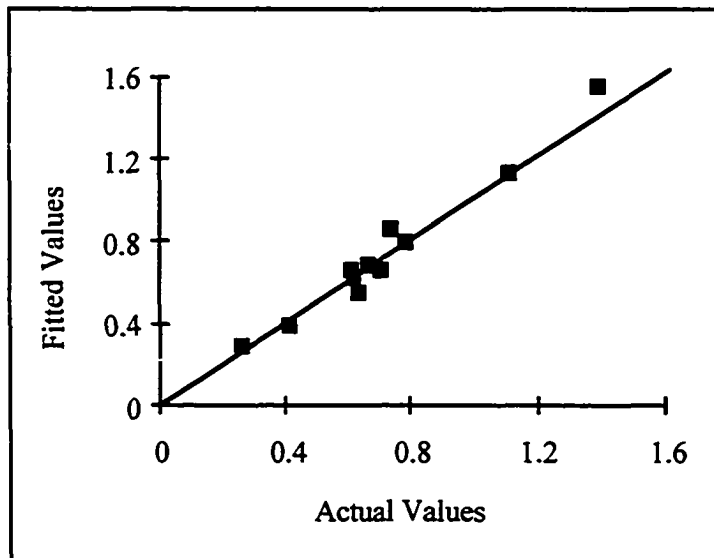
Figure 3.7. Actual versus fitted mold filling times using regression analysis

48

3.1.7 Cascade Correlation Algorithm

Although the linear regression model defined above was a suitable approximation for the nonlinear relationship between mold filling time and the three significant factors, mold temperature, injection pressure and fiber volume, this may not always be the case. Since there are inherent nonlinearities in every process, this is a reasonable assumption to make. Therefore, when a suitable linear approximation cannot be found, nonlinear regression must be pursued and along with it, a whole new set of challenges.

Nonlinear regression parameters are more likely to have physical meaning, although defining the initial model is not a trivial task and extremely difficult when the process is not well known. Least-squares estimation, well developed in linear regression, becomes much more difficult in nonlinear regression. Parameter estimation is iterative, not automatically successful and the properties of estimators are accessible only for large samples or in cases where the model being estimated has properties close to those of a linear model [Swain, 1990].

Due to the disadvantages of nonlinear regression techniques, the cascade correlation algorithm was investigated for its feasibility in design optimization of RTM parts.

3.1.7.1 Introduction

The cascade correlation algorithm (CCA) is included among several constructive learning paradigms that have been developed. Examples of other constructive neural network structures are the tiling algorithm [Mezard and Nadal, 1989] and the upstart algorithm [Frean, 1990]. Constructive neural networks begin with a minimal structure and "construct" nodes, as necessary, until learning takes place. The advantages of these constructive learning algorithms is that they provide a method for adaptively determining the network connectivity, avoiding a-priori choices, and the weights to solve specific

49

function approximation and pattern classification tasks through supervised learning [Honavar and Uhr, 1991].

Development of CCA was initiated to overcome limitations of the back-propagation learning algorithm [Rummelhart, *et al.*, 1986]. One of the major drawbacks of this algorithm is the time taken to learn, believed to be the result of the step-size problem and the moving target problem [Fahlman and Lebiere, 1991]. In back-propagation, error reduction occurs by taking the partial first derivative of the overall error function with respect to each weight in the network and performing a gradient descent. In order for convergence, an infinitesimal number of steps must be taken, which causes a drastic increase in learning time. For this reason, CCA looks at not only the slope of the error function, but its higher-order derivatives as well; i.e., the network utilizes information about the curvature of the error function at the current position in weight space.

The second problem - moving target - occurs when each unit in the network changes simultaneously to reduce the overall error. Since the units do not have any direct link with each other, each unit is trying to solve a problem that changes constantly. CCA overcomes this phenomenon by allowing only one hidden unit in the network to be added at a time.

Cascade correlation requires supervised learning, which means that a set of outputs is provided for each set of inputs during learning. There are two primary features of the cascade correlation algorithm. One is the cascade architecture, where hidden units are added to the network one at a time, as necessary. Once these hidden units are created, they do not change. The second feature is the nature of the learning algorithm that adds hidden units, which maximizes the magnitude of the correlation between the hidden unit's output and the residual error signal at the output layer [Fahlman and Lebiere, 1991].

CCA performs gradient descent in the space of network topology as well as weights. Initially, the network structure contains no hidden nodes (Figure 3.8). Each input is

50

connected to each output, with an adjustable weight corresponding to each connection. A bias input is also present, permanently set to +1. The network attempts to establish a relationship between the input-output patterns; a patience parameter determines whether or not the error is decreasing fast enough during a sequence of training epochs. If the patience parameter is exceeded, a pool of candidate nodes is generated, each connected to all existing nodes in the network. All candidates in the pool are trained in parallel for a specified number of epochs after which time, a final candidate is selected. This selection process is based on the candidate with the maximum correlation with the overall network error. Once a hidden unit is added to the network (Figure 3.9), its input weights are frozen. Repeating the same learning procedure, but now with an additional unit, the network again attempts to learn. If the error is too large after training reaches an asymptote, meaning no significant additional learning occurs, a second additional hidden unit is added to the network (Figure 3.10) using the procedure described above, its input weights are frozen and learning continues. Hidden units are added until the error drops to a desired level.

In Figures 3.8-3.10, the connections between the input units and output units and the connections between the hidden units and output units are denoted by an X. This signifies that these connections are trained repeatedly during learning. The connections between the input units and hidden units and the connections among all hidden units are marked with a box. After each new unit is added to the network, its weighted connections are frozen throughout the duration of the training phase.

51
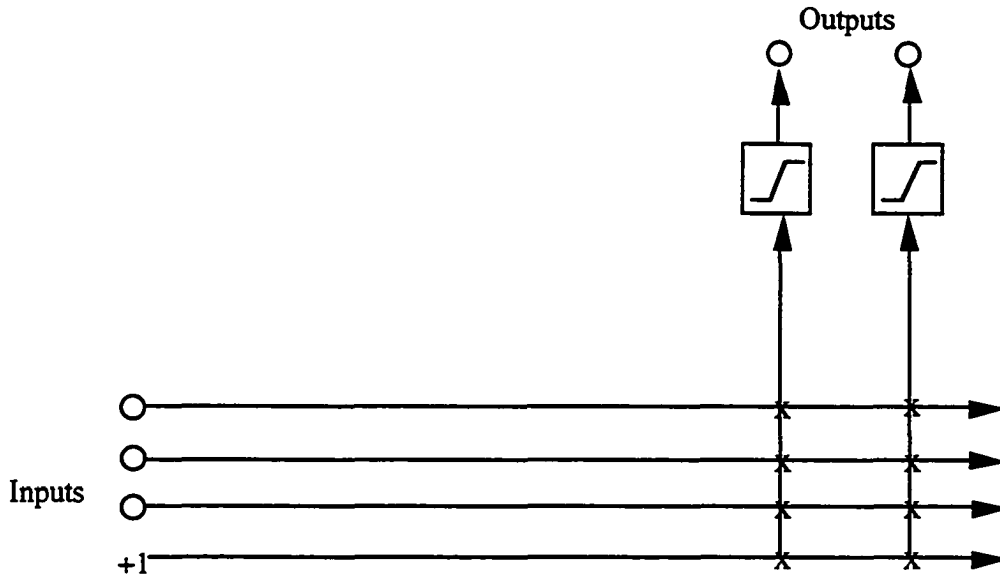
Figure 3.8. Cascade architecture - initial state
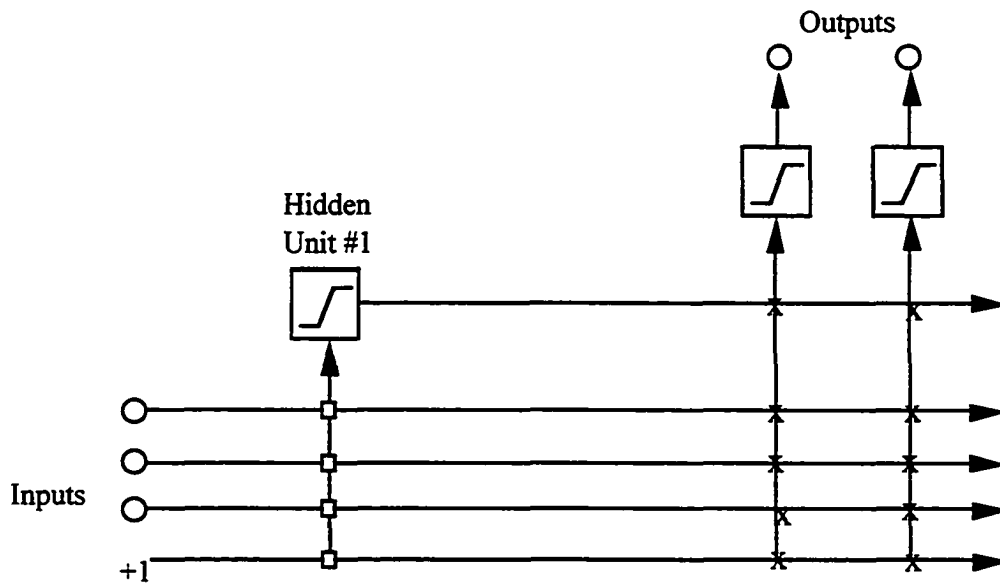
Figure 3.9. Cascade architecture - one hidden unit

52
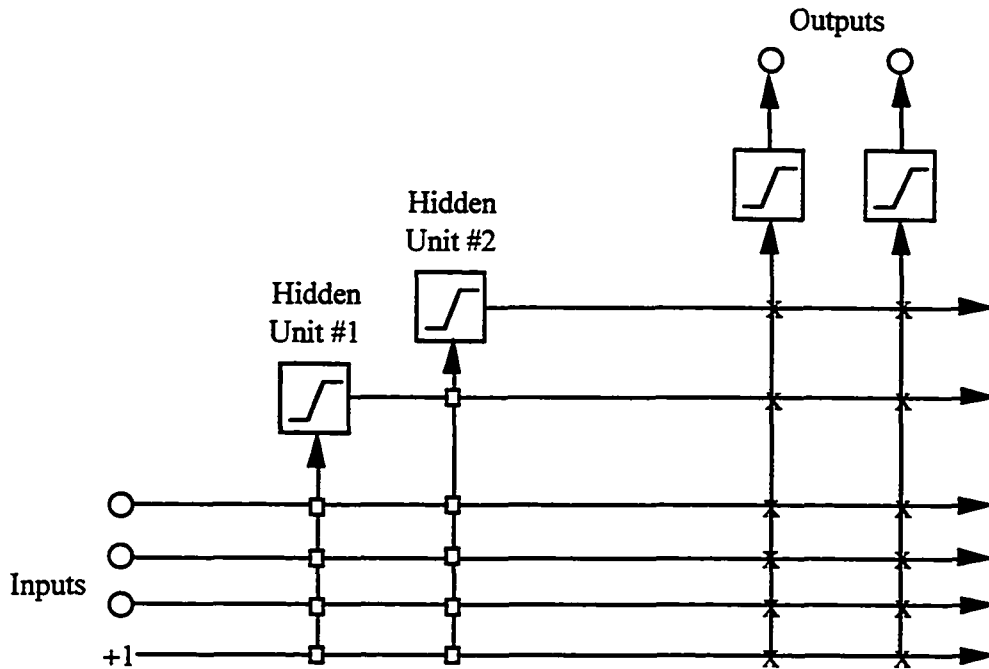
Figure 3.10. Cascade architecture - two hidden units

3.1.7.2 Output Unit Training

Output units are trained to minimize the sum-squared measure E, given by

$$E = \frac{1}{2} \sum_{o,p} (y_{op} - t_{op})^2$$ (3.26)

where

y_{op} = observed value of output o for training pattern p

t_{op} = target output

E is minimized by gradient descent using

$$\partial E / \partial w_{oi} = \sum_{p} (y_{op} - t_{op}) f'_p I_{ip}$$ (3.27)

where

53

f'_p = derivative of the activation function of the output unit for pattern p

I_{ip} = value of the input (or hidden unit) i

w_{oi} = weight connecting input i to output unit o

3.1.7.3 Candidate Unit Selection

As mentioned previously, if the overall error exceeds the desired level, a new hidden unit is added to the network. To create a new hidden unit, a candidate unit is added to the network by connecting it to all the input units and to every hidden unit. Using the training set, the candidate unit's input weights are adjusted to maximize C, where C is defined as

$$C = \sum_o \left| \sum_p (V_p - \overline{V})(E_{op} - \overline{E_o}) \right| \qquad (3.28)$$

where

o = network output where the error is measured

p = training pattern

$\overline{V}$ = average of the candidate unit's value over all patterns

$\overline{E_o}$ = residual output error observed at unit o over all patterns

In other words, the objective of candidate selection is to maximize the magnitude of the correlation between the candidate unit's value and the residual output error observed at the output units.

To maximize C, the value of $\partial C / \partial w_i$, the partial derivative of C with respect to each of the candidate unit's incoming weights, (w_i), must be calculated. This value is determined by the equation

$$\partial C / \partial w_i = \sum_{p,o} \sigma_o \left(E_{op} - \overline{E_o} \right) f'_p I_{ip} \qquad (3.29)$$

where

54

σ_o = sign of correlation between candidate unit's value and output o.

f'_p = derivative of pattern p of the candidate unit's activation function with respect to the sum of its inputs.

I_{ip} = input the candidate unit receives from unit i for pattern p.

After computing $\partial C / \partial w_i$ for each incoming connection, a gradient ascent is performed to maximize C, using the quickprop algorithm to train the input weights. When C no longer improves significantly, the new candidate is added to the network and its input weights are frozen.

3.1.7.4 Quickprop Algorithm

When minimizing E to update the candidate unit's weights and maximizing C to update the output connection weights, a method has been developed [Fahlman, 1988] to achieve good convergence for the weights in a reasonable number of cycles. This is accomplished using the quickprop algorithm. If we consider S to be the slope, either $\partial E / \partial w$ or $-\partial C / \partial w$, the weight change is determined by

$$\Delta w_t = \begin{cases} \varepsilon S_t, & if \ \Delta w_{t-1} = 0 \\ \dfrac{S_t}{S_{t-1} - S_t} \Delta w_{t-1}, & if \ \Delta w_{t-1} \neq 0 \ and \ \dfrac{S_t}{S_{t-1} - S_t} < \mu \\ \mu \Delta w_{t-1}, & otherwise \end{cases} \tag{3.30}$$

where

ε = parameter that controls the linear steps to initiate the algorithm.

S_i = slope at time i, where i represents t or $t-1$.

μ = parameter that controls the maximum step-size, compared to the previous step.

Weights are then updated using

55

$$w_{t+1} = w_t + \Delta w_t \qquad\qquad (3.31)$$

3.1.8 Welding Experiments Using Cascade Correlation Algorithm

A set of experiments was performed to investigate the feasibility of using CCA to accurately predict quality measures given a set of independent variables. This is the requirement of a neural network applied to the resin transfer molding process.

In this experiment, the welding data was utilized from research done by Andersen, *et al*, [1990] where gas tungsten arc welding (GTAW) was studied. In GTAW, an arc is initiated between a pointed tungsten electrode and the surface of the welded workpiece. The physical geometry of the molten weld pool is a major factor in determining the structural adequacy of the weld, such as strength. Several welding factors, such as welding voltage, wire feed rate, electrode tip angle and shielding gas type, affect the finished weld. Some of the measures of weld quality are penetration of the weld pool, bead width and height of the reinforcement. Due to the interactions among the parameters and nonlinearities of the GTAW system, it is difficult to control the process through traditional techniques. Therefore, the application of a neural network architecture is a feasible alternative. In this research, the cascade correlation algorithm was utilized.

The accuracy of the cascade correlation algorithm in predicting the weld quality was evaluated. A total of 42 data sets were used: 31 were selected for training purposes and the remaining 11 were used for testing the network. The selection of the data sets was peformed on a random basis. Appendix B (Table B.1 and B.2) displays the 42 sets of welding parameters and their corresponding quality measures.

Table 3.10 shows the testing results using the cascade correlation algorithm. Figures 3.11-3.14 display the predicted weld quality measures against the actual measures.

56

Table 3.10. Welding test results of cascade correlation algorithm

Weld Number	Bead width (mm)	Penetration (mm)	Reinforcement Height (mm)	Cross Section Area (mm²)
32	6.01	1.29	2.01	7.39
33	5.32	1.60	0.74	2.87
34	6.48	1.42	1.00	4.24
35	7.36	2.46	0.96	6.06
36	6.35	1.36	2.04	8.58
37	8.03	1.41	0.45	2.32
38	7.84	1.26	0.56	3.00
39	8.38	0.87	0.8	3.96
40	9.24	2.46	0.39	2.67
41	10.2	1.19	1.00	6.31
42	8.90	2.04	0.30	1.70
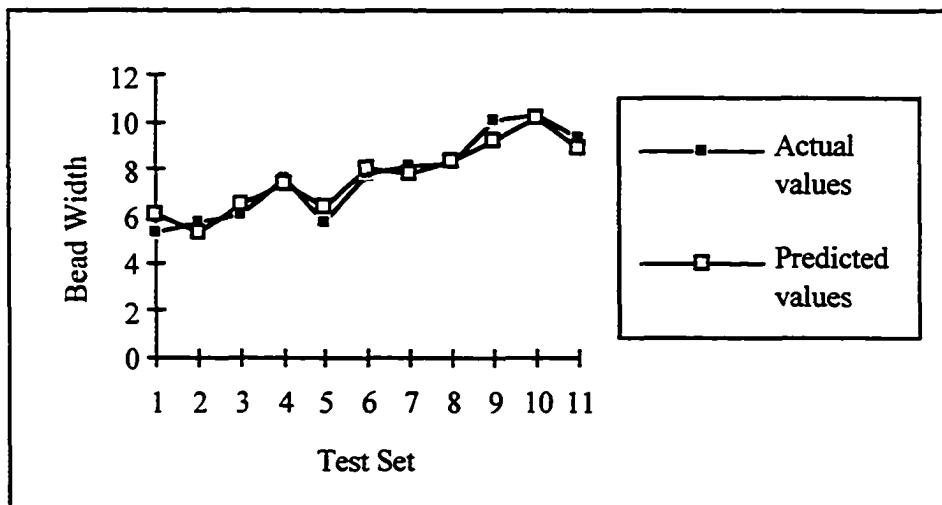
Figure 3.11. Predicted versus actual bead width

57
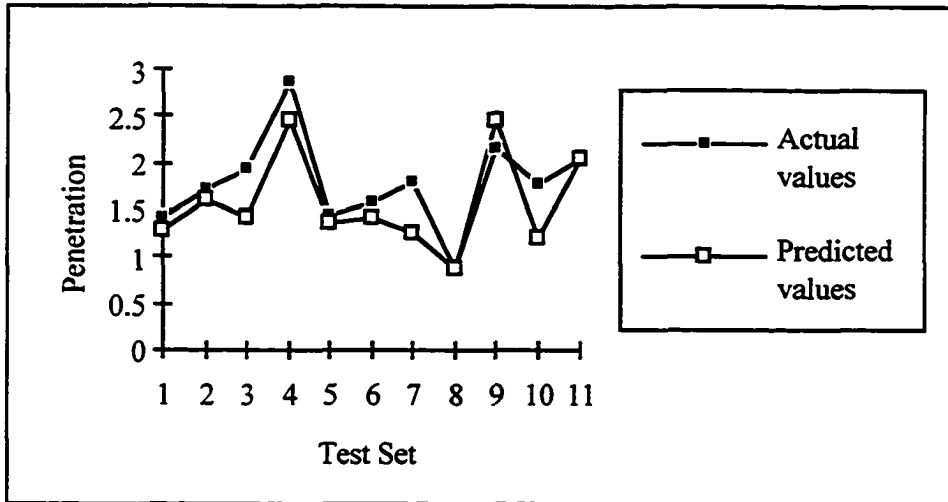
Figure 3.12. Predicted versus actual penetration
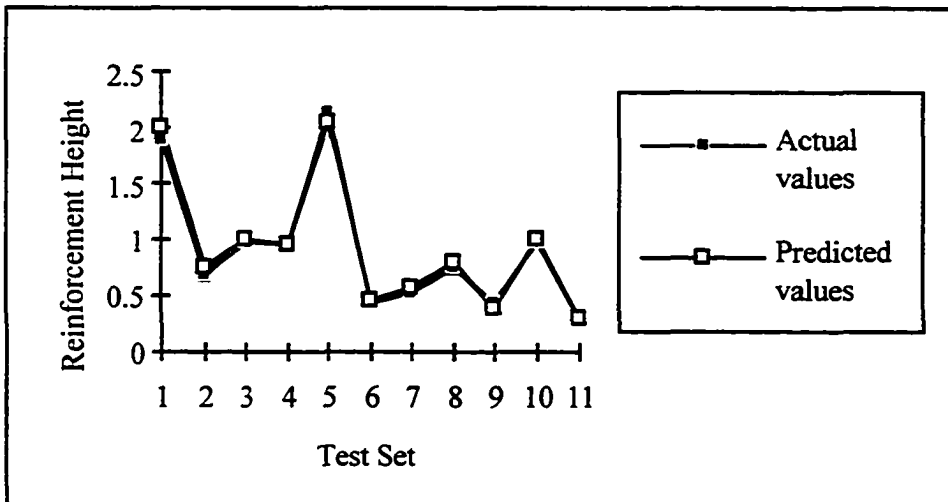
Figure 3.13. Predicted versus actual reinforcement height

58
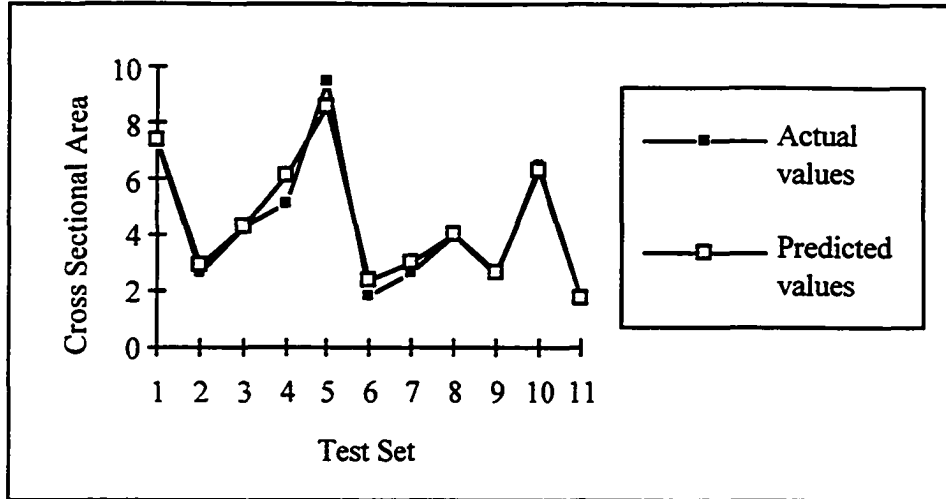
Figure 3.14. Predicted versus actual cross-sectional area

3.1.9 Statistical Analysis

A stastical analysis was conducted to compare the actual results with the neural network results for Figures 3.11-3.14. The difference in the actual and predicted values for bead width, penetration, reinforcement height and cross-sectional area were calculated. The test statistic for testing the hypotheses

$$H_0: \mu_d = 0$$

$$H_1: \mu_d \neq 0$$

is calculated by the following equation:

$$t_0 = \frac{\bar{d}}{S_d / \sqrt{n}} \tag{3.32}$$

where

$$S_d = \left[\frac{\sum\limits_{j=1}^{n} (d_j - \bar{d})^2}{n-1} \right]^{1/2} = \left[\frac{\sum\limits_{j=1}^{n} d_j^2 - \frac{1}{n} \left(\sum\limits_{j=1}^{n} d_j \right)^2}{n-1} \right]^{1/2} \tag{3.33}$$

59

If $t_{\alpha,n-1} > t_0$, the hypothesis H_0: $\mu_d = 0$ cannot be rejected since there is no evidence to indicate that the two results are different. Table 3.11 shows the t-statistic ($\alpha = 0.025$), comparing the actual reading with the predicted reading, for Figures 3.16-3.23. From Table 3.11, it is evident that there is no significant difference between the actual and predicted values for the bead width, reinforcement and cross-sectional area. However, the penetration is significant at $\alpha = 0.025$ by a small margin. This is a reasonable result since the penetration is more difficult to measure accurately.

Table 3.11. Statistical analysis for welding data in Figures 3.11-3.14

Measure	t_0	n	$t_{\alpha,n-1}$
Bead width	-0.1037	10	2.228
Penetration	-2.4980	10	2.228
Reinforcement height	1.2120	10	2.228
Area	0.8224	10	2.228

3.1.10 RTM Experiments Using Cascade Correlation Algorithm

The cascade correlation algorithm was trained with the data from Table 3.4. The inputs provided to the network were the settings of the three design variables - mold temperature, injection pressure and fiber volume - and the output was the mold filling time. The network structure after training all twenty seven examples in Table 3.4 was ten hidden units, for a total of fourteen units.

Using the data in Table 3.8, the neural network was trained to predict the mold filling time. Table 3.12 shows the results of the testing session. From a plot of actual versus

60

fitted values, see Figure 3.15, it is apparent that the neural network does a good job of predicting the mold filling times.

Table 3.12. Predicted mold filling times from CCA

Actual mold fillling time, min	Predicted mold filling time, min
0.78697	0.78058
0.66755	0.70573
0.64040	0.55990
0.61208	0.67274
0.61994	0.57922
0.74090	0.92693
0.26631	0.28612
1.11403	1.05287
0.41797	0.37362
0.70861	0.72677
1.39591	1.25667
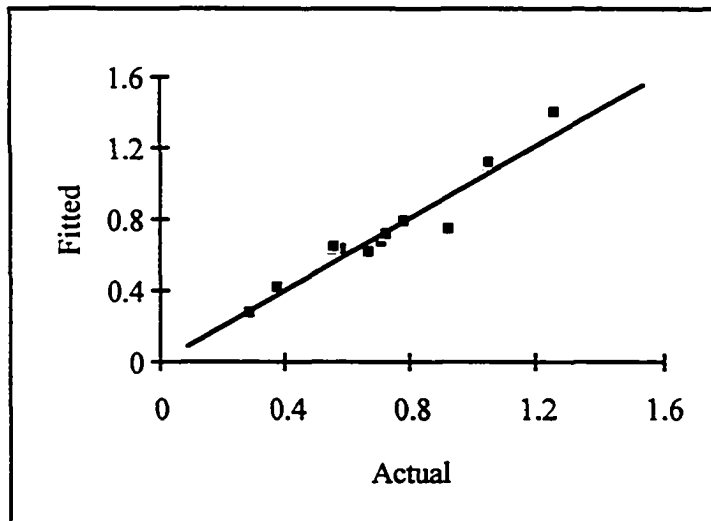
Figure 3.15. Actual versus predicted mold filling times using CCA

61

3.1.11 Conclusions

The cascade correlation was formulated for application to the resin transfer molding design optimization modeling procedure. Using data provided from simulation experiments, the cascade correlation algorithm established a relationship between the design variables - mold temperature, injection pressure and fiber volume - and the mold filling time. The results were compared with modeling efforts using regression analysis. The conclusions from this study are summarized below:

1. The CCA was able to define a relationship between the design variables and the mold filling time that was just as accurate as the regression techniques.

2. Identifying the model was significantly faster using CCA than regression analysis. In regression, a series of diagnostic checks were necessary to test the validity of the model since a high R^2 value did not necessarily mean that the model was adequate.

3.2 Process Control

3.2.1 Cure Monitoring Using CCA

RTM is a typical example of a material processing operation that is characterized by nonlinearities and interactions among process variables. Due to its complexity, the RTM process requires an efficient control procedure to maintain consistent quality of each part. The degree of cure is an important processing variable that affects the shear strength and is the focus of the process control scheme. The need for an intelligent, automated system results from the fact that the standard cure cycles recommended for a specific resin are often inadequate. Resin variations from one batch to another can cause this method of curing to produce final composite parts with widely varying properties, despite identical

62

cure schedules . This is due to the fact that the molecular state of the curing resin is ignored by a strict time/temperature curve [Kranbuehl, et al., 1994].

Using data collected on a commercial epoxy system, Tactix 123 (DOW Chemical) and Jeffamine D400 curing agent (Texaco), the information in Table 3.13 was obtained from IR spectroscopy analysis, conducted by Dara Woerdeman at NIST. The ratio was calculated by taking the ratio of the heights of the diminishing epoxide ring peak of 970 cm^{-1} to the internal standard peak of 1185 cm^{-1}. Percent monomer refers to a measure of the degree of chemical conversion, where (1 - percent monomer) equals the degree of cure from 0 to 1; 1 means that the cure is 100% complete.

The cascade correlation algorithm was trained using the data in Table C.1 and testing examples are provided in Table C.2. Both tables are found in Appendix C. Inputs to the neural network were the time and temperature information; outputs were the percent monomer, related to the degree of cure, and the ratio. The threshold was selected as 0.05 and when training was complete, the network consisted of 29 nodes total, of which 26 were hidden nodes.

Figures 3.16 and 3.17 show the results of the testing session for predicting the ratio and the % monomer, respectively. A breakdown of the IR spectroscopy ratio and percent monomer testing results by cure temperature are provided in Figures 3.18-3.20 and Figures 3.21-3.23, respectively. The accuracy of the cascade correlation was better in predicting the IR spectroscopy ratios. In Figure 3.21, there is a significant difference between the actual and predicted % monomer at 99.5 seconds. This is believed to be a suspect data point since there is the possibility of human error in collecting IR data.

63

Table 3.13. Actual versus predicted IR data using CCA

Temperature	Time	Actual % Monomer	Predicted % Monomer	Actual Ratio	Predicted Ratio
50	16.5	0.1288	0.13845	0.984	0.99339
50	49.75	0.1221	0.1063	0.932	0.95965
50	99.5	0.1068	0.06295	0.816	0.69431
50	149.25	0.0848	0.08469	0.647	0.64025
50	199.25	0.0616	0.06186	0.47	0.50809
50	249	0.0464	0.04226	0.354	0.34846
50	288.75	0.0333	0.03716	0.254	0.2673
50	313.5	0.0289	0.03246	0.221	0.21313
50	348.5	0.0238	0.02675	0.181	0.15037
60	10.5	0.1195	0.11067	0.979	0.98233
60	21	0.1158	0.11528	0.948	0.97343
60	42.25	0.1057	0.10389	0.865	0.89421
60	74.25	0.0829	0.07684	0.678	0.70105
60	84.75	0.0766	0.06598	0.627	0.5849
60	106	0.0598	0.05792	0.489	0.4831
60	137.75	0.043	0.0433	0.352	0.33509
60	169.5	0.0277	0.03375	0.227	0.22894
60	180.25	0.024	0.03141	0.196	0.20232
80	19.75	0.0896	0.08935	0.724	0.71009
80	26.25	0.0759	0.06913	0.614	0.56771
80	39.25	0.0468	0.03922	0.378	0.39252
80	46	0.0366	0.02771	0.296	0.29241
80	59.25	0.0234	0.02659	0.19	0.19479
80	79	0.0112	0.01132	0.091	0.08088
80	98.75	0.0064	0.00986	0.052	0.05019
80	118.5	0.0035	0.00894	0.028	0.03646
80	128.5	0.0033	0.00718	0.027	0.02623

64
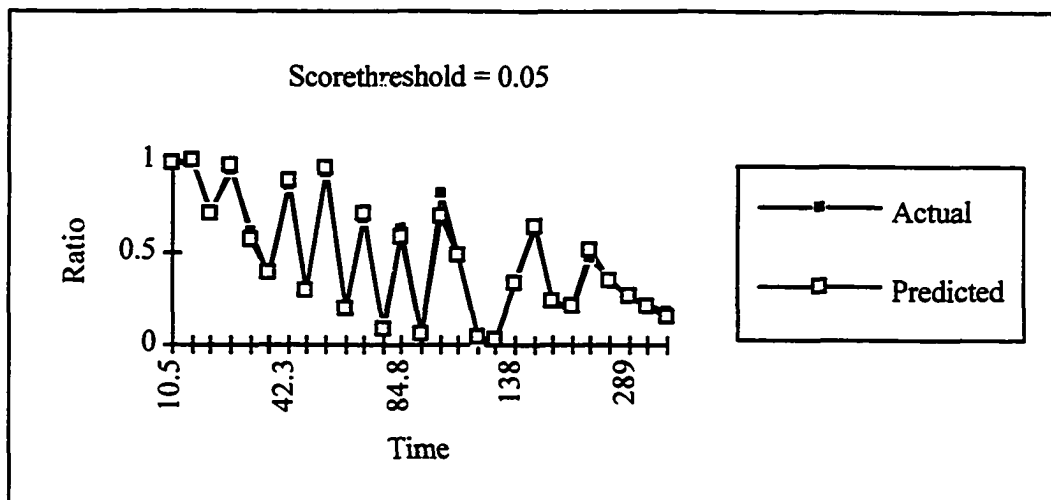
Figure 3.16. Actual versus predicted IR spectroscopy ratio using CCA
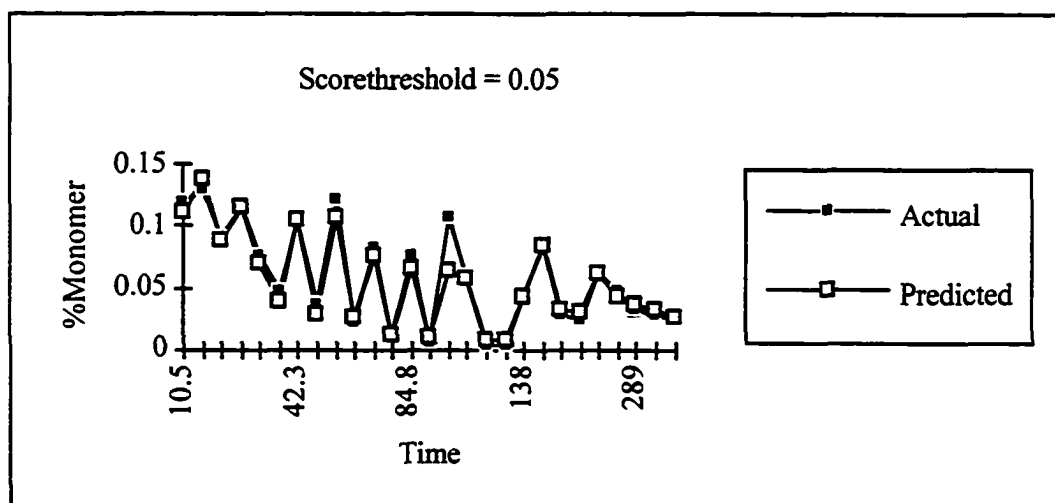
Figure 3.17. Actual versus predicted degree of cure using CCA

65
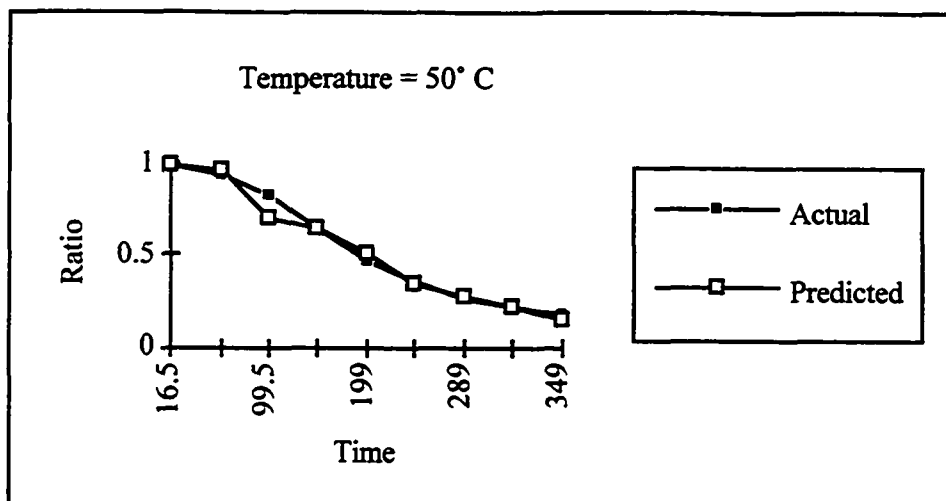
Figure 3.18. Actual versus predicted IR spectroscopy ratio at 50° C
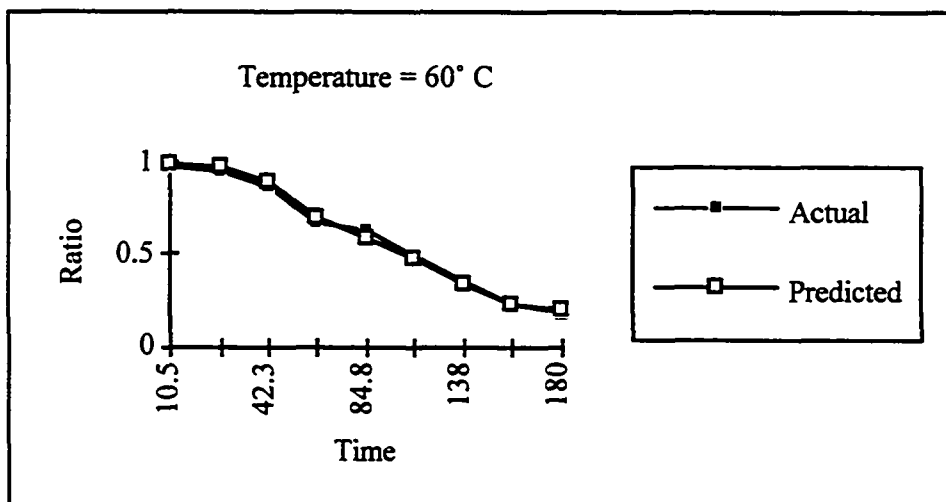
Figure 3.19. Actual versus predicted IR spectroscopy ratio at 60° C

66
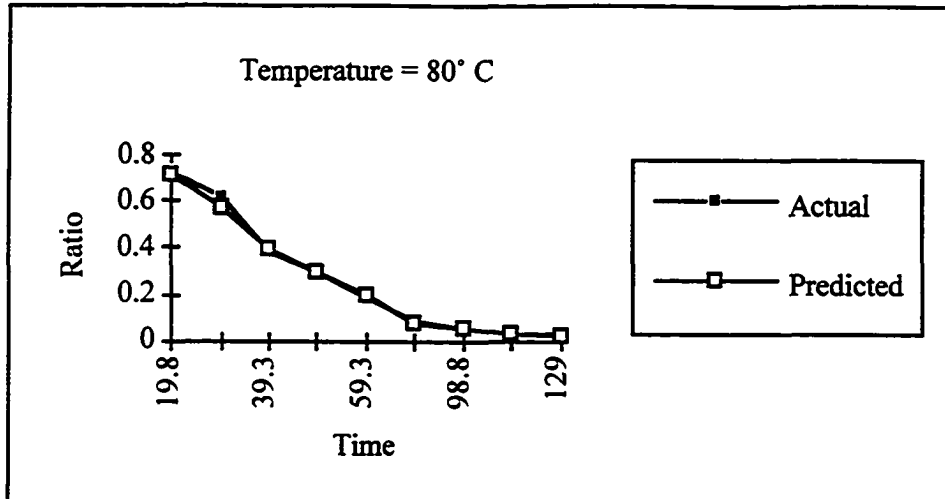
Figure 3.20. Actual versus predicted IR spectroscopy ratio at 80° C
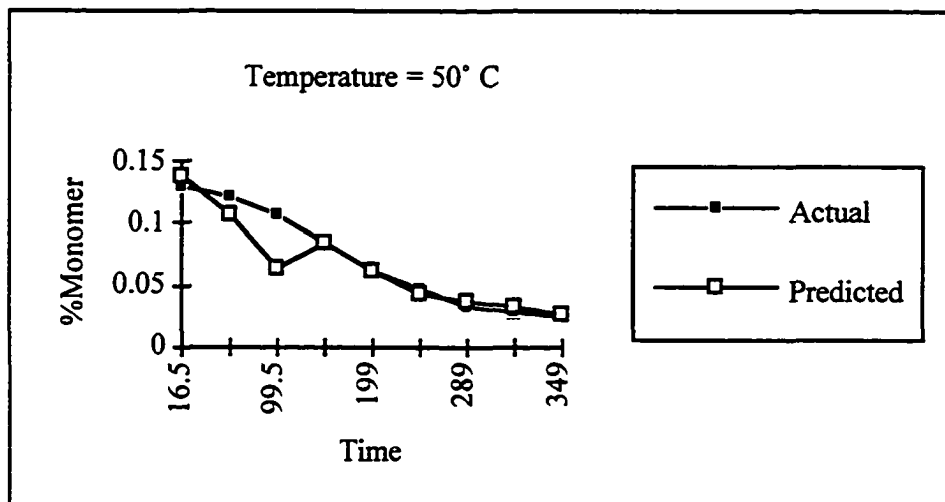
Figure 3.21. Actual versus predicted degree of cure at 50° C

67
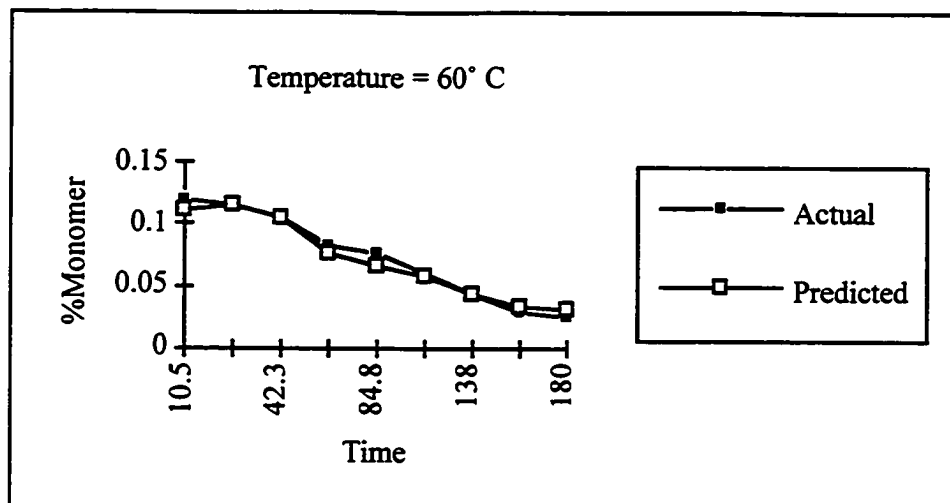
Figure 3.22. Actual versus predicted degree of cure at 60° C
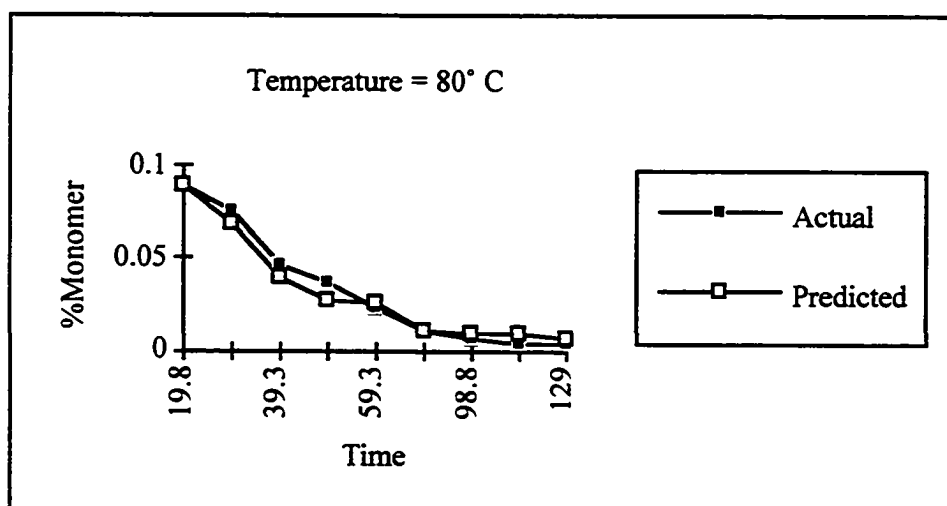
Figure 3.23. Actual versus predicted degree of cure at 80° C

68

3.2.2 Statistical Analysis

A stastical analysis was conducted to compare the actual results with the neural network results for Figures 3.16-3.23. Table 3.14 shows the t-statistic ($\alpha = 0.025$), comparing the actual reading with the predicted reading, for Figures 3.16-3.23. From Table 3.14, it is apparent that there is no significant difference between the actual and predicted ratios. A similar conclusion is drawn for the percent monomer completed.

Table 3.14. Statistical analysis for cure data in Figures 3.16-3.23

Figure	t_0	n	$t_{\alpha,n-1}$
3.16	0.6687	27	2.056
3.17	1.2584	27	2.056
3.18	0.5977	9	2.306
3.19	-0.3583	9	2.306
3.20	0.9192	9	2.306
3.21	0.8958	9	2.306
3.22	0.8719	9	2.306
3.23	0.4475	9	2.306

3.2.3 Conclusions

The cascade correlation algorithm was tested for its suitability in predicting the degree of cure during processing of a resin transfer molded part. IR spectroscopy data was collected from a commercial resin system and used for analyzing CCA as a cure monitoring tool. Inputs to the network included cure temperature and cure time, while

69

outputs from the network were the percent monomer, related to the degree of cure, and the ratio of the heights of the diminishing epoxide ring peak of 970 cm^{-1} to the internal standard peak of 1185 cm^{-1}. Two conclusions were a result of this study.

1. CCA was able to provide accurate prediction of both the percent monomer and the ratio given inputs of the cure time and cure temperature.

2. CCA has the potential to become a useful tool in predicting the degree of cure during the cure stage in resin transfer molding.

In the future, wavelength data from evanescent wave sensing will be utilized in the cascade correlation algorithm to determine the degree of cure for the purpose of intelligent process control of the cure stage. At this time, however, the wavelenth data is not available.

3.3 Summary of Research Investigations

In summary, conclusions drawn from the research investigations are:

- The cascade correlation algorithm was found to be a suitable replacement for regression analysis in the efficiency and accuracy of modeling. From preliminary studies, the CCA neural network model required less development time and guesswork in design optimization modeling for resin transfer molding.

- In process monitoring, the CCA was analyzed for its suitability in predicting the degree of cure at varying stages throughout the resin transfer molding process. Given the cure time and cure temperature, CCA was able to predict the cure percentage accurately and efficiently.

70

CHAPTER 4

METHODOLOGY

4.1 Background

One of the objectives of this research, as mentioned in the first chapter, is to determine the correlation between a select number of product and process design variables, and specific quality and performance measures. The product and process design variables of interest are mold preheat temperature, mold outlet pressure, driving pressure, fiber volume and fiber architecture. Quality measures include the void content and interlaminar shear strength within the final part, while the mold filling time is the performance measure.

In composites manufacturing, nonlinearities exist in the resin cure kinetics, the formation of residual porosity and the development of the fiber/resin interfacial region. It is expected that these physical nonlinearities will interact strongly with the processing parameters. For example, injection rate, injection pressure and temperature cycle control, to some degree, determine the resin cure and the degree of porosity in the part. In addition, it is possible that interactions of the processing variables are also significant. In light of the presence of nonlinearities in the process, an alternative to traditional regression techniques was desired for establishing the relationship between the design variables and the response variables. In chapter 3, the cascade correlation algorithm was found to be a good tool for modeling those relationships.

71

4.2 Genetic Algorithms

The use of genetic algorithms in this project is possible due to the work done previously by Lin [1994], which involved the application of genetic algorithms to mechanical tolerancing problems.

4.2.1 Advantages

Genetic algorithms have drawn much attention in solving a wide range of optimization problems with their ease of understanding and implementation [Goldberg, 1989]. GAs are search procedures based on the mechanics of natural genetics and natural selection. In addition, GAs are different from traditional search methods in the following ways: 1) they work with a coding of the design variables as opposed to the variables themselves -- continuity of parameter space is not a requirement; 2) they search from a population of points, not a single point -- parallel processing of points reduces the chance of trapping into a local optima; 3) they use probabilistic transition rules, not deterministic transition rules -- leads to high quality solutions; 4) they require only the objective function values -- minimal requirements broaden GA's application.

4.2.2 GA schematic

Figure 4.1 [Lin, 1994] displays a schematic of the genetic algorithm. An initial population is generated randomly and encoded as a bit-string representation. Each member of the population is evaluated based on their fitness, determined by the value of the defining function; i.e., the inputs into the genetic algorithm are n population members and the outputs from the genetic algorithm are n fitness functions corresponding to each member of the population. GA operators are performed on the most "fit" members of the population to form a new generation. A set of parameters, such as mutation and crossover probabilities, are defined by the users.

72
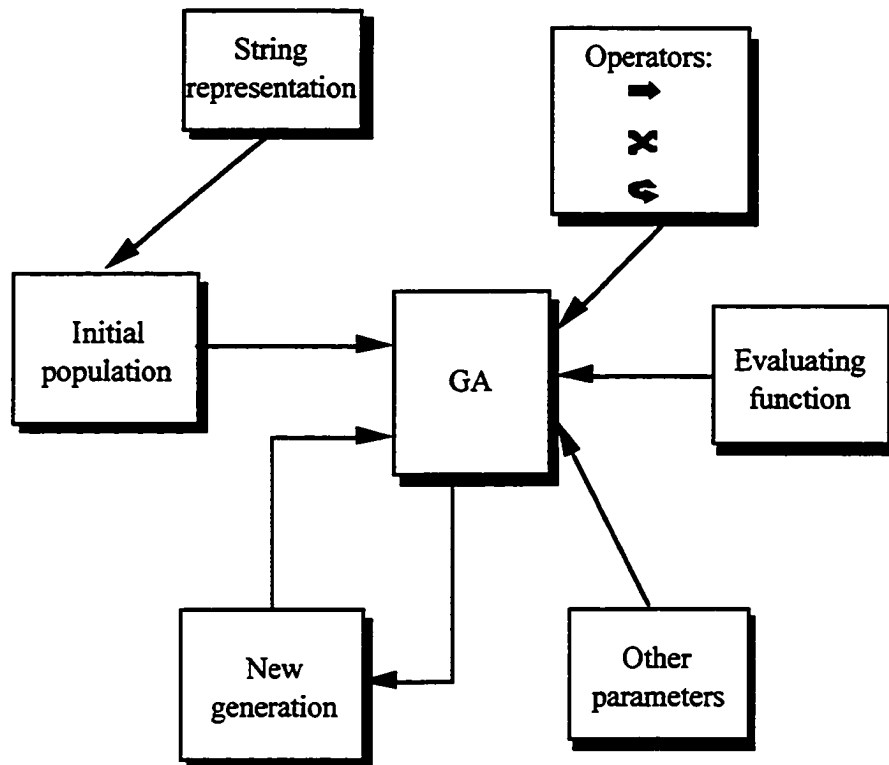
Figure 4 .1. Schematic of the genetic algorithm

4.2.3 GA components

There are three basic components necessary for the successful implementation of a genetic algorithm. Initially, there must be a code or scheme that allows for a bit string representation of possible solutions to the problem. Next, a suitable function must be devised that allows for a ranking or fitness assessment of any solution. The final, and perhaps most important components, are the transformation functions that mimic the biological evolution process when applied to a population of chromosomal representations of solutions to the problem. Once a population of solutions is generated,

73

the genetic search can proceed to produce new solutions with a higher level of fitness than members of the current population. The search steps are repeated for successive generations of the population, until no further improvement in the fitness is attainable. The member in this generation with the highest level of fitness is the optimal solution.

4.2.3.1 Variable representation

Integer, discrete and real values are accommodated by the genetic algorithm coding and decoding scheme. Integer variables involve direct binary encoding and decoding, while real variables necessitate that a numerical operation be performed. Discrete variables are represented by a one-to-one variable mapping scheme. An example of each of the bit string representations is provided below:

- Integer: direct binary encoding and decoding

$$1\ 1\ 1\ 0\ 1\ 0_2 = 58_{10}$$

- Discrete: variable mapping scheme

0	1	2	3	4	5...
1/16	3/16	4/16	7/16	8/16	10/16...

- Real: numerical operation

$$X \frac{U-L}{2^m - 1} + L; \quad 2^m \geq \frac{U-L}{A_c} + 1$$

U: upper bound

L: lower bound

m: chromosome length

A_c: desired accuracy

X: decoded integer

74

4.2.3.2 Fitness evaluation

Each of the population members are evaluated by their corresponding function values. For example, suppose the objective is to minimize $f(x) = x^2$, given a set of constraints. The member that has the highest value of $f(x)$, without violating any of the constraints, will be selected as a member for the next population.

4.2.3.3 GA operators

The GA operators, reproduction, crossover and mutation, play an active role in defining the new population members in each iteration of the genetic algorithm. Reproduction involves copying one string from the previous population into the next generation. This operation is performed on the current population members with the highest fitness value. In the crossover operation, two solutions exchange parts of their string to form two new solutions. A crossover location and crossover probability must be specified for this operator. The final operator, mutation, randomly selects a specific bit and changes its value, given a probability of mutation. An example of each of the three GA operators is given as the following:

- Reproduction:

  1 0 0 1 1 0 1   →   1 0 0 1 1 0 1

- Crossover:

  1 0 0 * 1 1 0 1   →   1 0 0 0 1 1 0

  0 1 1 * 0 1 1 0   →   0 1 1 1 1 0 1

  (* = crossover location)

- Mutation:

  1 0 0* 1 1 0 1   →   1 0 1 1 1 0 1

  (* = mutation site)

75

4.3 Mathematical Model for Design Optimization

4.3.1 Notations

This section defines the notations used in the product and process design optimization model:

v_c = void content, % by volume

v_r = void content, % by volume

P_d = driving pressure, psi

P_{d_u} = upper limit on driving pressure, psi

P_{d_l} = lower limit on driving pressure, psi

P_o = outlet pressure, psi

P_{o_u} = upper limit on driving pressure, psi

P_{o_l} = lower limit on driving pressure, psi

F = fiber volume

T = mold temperature, °F

T_l = lower limit on temperature, °F

T_u = upper limit on temperature, °F

t = mold filling time, min

S_H = shear strength of part, N/m^2

S_{H_r} = minimum allowable shear strength of part, N/m^2

4.3.2 Constraints

Constraints exist in any system, which is why it is important to accurately recognize, formulate and satisfy all necessary constraints. In the RTM design optimization problem, three categories of constraints are imposed: process constraints, quality constraints and part characteristic constraints.

76

4.3.2.1 Process constraints

The process constraints considered in RTM design optimization are described below:

• Driving pressure

$$P_{d_l} \leq P \leq P_{d_u} \qquad (4.1)$$

An upper limit on the driving pressure is necessary since, if the pressure is too high, displacement of the aligned fibers will occur; this phenomenon is known as "fiber wash" and has a detrimental impact on the strength of the finished part. A lower limit must be satisfied or the resin may not completely fill the part before curing initiates.

• Outlet pressure

$$P_{o_l} \leq P \leq P_{o_u} \qquad (4.2)$$

An upper limit on the outlet pressure is important. If the outlet pressure is higher than the inlet pressure, as derived from the driving pressure, the resin will flow backwards in the mold. However, if the outlet pressure is too low, it will increase the driving pressure to a point where excessive fiber wash or air entrapment may occur.

• Mold temperature

$$T_l \leq T \leq T_u \qquad (4.3)$$

A second constraint sets the lower and upper limits for the mold temperature. There is an optimal range for the temperature at which the resin has sufficient flow during the mold filling stage, yet premature resin cure is inhibited.

4.3.2.2 Quality constraints

• Void percentage

77

The following constraint defines the maximum void percentage that is acceptable in the final part:

$$v_c \leq v_r \qquad (4.4)$$

The above constraints ensure that the quality of the part is adequate in regard to the size and frequency of voids. Voiding affects the strength of the part due to areas of insufficient resin impregnation in the fiber matrix. In the long term, the life of the part is reduced since void regions are more susceptible to fatigue failure.

4.3.2.3 Part characteristic constraints

• Part strength

The following constraint ensures that the interlaminar shear strength of the part is maintained at an acceptable level:

$$S_H \geq S_{H_r} \qquad (4.5)$$

4.3.3 Objective Functions

There are three objectives in the RTM design optimization model: (1) minimization of the mold fillling time, (2) minimization of the void content and (3) maximization of the interlaminar shear strength of the part

• Minimization of the mold filling time

The minimization of the mold filling time is a function of the fiber architecture, driving pressure, outlet pressure and mold temperature. For example, it is expected that the mold filling time will decrease as the driving pressure increases. The mold temperature affects the viscosity of the resin; therefore, for higher mold temperatures the filling time is reduced.

$$Min\ t = f_1(F, P_d, P_o, T) \qquad (4.6)$$

78

• Minimization of the void content

Driving and outlet pressures are the major variables that affect the void content within the part.

$$Min\ v_c\ =\ f_3(P_d, P_o) \qquad (4.7)$$

• Maximization of the part strength

The strength of the part is determined, most obviously, by the type of resin and fiber used. If the resin and fiber are compatible, such that good adhesion and wetting occurs, the mechanical properties of the finished part are enhanced. In addition to the resin and fiber, the fiber architecture is expected to have an impact on the overall strength. Driving and outlet pressures, and mold temperature have a combined effect on the strength since these parameters determine the wetting of the fibers and the final macrostructure of the part.

$$Max\ S_H\ =\ f_3(F, P_d, P_o, T) \qquad (4.8)$$

4.3.4 General Model

The task is to optimize the three objective functions, mold filling time (t), void vontent (v_c) and part strength (S_H), subject to the constraints of driving pressure, outlet pressure and mold temperature. The design optimization problem is formulated mathematicallly as follows:

$$Min\ t,\ v_c$$
$$Max\ S_H$$

Subject to:

$$P_{d_l} \leq P \leq P_{d_u}$$
$$P_{o_l} \leq P \leq P_{o_u}$$
$$T_l \leq T \leq T_u$$
$$v_c \leq v_r$$
$$S_H \geq S_{H_r}$$

79

The solution of the above equations will provide an optimal product and process design that results in efficient and robust manufacturing, and that produces parts of consistently high quality. Thus, an integrated product and process design approach is used for enhancing the resin transfer molding process.

4.4 Solution Procedure

The cascade correlation algorithm is integrated into the genetic algorithm, as shown pictorially in Figure 4.2. Beginning with a set of experiments, the quality and performance measures are obtained by one of two methods: the actual resin transfer molding process or a simulation model of the process. When using the simulation model, however, it is imperative that it is validated by the actual process to ensure that the simulation provides accurate results.

Once the results are obtained, the next step is optimization using the GA-CCA system. A more detailed picture of the GA-CCA system is provided in Figure 4.3. Design variables $[x_1, x_2, x_3, x_4]$ are used to generate the initial population members. The cascade correlation algorithm provides the objective function values for each population member based on experience provided by previous training of the network. Using this fitness information, the genetic algorithm will select the members that will continue into the next generation. Once again, the new members are evaluated by their fitness; the process repeats for the maximum number of generations or until a suitable solution is found.

4.4.1 Design Optimization Using GA-CCA System

Utilizing the data in Table 3.4, the cascade correlation algorithm was trained and the weights saved into a file. The weights are then used in the GA-CCA system to determine the objective function value for each population member. A maximum of fifty generations

80

was selected and the mold filling time is minimized with respect to the mold temperature, injection pressure and fiber volume. Table 4.1 shows the optimization results using the integrated GA-CCA system and Table 4.2 provides the optimum settings using the regression model as the GA objective function value.

4.5 Intelligent Process Control

Due to the presence of system nonlinearities and complexities, the RTM process requires an efficient control procedure to maintain consistent quality of each part. The need for an intelligent, automated system results from the fact that the standard cure cycles recommended for a specific resin are often inadequate. Resin variations from one batch to another can cause this method of curing to produce final composite part with widely varying properties, despite identical cure schedules. Figure 4.4 outlines the intelligent process control scheme. This work is proposed for future study, but is included in this manuscript as an important step beyond optimization.

81
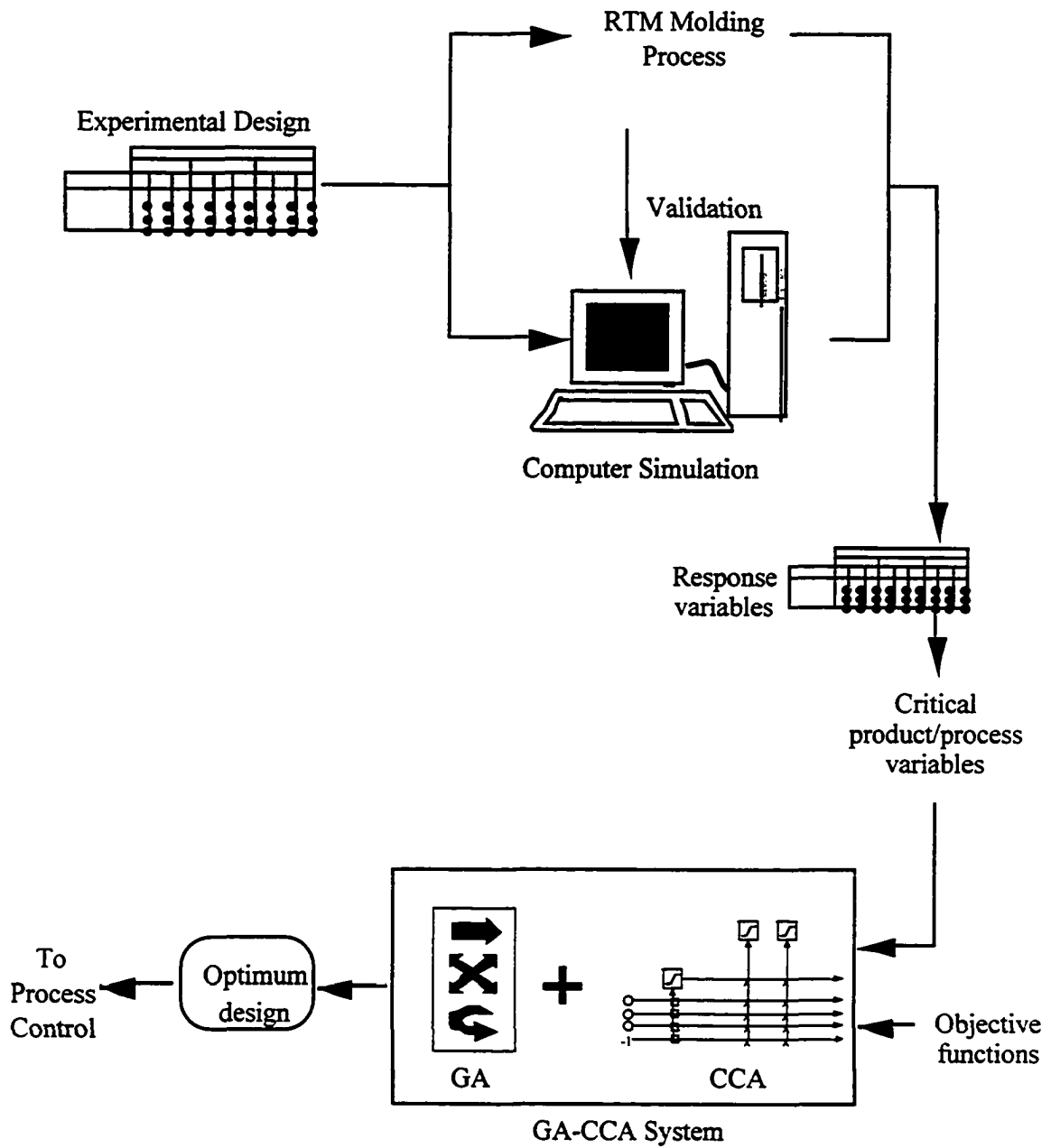
Figure 4.2. Integrated product and process design optimization scheme

82
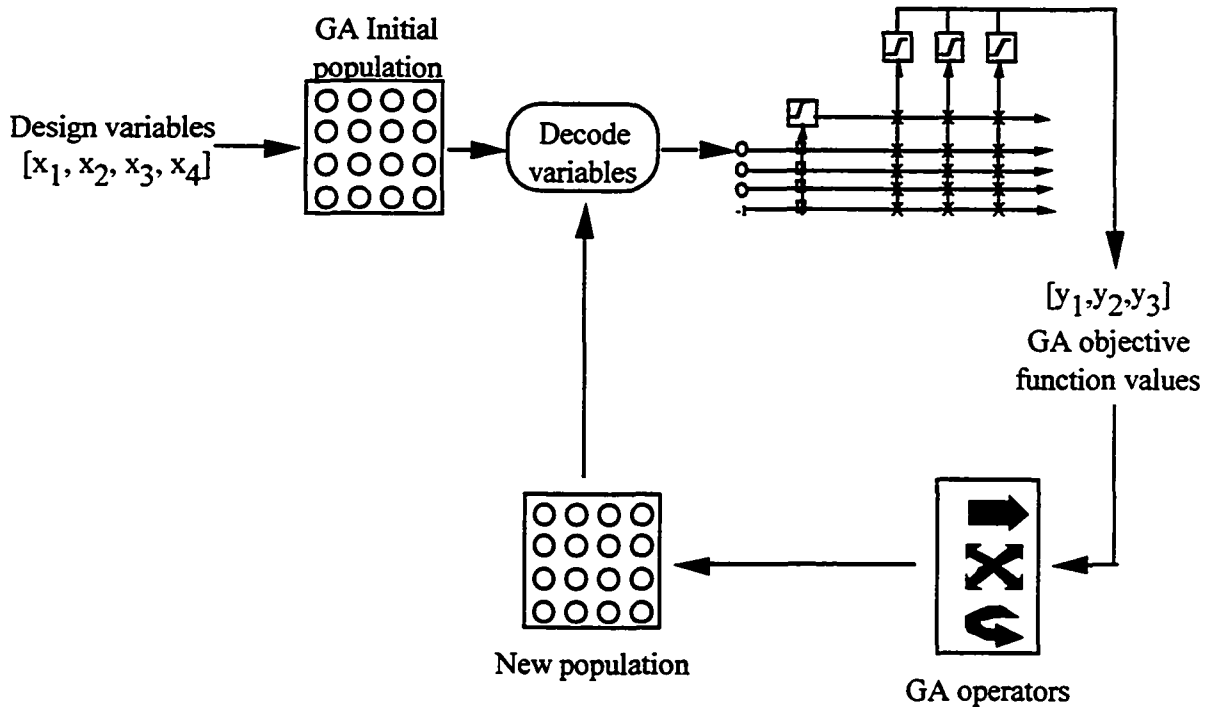
Figure 4.3. GA-CCA system

Table 4.1. Optimization results for mold filling time using GA-CCA system

Mold temperature, °C	Injection pressure, psi	Fiber volume, % by weight	Mold filling time, min
171	· 127	46	0.1773

Table 4.2. Optimization results for mold filling time using regression

Mold temperature, °C	Injection pressure, psi	Fiber volume, % by weight	Mold filling time, min
171	125	45.5	0.1908

83
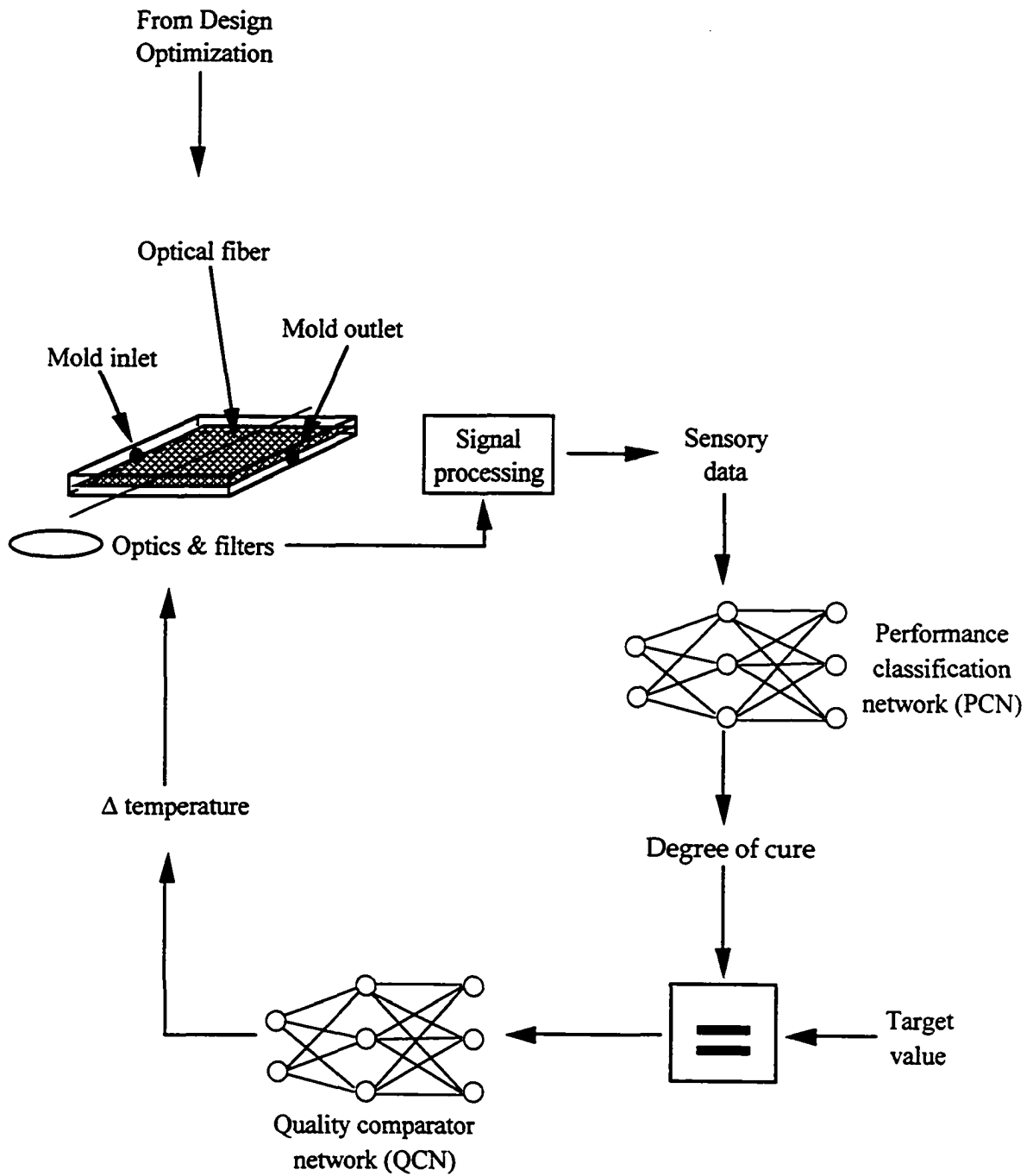
Figure 4.4. Process control scheme

4.6 Process Modeling and Simulation

The manufacturing of large fiber-reinforced composites by resin transfer molding has lacked a firm science basis. At present, much of the tooling, preform design and process development for a new RTM part is determined through trial and error. Currently, research is underway to develop a mathematical model that can describe the flow behavior of resins through various molding tools loaded with different preform architectures, and that can characterize the physical and chemical change that occur during the process.

The RTM process has three phases: resin flow, heat transfer, and cure reaction. These phases can be modeled and simulated utilizing numerical techniques. The development of a simulation model can provide the following results:

(1) An adequate positioning of the injection ports and air vents to ensure complete filling of the mold without entrapping air.

(2) A clear picture of the physics and chemistry involved in RTM before carrying out the physical processing. This is central to the mold and process design.

(3) Through simulation, the effect of different combinations of variables on the quality and process performance can be evaluated, generating adatabase for intelligent control.

4.6.1 Process Modeling

In order to generate a complete and effective model of the resin transfer molding process, the simulation should incorporate all three phases: resin flow, heat transfer and cure reaction. Appendix D provides more detail on the equations used for modeling these phases.

85

4.6.2 Simulation

A simulation model was developed by graduate students, Zhang and Wu. The model includes the resin flow and heat transfer phases of resin transfer molding. Validation of the resin flow phase was performed utilizing data provided by Brunswick Defense.

4.6.2.1 Numerical Solution of RTM Process Models

A finite difference analysis (FDA) method is employed to solve the RTM process models. Control volume and boundary element techniques have been investigated and are being utilized in the RTM simulation procedure.

An important issue in the simulation of the mold filling process is the numerical treatment of the moving boundary. Since the resin is continually changing shape as it advances within the mold, the geometry of the resin-saturated region is defined several times during the analysis. The fixed grid approach is being utilized for meshing. The governing equation for the pressure is solved using a finite difference method and the flow front is advanced using a control volume technique. A sample output from the RTM process simulation, resin flow stage, is shown in Figure 4.5.

Since resin transfer molding involves such a large number of variables, there is a significant number of combinations that exist which cannot feasibly be handled through experimentation. However, by verifying the simulation model based on experimental data over a broad range of part geometries and resin and fiber systems, an unlimited number of combinations can be selected without a significant amount of time, cost and material waste. Through the concurrent knowledge of the process and materials, a representative and flexible simulation of resin transfer molding can be developed. The simulation model was used to: 1) identify the effects of changes in product and process design variables on the mold filling time; 2) compare the results of regression and neural network techniques in establishing a model for mold filling time.

86
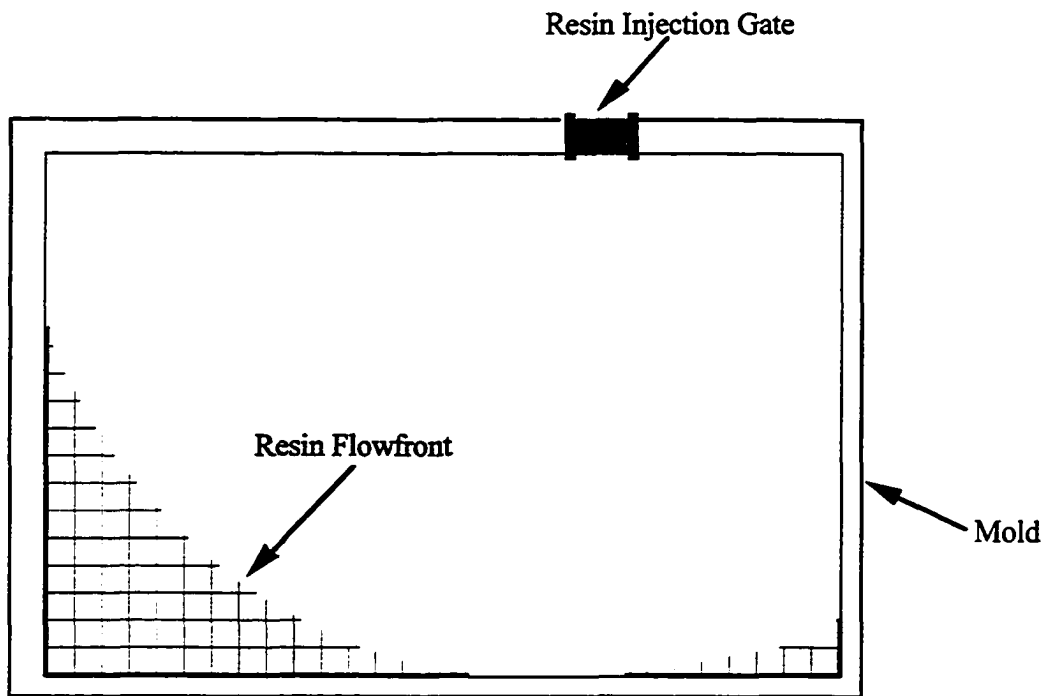
Figure 4.5. Resin flow simulation output

4.6.2.2 Validation of Simulation Model

Validation of the simulation model is vital to assure its useful application to the real RTM process. The flow model was validated in terms of the mold filling time. For a 20" x 20" flat, rectangular part, the filling time was estimated to be less than five minutes. This data was obtained from an RTM engineer at Brunswick Defense. After running the simulated version of the flow stage, mold filling times were approximately four minutes, which was in agreement with the information provided by the actual process.

87

CHAPTER 5

INTEGRATED PRODUCT AND PROCESS DESIGN OPTIMIZATION
AN EXAMPLE IN RESIN TRANSFER MOLDING

5.1 Introduction

An integrated product and process design optimization problem in resin transfer molding using the GA-CCA system, described in Chapter 4, is illustrated in this chapter. The experimental design is introduced and the results of experimentation are provided.

5.2 Experimental Design

The experimental design procedure in this study utilizes a central composite design due to its efficiency; i.e, the maximum number of levels for each factor are investigated with a limited number of experiments. The total number of experiments conducted was nineteen. Table 5.1 describes the settings for each factor in the complete set of experiments.

5.3 Experimental Procedure

5.3.1 Experimental Setup

A rectangular mold of dimensions 13.97 x 15.27 x 0.98 cm was used in this study. The reinforcement was a unidirectional fiberglass material, Knytex D155, with the fibers

88

aligned perpendicular to the direction of resin flow. Figure 5.1 shows a sketch of the mold

Table 5.1. Experimental design in resin transfer molding process

Expmt #	Cure temperature, ° C	Outlet pressure, psi	Driving pressure, psi	Fiber volume, % by weight
1	70	-9	14	22
2	110	-9	14	24
3	70	-3	14	24
4	110	-3	14	22
5	70	-9	27	24
6	110	-9	27	22
7	70	-3	27	22
8	110	-3	27	24
9	130	-6	20	23
10	50	-6	20	23
11	90	0	20	23
12	90	-12	20	23
13	90	-6	34	23
14	90	-6	6	23
15	90	-6	20	25
16	90	-6	20	21
17	90	-6	20	23
18	90	-6	20	23
19	90	-6	20	23

components in the experiment. The resin injection inlet was located at the center of one end of the mold and venting took place at the opposite end of the mold at the outlet. Since the fiberglass layers did not completely cover the area of the mold, a sealant was used to hold the layers intact and to prevent an "edge effect" from occurring. The resin system,

89

Tactix 123 (Dow) with Jeffamine D400 (Texaco) curing agent, was selected due to its common use and wide range of applications in commercial products. Since there was no reinforcement in a small region immediately beyond the injection inlet, this allowed for uniform flow of the resin; in essence, the injection gate ran the entire width of the mold.

Pressure transducers were located at both the inlet and outlet of the mold to monitor the pressures at each location. RTD's positioned at the bottom and top of the mold collected temperature data. Prior to its injection into the mold, the resin was degassed for approximately ten minutes. A small piece of glass tubing was inserted immediately after the mold outlet to track the mold filling time for each part.

Figure 5.2 shows a detailed sketch of the experimental setup.
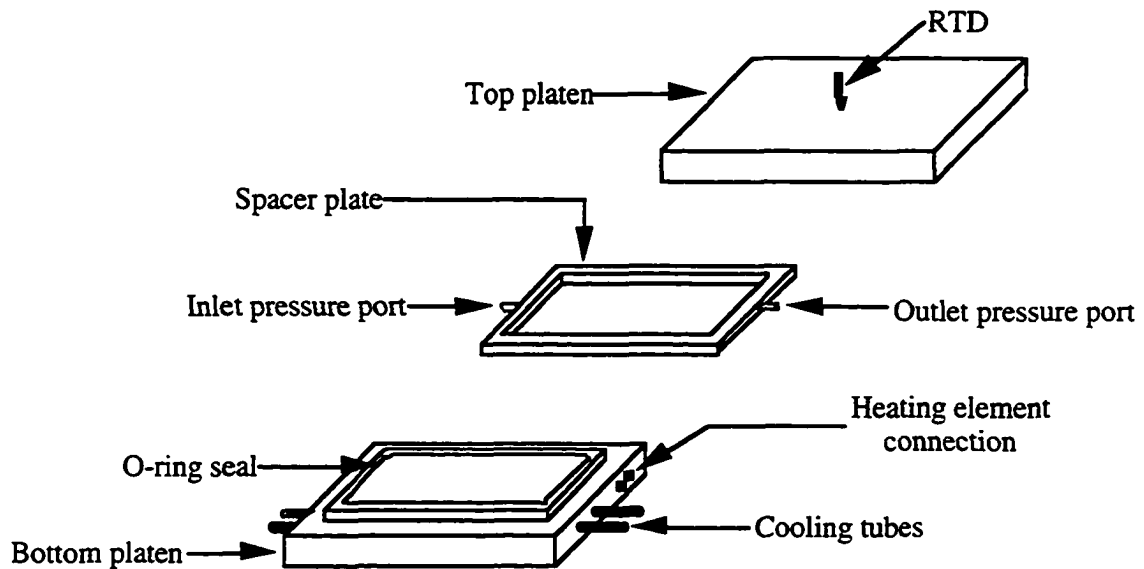
Figure 5.1. Mold components in resin transfer molding
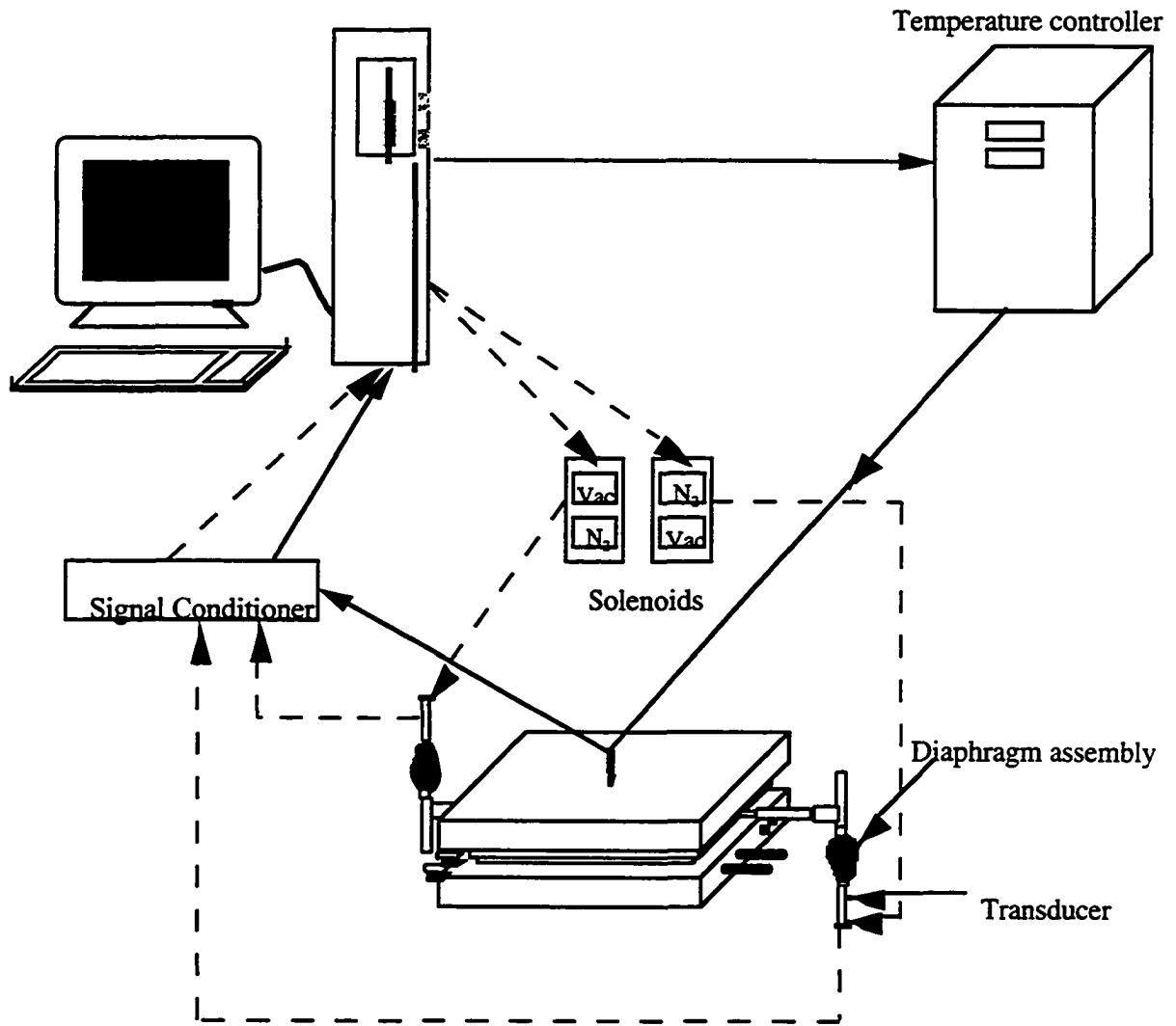
Figure 5.2. Experimental setup in resin transfer molding

5.3.2 Specimen Description

Figure 5.3 shows the layout of a typical laminate fabricated with the fibers oriented perpendicular to the flow direction. Specimens 1 through 12 were used for interlaminar shear testing, specimens A1 through A12 and B1 through B12 were utilized in determining the void content. The width of each specimen was cut to the same dimension

91

as the thickness, which was approximately 9.25 mm. The length of specimens 1 through 12 were approximately 88.9 mm. and were cut from the center of the laminate. Specimens A1 through A12 and B1 through B12 were used only in determining the void content; therefore, there was no designation regarding the length of these sections.

Outlet

A12	12	B12
A11	11	. B11
A10	10	B10
A9	9	B9
A8	8	B8
A7	7	B7
A6	6	B6
A5	5	B5
A4	4	B4
A3	3	B3
A2	2	B2
A1	1	B1

9.25 mm

|◄────── 88.9 mm ──────►|

Inlet
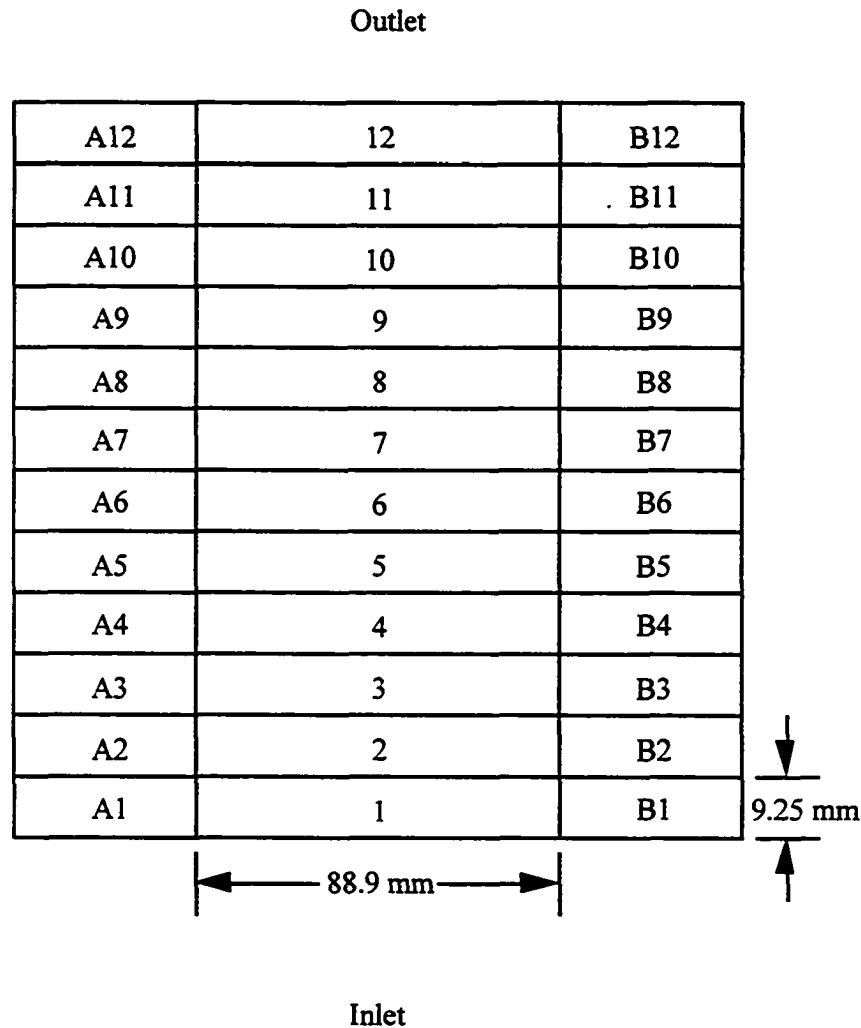
Figure 5.3. Specimen layout for a typical laminate

92

5.3.3 Composite Density

Density measurements of the composite samples were made through weight and volumetric measurements. Figure 5.4 depicts the location of each of the 12 measurements made on each specimen in determining the volume. Appendix E lists all 12 measurements for each specimen, as well as their weights. Referring to Figure 5.4, the volume of each specimen was calculated by the following equations:

length = (measurement 7 + measurement 8 + measurement 9 + measurement 10)/4   (5.1)

width = (measurement5 + measurement 6 + measurement 11 + measurement 12)/4   (5.2)

height = (measurement1 + measurement 2 + measurement 3 + measurement 4)/4   (5.3)

$$\text{volume} = \text{length} * \text{width} * \text{height, cm}^3 \qquad (5.4)$$

A density measurement was determined for each specimen in the laminate. For the density measurements, the following calculation was used:

$$\text{density} = \text{mass/volume, g/cm}^3 \qquad (5.5)$$
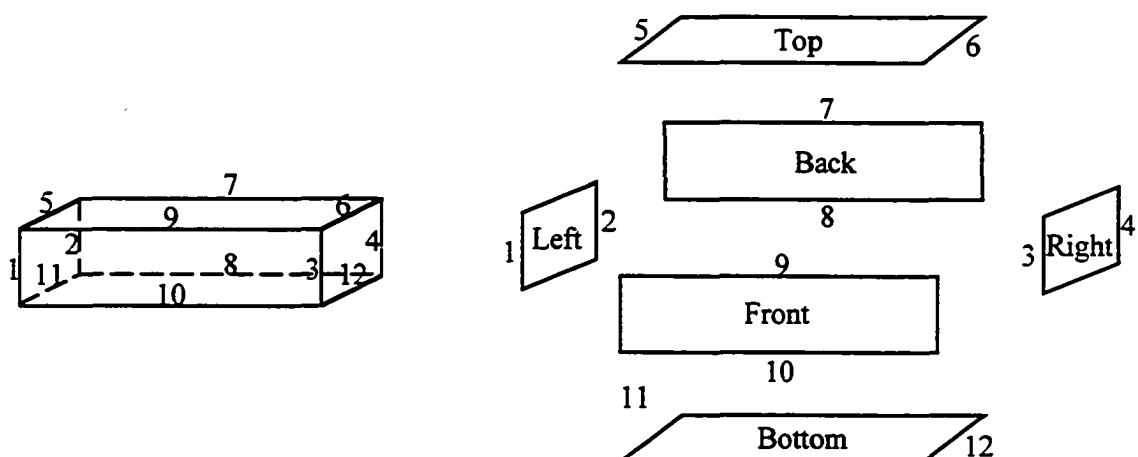
Figure 5.4. Measurements taken on each specimen for calculating volume

93

Table 5.2. Average calculated densities

Experiment #	Average density, g/cm^3
1	2.0177
2	2.0028
3	1.7557
4	1.9355
5	2.0382
6	1.9404
7	2.0341
8	2.0013
9	1.9121
10	1.9507
11	1.9389
12	1.8943
13	1.9161
14	1.9005
15	1.9558
16	1.8761
17	1.9414
18	1.9198
19	1.9659

5.3.4 Fiber Content

For each experiment, the fiber layers were weighed. Since each layer was cut to a final dimension of 13.97 x 15.24 cm (5.5 x 6 in), the area of the fiber was 212.9028 cm^2 (33 in^2). Knowing these measurements, an areal density was calculated by the following equation:

$$\text{areal density} = (\text{total fiber mass/\# layers})/212.9028, \text{g/cm}^2 \qquad (5.6)$$

94

To determine the fiber mass in each specimen, the following equation was used:

$$\text{fiber mass} = (\text{area of specimen})(\text{areal density})(\#\text{layers}), \text{g} \qquad (5.7)$$

Finally, the fiber content for each specimen is determined by:

$$\text{fiber content} = (\text{fiber mass})/\text{total mass} * 100\%, \text{g} \qquad (5.8)$$

5.3.5 Void Content

Void content of the composite specimens was calculated from the values obtained by measuring the fiber content and density values. The average void content for each experimental part is provided in Table 5.3. In calculating the void content, the following formula was used:

$$v_c = 1 - d_c\left(\frac{w_f}{d_f} + \frac{w_r}{d_r}\right) \qquad (5.9)$$

where

v_c = void volume fraction
d_c = composite density
d_f = fiber density
d_r = resin density
w_f = fiber weight fraction
w_r = resin weight fraction

The value for the fiber density was determined experimentally using the displacement method and calculated to be 2.37 g/cm^3. This value is slightly lower than the e-glass value provided in ASTM D2734, which is 2.54 g/cm^3. This is a reasonable result since the unidirectional fabric in this study contains bundles of fibers (tows) held together by polyester threads. There is a certain amount of volume consumed by the spacing between fiber bundles, resulting in a lower density. Differences in curing, heat and pressure from

95

the reinforcement surface all change the composite resin density from the bulk resin density (ASTM D2734). Therefore, a single resin density could not be used for each composite plaque. In order to estimate the resin density for each of the nineteen parts, two assumptions are made. First, it is assumed that the specimen with the largest density value has the fewest number of voids. Since the center specimens (1 through 12 in Figure 5.3) are the most dimensionally accurate, a single specimen is selected from this group to calculate the overall resin density. The second assumption is that the specimen selected is relatively void free. Obviously, this can not be stated for parts that contain visible voiding throughout, such as those found in higher temperature experiments. In these cases, the minimum resin density determined in the lower temperature experiments is used. This results in a possible underestimation of the void content within the part; however, it is a measure of the minimum voiding that exists and is used as a relative comparison with other plaques.

5.3.6 Strength

The strength tests are conducted at room temperature using the guidelines outlined in ASTM D-2344. A three-point loading fixture is utilized with a length/thickness ratio of 7 and a span/thickness ratio of 5, as recommended for glass fiber-reinforced composites. The speed of testing is at a rate of crosshead movement of 1.3 mm/min. When performing the testing, it was observed that two failure mechanisms occurred simultaneouly. Initially, due to the "softness" of the composite material, the upper loading nose compressed the specimen locally. After a longer period of time, interlaminar shear took place. Since two failure modes must be considered in this test, the maximum load during experimentation is used to determine an overall strength, although it can not accurately be considered interlaminar shear strength. Results of the tests are given in Table 5.3. Appendix F

96

provides a listing of the calculated strength for each specimen tested in terms of an average, as well as plots of strength versus void content for each experiment.

Table 5.3. Experimental results in resin transfer molding process

Expmt #	Average void content, %	Strength, lbs	Filling time, sec
1	0	792.347	1930
2	3.3	946.777	360
3	1.5	826.083	960
4	4.7	979.004	140
5	0	699.87	960
6	1.3	860.263	85
7	3.5	883.345	40
8	5.8	797.294	205
9	7.6	894.043	55
10	0	869.838	13980
11	0	755.06	230
12	1.9	798.118	70
13	0	846.946	95
14	5.28	810.547	short shot
15	1.1	899.769	240
16	0	755.06	55
17	0	856.323	165
18	1.4	961.914	270
19	1.4	845.541	430

5.4 Analysis of Results

5.4.1 Significance Tests

Utilizing the data in Table 5.3, a statistical F-test is performed to determine the input variables that are significant in affecting the response variables. Tables 5.4 - 5.6 provide the results of this test.

97

Table 5.4. Significance test for void content

Predictor	Coefficient	Stdev	t-ratio	p
Constant	0.9330	1.1790	0.79	0.459
Cure temperature (x_1)	1.5812	0.5104	3.10	0.021
Outlet pressure (x_2)	0.4438	0.5104	0.87	0.418
Driving pressure (x_3)	-0.5913	0.5104	-1.16	0.291
Fiber volume (x_4)	0.2063	0.5104	0.40	0.700
$(x_1)^2$	0.7167	0.4659	1.54	0.175
$(x_2)^2$	0.0042	0.4659	0.01	0.993
$(x_3)^2$	0.4267	0.4659	0.92	0.395
$(x_4)^2$	-0.0958	0.4659	-0.21	0.884
x_1x_2	0.1125	0.7218	0.16	0.881
x_1x_3	-0.3625	0.7218	-0.50	0.633
x_1x_4	0.6375	0.7218	0.88	0.411
$x_1x_2x_3x_4$	0.5270	1.0210	0.52	0.624

Table 5.5. Significance test for strength

Predictor	Coefficient	Stdev	t-ratio	p
Constant	887.93	50.85	17.46	0.000
Cure temperature (x_1)	26.88	22.02	1.22	0.268
Outlet pressure (x_2)	6.27	22.02	0.28	0.785
Driving pressure (x_3)	-14.42	22.02	-0.65	0.537
Fiber volume (x_4)	2.78	22.02	0.13	0.904
$(x_1)^2$	-1.50	20.10	-0.07	0.943
$(x_2)^2$	-27.83	20.10	-1.38	0.215
$(x_3)^2$	-14.79	20.10	-0.74	0.489
$(x_4)^2$	-15.13	20.10	-0.75	0.480
x_1x_2	-30.99	31.14	-1.00	0.358
x_1x_3	-29.13	31.14	-0.94	0.386
x_1x_4	6.82	31.14	0.22	0.834
$x_1x_2x_3x_4$	19.45	44.04	0.44	0.674

Table 5.6. Significance test for mold filling time

Predictor	Coefficient	Stdev	t-ratio	p
Constant	288	117725	0.00	0.998
Cure temperature (x_1)	-1934	50977	0.04	0.971
Outlet pressure (x_2)	-104	50977	0.00	0.998
Driving pressure (x_3)	-125119	50977	2.45	0.049
Fiber volume (x_4)	41	50977	0.00	0.999
$(x_1)^2$	1682	46535	0.04	0.972
$(x_2)^2$	-35	46535	0.00	0.999
$(x_3)^2$	124940	46535	2.68	0.036
$(x_4)^2$	-35	46535	0.00	0.999
x_1x_2	224	72092	0.00	0.998
x_1x_3	210	72092	0.00	0.998
x_1x_4	49	72092	0.00	0.999
$x_1x_2x_3x_4$	-126225	101953	-1.24	0.262

In Table 5.4, the significance of the predictor variables with respect to the void content is provided. Temperature is the most significant variable, as expected (see Table 5.3). The overall strength of the composite part is not influenced to a large extent by any of the predictor variables, as seen in Table 5.5; however, temperature and outlet pressure are more highly correlated with strength than any other factors. Table 5.6 provides the significance test for filling time, which shows that the driving pressure is the most significant variable.

5.4.2 Design Optimization

Before the design optimization stage, training of the neural network takes place. Using the four input variables (cure temperature, outlet pressure, driving pressure and fiber

99

volume), the cascade correlation algorithm is trained to predict the values of the output variables (void content, strength and mold filling time). Experiment 10 had an unusually high mold filling time and experiment 14 was a short shot, i.e., the mold did not completely fill with resin; therefore, these are not included as mold filling time data.

After training the cascade correlation algorithm, the genetic algorithm is utilized for determining optimal design for the resin transfer molding process. The optimal variable settings of cure temperature, outlet pressure, driving pressure and fiber volume are shown in Tables 5.7-5.9 for minimizing void content, maximizing composite strength and minimizing mold filling time, respectively. Ten runs were performed for each objective function. It should be noted that for void content, a quality rating is used to determine part quality. Since 5 percent voiding within a composite part is considered unacceptable, any plaque that contained 5 percent voiding or higher was assigned a value of "1", or unacceptable. Parts with 4 percent voiding or less are given a quality rating of "0".

Table 5.7. Optimal designs for minimizing void content

Run #	Cure temperature, ° C	Outlet pressure, psi	Driving pressure, psi	Fiber volume, # layers
1	59.50	-11.05	18.75	23
2	67.10	-12.00	16.85	25
3	56.65	-11.05	21.60	22
4	52.85	-10.10	27.30	24
5	50.95	-11.05	29.20	21
6	50.00	-12.00	14.00	22
7	51.90	-12.00	25.40	23
8	51.90	-11.05	26.35	25
9	53.80	-10.10	14.00	25
10	60.45	-10.10	19.70	21

Table 5.8. Optimal designs for maximizing strength

Run #	Cure temperature, ° C	Outlet pressure, psi	Driving pressure, psi	Fiber volume, # layers
1	123.93	-4.00	21.99	21
2	118.93	-5.00	17.00	25
3	90.96	-9.00	27.99	21
4	60.99	-11.00	21.97	21
5	105.94	-11.00	24.99	23
6	88.92	-5.00	16.00	22
7	97.95	-5.00	31.98	21
8	51.00	0.00	27.99	24
9	58.99	-3.00	23.99	23
10	124.93	-10.00	23.99	25

Table 5.9. Optimal designs for minimizing mold filling time

Run #	Cure temperature, ° C	Outlet pressure, psi	Driving pressure, psi	Fiber volume, # layers
1	126.00	-11.00	34.00	24
2	114.00	-8.00	32.00	22
3	125.00	-2.00	31.00	23
4	124.00	-2.00	34.00	21
5	100.00	-10.00	32.00	21
6	129.00	-11.00	28.00	23
7	129.00	-8.00	26.00	22
8	107.00	-9.00	33.00	25
9	123.00	-6.00	32.00	22
10	124.00	-3.00	28.00	25

101

Although the genetic algorithm provides varying solutions for optimizing each objective function - minimizing void content, maximizing strength and minimizing mold filling time - the objective function values are the same. In Table 5.7, the minimum void content found by the genetic algorithm is 0 percent voiding. An overall part strength of 824 lbs is provided for the solutions in Table 5.8. Finally, the mold filling time solutions in Table 5.9 correspond to a time of approximately 80 seconds.

After determining the individual solutions for minimizing void content, maximizing strength and minimizing mold filling time, the genetic algorithm is utilized for optimizing the resin transfer molding process with multiple objective functions. The results are shown in Table 5.10. As expected, there are tradeoffs when deciding the settings for cure temperature, outlet pressure, driving pressure and fiber volume.

Table 5.10. Optimal designs for multiple objective functions

Run #	Cure temperature, ° C	Outlet pressure, psi	Driving pressure, psi	Fiber volume, # layers	Void content	Strength, lbs	Filling time, sec
1	52	-8	32	23	0.228	738.867	269.05
2	53	-12	33	22	0.243	728.348	152.38
3	50	-5	28	22	0.275	751.628	307.14
4	61	-8	29	21	0.343	750.453	114.29
5	65	-12	33	23	0.249	743.037	152.38
6	51	-3	28	24	0.212	765.100	533.33
7	62	-12	32	25	0.160	753.579	411.90
8	69	-9	34	21	0.384	737.137	221.43
9	62	-12	30	23	0.230	752.447	261.90
10	58	-4	32	24	0.241	753.485	309.52

102

From the significance test results in Section 5.4.1, temperature has a higher correlation with void content, strength and mold filling time than any other variable. In addition, strength is influenced to some degree by the outlet pressure. For each objective function, the genetic algorithm is used to determine the process variable settings that result in a design that is insensitive to in-process fluctuations. These process variable settings are provided in Tables 5.11 - 5.14. In Table 5.11, the optimal temperatures are low since the void content is known to increase significantly when the cure temperature extends beyond 100° C (see Table 5.3). Random fluctuations in temperature of +/- 10° C were included in the genetic algorithm for this optimization step. In the case of minimizing the sensitivity of strength to temperature fluctuations, as shown in Table 5.12, the cure temperature solutions were on the lower end of the possible temperature range of 50° C - 130° C. The outlet pressure was varied +/- 2 psi in Table 5.13 to measure the sensitivity of the strength to in-process pressure fluctuations. Finally, as seen in Table 5.14, the mold filling time was optimized in the presence of random temperature fluctuations.

Table 5.11. Solutions for minimizing Δ void content with temperature fluctuations

Run #	Cure temperature, ° C	Outlet pressure, psi	Driving pressure, psi	Fiber volume, # layers	Void content	Δ void content
1	51	-5	24	25	0.153	0
2	57	-7	22	25	0.155	0
3	57	-4	15	25	0.160	0
4	58	-9	17	25	0.135	0
5	53	-9	30	25	0.146	0
6	57	-11	22	25	0.130	0
7	54	-11	24	24	0.158	0
8	55	-6	20	25	0.151	0
9	57	-11	19	24	0.157	0
10	71	-9	15	25	0.173	0

103

Table 5.12. Solution for minimizing Δ strength with temperature fluctuations

Run #	Cure temperature, °C	Outlet pressure, psi	Driving pressure, psi	Fiber volume, # layers	Strength , lbs	Δ strength, lbs
1	65	-5	32	24	755.287	0
2	52	-11	34	24	732.807	0
3	83	-11	33	21	752.507	0
4	79	-9	31	22	764.538	0
5	59	-2	34	22	739.213	0
6	57	-7	29	21	747.545	0
7	56	-4	32	24	751.438	0
8	52	0	32	21	738.119	0
9	56	-7	32	23	743.590	0
10	51	-10	27	25	766.620	0

Table 5.13. Solutions for minimizing Δ strength with outlet pressure fluctuations

Run #	Cure temperature, °C	Outlet pressure, psi	Driving pressure, psi	Fiber volume, # layers	Strength , lbs	Δ strength, lbs
1	51	-5	32	24	755.287	0
2	52	-11	34	24	732.807	0
3	83	-11	33	21	752.507	0
4	79	-9	31	22	764.538	0
5	59	-2	34	22	739.213	0
6	57	-7	29	21	747.545	0
7	56	-4	32	24	751.438	0
8	52	0	32	21	738.119	0
9	56	-7	32	23	743.590	0
10	51	-10	27	25	766.620	0

Table 5.14. Solutions for minimizing Δ filling time with driving pressure fluctuations

Run #	Cure temperature, °C	Outlet pressure, psi	Driving pressure, psi	Fiber volume, # layers	Filling time, sec	Δ filling time
1	116	-1	34	22	90	0
2	128	-6	28	23	125	0
3	116	-5	29	21	89	0
4	126	-10	33	23	118	0
5	122	-2	30	21	93	0
6	129	-4	33	22	101	0
7	128	0	34	21	82	0
8	122	-4	33	21	87	0
9	96	-12	33	21	94	0
10	126	0	30	21	99	0

105

CHAPTER 6

CONCLUSIONS

Although the RTM process has become better understood in recent years, there is still a great deal of knowledge to be attained in this field of material processing. One area in particular that needs attention is that of integrated product/process design. In many instances, the product and process design variables are selected arbitrarily and modified as needed during prototype development, which results in wasted time and resources. For this reason, it is important to develop a systematic procedure for design optimization. In addition, to ensure the quality of the product during the production stage, an accurate method of process control is necessary. The genetic algorithm - cascade correlation algorithm procedure developed in this research was employed for systematic product design selection. In addition, a robust design was determined so that part quality is maintained in the presence of fluctuations in the process variables. Since the resin transfer molding process is a complicated process exhibiting many nonlinearities, there is a need for an accurate process control procedure. In this research, the cascade correlation algorithm was applied as a control mechanism for the curing stage to enhance part-to-part reproducibility.

6.1 Contributions

This research has undertaken a systematic investigation into the resin transfer molding process, with the following contributions being made.

106

1. Integration of product and process design in the resin transfer molding process. By incorporating both aspects, there are fewer limitations placed on the production of composite parts. This allows for more flexibility and enhancement of the final product.

2. Robust design of the processing parameters. This is an important task for the production of composite parts in the resin transfer molding process due to the highly nonlinear behavior of the system. Changes in curing temperatures and pressures during the process, as well as the resin batch used, can alter the process as to create a shift in the desired part quality.

3. Modeling of the resin transfer molding process using the cascade correlation algorithm. Neural networks are likely candidates for the modeling of nonlinear systems. Through proper training, the cascade correlation algorithm is developed into an accurate predictive model for determining the final part characteristics given a set of processing parameters.

4. Application of genetic algorithms to the optimization of product and process design parameters. An efficient and effective solution procedure was desired for optimizing the resin transfer molding process. The genetic algorithm approach satisfied these requirements. In addition, the incorporation of the cascade correlation algorithm into the genetic algorithm allows for implicit and explicit objective function representation.

5. The cascade correlation algorithm was tested for its feasibility in tracking degree of cure. Using IR data, CCA was able to accurately predict the degree of cure at a specified point in time.

107

6.2 Suggestions for Future Studies

Although this research has taken steps towards gaining a better understanding of the resin transfer molding process and, therefore, developing a systematic procedure for optimizing product and process design, there remains a need for further areas of research. Listed below are a few of those areas.

1. Development of a resin transfer molding database. This is by no means a small task. The above research dealt with a specific resin/fiber system. It is of great interest to resin transfer molding manufacturers to have an extensive library of guidelines for a number of resin and fiber systems, as well as fiber architectures.

2. Application of neural networks to database development. Since it would take many year of work and experimentation to create an extensive database, neural network technology can be utilized to reduce the amount of development time. Through knowledge of existing systems and their optimal parameters, a neural network has the capability of determining the optimum design for a new resin transfer molding system.

3. Investigation of the effects of varying fiber architectures on mechanical properties, mold filling, etc. In this research, a unidirectional fabric was used with each layer oriented in the same direction. It would be of interest to alternate the fiber direction from one layer to the next to determine its effect on RTM processing and final mechanical properties of the composite.

4. Process control for mold filling and heat transfer stages. It may be feasible to investigate the effects of mold filling and heat transfer on the final part quality. By carefully monitoring the critical processing variables during these stages, the resin transfer molding process will be optimized at each step.

5. Application of the GA-CCA system to other manufacturing processes.

108

APPENDIX A

AUTOREGRESSIVE (AR) MODEL

An auto regressive process is represented by a difference equation of the following form:

$$X(n) = \sum_{i=1}^{p} \phi_i \; X(n\text{-}i) + e(n) \tag{A.1}$$

where $X(n)$ is the time random sequence, ϕ_i , $i = 1, \ldots, r$ are parameters, and $e(n)$ is a sequence of independent and identically distributed zero-mean Gaussian random variables with constant variance, that is,

$$E\{e(n)\} = 0 \tag{A.2}$$

$$E\{e(n)e(j)\} = \begin{cases} \sigma_N^2, & \text{for } n = j \\ 0 & \text{for } n \neq j \end{cases} \tag{A.3}$$

$$f_{e(n)} \; (l) = \frac{1}{\sqrt{2\pi}\,\sigma_N} \; exp\left\{\frac{-\lambda^2}{2\sigma_N^2}\right\} \tag{A.4}$$

The sequence $e(n)$ is known as white Gaussian noise. Thus, an auto regressive process is a linear difference equation model when the input or forcing function is white Gaussian noise [Jangi and Yogendra, 1991].

109

APPENDIX B

WELDING TRAINING AND TESTING DATA

Table B.1. Welding training data

Weld Number	Arc Current (A)	Arc Voltage (V)	Travel Speed (mm/s)	Wire speed (mm/s)	Bead width (mm)	Penetration (mm)	Reinforcement Height (mm)	Cross Section Area (mm^2)
1	150	9.6	1.91	2.12	6.95	2.60	0.37	1.87
2	150	9.6	1.91	4.23	7.04	2.70	0.64	2.87
3	150	9.6	1.91	6.35	6.93	2.63	0.86	4.13
4	150	9.6	1.91	8.47	6.87	2.47	1.02	4.94
5	100	9.0	1.19	2.12	5.49	1.75	0.59	2.55
6	100	9.0	1.19	4.23	5.23	1.77	0.88	3.33
7	100	9.0	1.19	6.35	5.51	1.50	1.43	5.34
8	100	9.0	1.19	10.58	5.47	1.18	2.10	8.68
9	100	9.0	1.82	2.12	4.60	1.74	0.60	2.05
10	100	9.0	1.82	6.35	4.64	1.62	1.07	3.51
11	100	9.0	1.82	8.47	4.68	1.29	1.25	4.18
12	150	9.6	2.88	4.23	6.81	1.93	0.47	2.12
13	150	9.6	2.88	6.35	7.23	2.00	0.60	2.55
14	150	9.6	2.88	8.47	7.05	1.83	0.78	3.51
15	150	9.6	1.44	2.12	7.45	3.21	0.42	2.42
16	150	9.6	1.44	4.23	7.58	3.10	0.63	3.47
17	100	9.0	0.89	2.12	5.59	1.29	0.66	2.75
18	100	9.0	0.89	4.23	5.66	1.85	1.09	4.53
19	100	9.0	0.89	6.35	5.53	1.36	1.64	6.59
20	200	10.5	4.19	2.12	7.66	1.33	0.21	0.92
21	200	10.5	4.19	2.12	6.64	1.51	0.21	0.83
22	200	10.5	4.19	4.23	8.00	1.50	0.34	1.58
23	200	10.5	4.19	10.58	7.86	1.06	0.59	2.98
24	200	10.5	4.19	12.70	8.12	1.11	0.69	3.66
25	200	10.5	4.19	16.93	8.66	0.72	0.82	4.73

110

Table B.1--continued

Weld Number	Arc Current (A)	Arc Voltage (V)	Travel Speed (mm/s)	Wire speed (mm/s)	Bead width (mm)	Penetration (mm)	Reinforcement Height (mm)	Cross Section Area (mm²)
26	200	10.5	4.19	21.17	8.75	0.55	0.94	5.61
27	200	10.5	2.12	8.47	9.76	2.50	0.78	4.93
28	200	10.5	2.12	16.93	11.09	1.11	1.18	8.51
29	200	10.5	2.79	12.70	9.45	1.58	0.83	5.11
30	200	10.5	2.79	16.93	9.58	0.89	1.05	6.52
31	200	10.5	2.79	8.47	9.31	2.28	0.63	3.64

Table B.2. Welding testing data

Weld Number	Arc Current (A)	Arc Voltage (V)	Travel Speed (mm/s)	Wire speed (mm/s)	Bead width (mm)	Penetration (mm)	Reinforcement Height (mm)	Cross Section Area (mm²)
32	100	9.0	1.19	8.47	5.35	1.43	1.89	7.27
33	100	9.0	1.82	4.23	5.70	1.73	0.69	2.64
34	150	9.6	2.88	10.58	6.06	1.94	0.97	4.23
35	150	9.6	1.44	6.35	7.55	2.86	0.95	5.06
36	100	9.0	0.89	8.47	5.78	1.44	2.13	9.44
37	200	10.5	4.19	6.35	7.80	1.58	0.44	1.85
38	200	10.5	4.19	8.47	8.09	1.80	0.53	2.59
39	200	10.5	4.19	14.82	8.27	0.87	0.75	4.00
40	200	10.5	2.12	2.12	10.08	2.16	0.42	2.55
41	200	10.5	2.12	12.70	10.24	1.76	0.97	6.48
42	200	10.5	2.79	2.12	9.35	2.05	0.30	1.74

111

APPENDIX C

INFRARED CURE DATA

Table C.1. Infrared data used in training CCA

Example	Temp, ° C	Time, min	% Monomer	Ratio
1	50	8.25	0.1283	0.979
2	50	25	0.1283	0.98
3	50	33.25	0.1262	0.963
4	50	41.5	0.1252	0.956
5	50	58	0.1204	0.919
6	50	66.25	0.1181	0.901
7	50	74.5	0.116	0.886
8	50	82.75	0.1136	0.867
9	50	91.25	0.1076	0.821
10	50	107.75	0.1013	0.774
11	50	116	0.0966	0.737
12	50	124.25	0.0933	0.712
13	50	132.5	0.0923	0.704
14	50	141	0.0882	0.673
15	50	157.5	0.0815	0.622
16	50	165.75	0.0783	0.597
17	50	174	0.0734	0.561
18	50	182.25	0.0717	0.548
19	50	190.75	0.0693	0.529
20	50	207.5	0.0612	0.467
21	50	215.75	0.06	0.458
22	50	224	0.054	0.412
23	50	232.5	0.0479	0.366
24	50	240.75	0.047	0.359
25	50	257.25	0.046	0.351
26	50	265.5	0.0417	0.318
27	50	273.75	0.0404	0.308
28	50	272	0.0366	0.279

112

Table C.1--continued

Example	Temp, ° C	Time, min	% Monomer	Ratio
29	50	280.5	0.036	0.275
30	50	297	0.0326	0.249
31	50	305.25	0.0302	0.231
32	50	321.75	0.0276	0.211
33	50	340	0.0267	0.204
34	60	5.25	0.1212	0.992
35	60	15.75	0.118	0.965
36	60	26.5	0.1139	0.932
37	60	31.75	0.111	0.909
38	60	37	0.1092	0.894
39	60	47.5	0.1025	0.839
40	60	52.75	0.0979	0.801
41	60	58	0.0939	0.768
42	60	63.5	0.0912	0.747
43	60	69	0.0879	0.719
44	60	79.5	0.0797	0.652
45	60	90	0.0707	0.579
46	60	95.25	0.0671	0.549
47	60	100.5	0.0639	0.523
48	60	111.25	0.0561	0.459
49	60	116.5	0.0524	0.429
50	60	121.75	0.0508	0.416
51	60	127	0.0472	0.387
52	60	132.5	0.0435	0.356
53	60	143	0.0403	0.33
54	60	148.25	0.0374	0.306
55	60	153.5	0.0352	0.288
56	60	159	0.0334	0.273
57	60	164.25	0.0306	0.251
58	60	175	0.0268	0.219
59	60	185.5	0.023	0.188
60	60	196	0.0204	0.167
61	60	190.75	0.0219	0.179
62	80	3.25	0.1238	1
63	80	6.5	0.1181	0.954
64	80	9.75	0.113	0.913
65	80	13	0.1053	0.851
66	80	16.25	0.0976	0.789

113

Table C.1--continued

67	80	23	0.0823	0.665
68	80	29.5	0.0672	0.543
69	80	32.75	0.0602	0.486
70	80	36.25	0.0547	0.442
71	80	42.75	0.0416	0.336
72	80	49.25	0.0312	0.252
73	80	52.5	0.0296	0.239
74	80	56	0.0268	0.217
75	80	62.5	0.0201	0.162
76	80	65.75	0.0194	0.157
77	80	69	0.0181	0.146
78	80	72.25	0.0137	0.11
79	80	75.75	0.013	0.105
80	80	82.25	0.0105	0.085
81	80	85.5	0.0096	0.077
82	80	88.75	0.0096	0.077
83	80	92	0.0075	0.061
84	80	95.25	0.0065	0.053
85	80	102	0.0049	0.04
86	80	105.5	0.0048	0.039
87	80	108.75	0.0045	0.036
88	80	112	0.004	0.032
89	80	115.25	0.0037	0.03
90	80	121.75	0.0032	0.026
91	80	125	0.0033	0.027

Table C.2. Infrared data used in testing CCA

Example	Temp, °C	Time, min	% Monomer	Ratio
50	16.5	0.1288	0.984	0.979
50	49.75	0.1221	0.932	0.98
50	99.5	0.1068	0.816	0.963
50	149.25	0.0848	0.647	0.956
50	199.25	0.0616	0.47	0.919
50	249	0.0464	0.354	0.901
50	288.75	0.0333	0.254	0.886
50	313.5	0.0289	0.221	0.867

114

Table C.2--continued

Example	Temp, ° C	Time, min	% Monomer	Ratio
50	348.5	0.0238	0.181	0.821
60	10.5	0.1195	0.979	0.774
60	42.25	0.1057	0.865	0.712
60	74.25	0.0829	0.678	0.704
60	84.75	0.0766	0.627	0.673
60	106	0.0598	0.489	0.622
60	137.75	0.043	0.352	0.597
60	169.5	0.0277	0.227	0.561
60	180.25	0.024	0.196	0.548
80	19.75	0.0896	0.724	0.529
80	26.25	0.0759	0.614	0.467
80	39.25	0.0468	0.378	0.458
80	46	0.0366	0.296	0.412
80	59.25	0.0234	0.19	0.366
80	79	0.0112	0.091	0.359
80	98.75	0.0064	0.052	0.351
80	118.5	0.0035	0.028	0.318
80	128.5	0.0033	0.027	0.308
60	21	0.1158	0.948	0.737
60	42.25	0.1057	0.865	0.712
60	74.25	0.0829	0.678	0.704
60	84.75	0.0766	0.627	0.673
60	106	0.0598	0.489	0.622
60	137.75	0.043	0.352	0.597
60	169.5	0.0277	0.227	0.561
60	180.25	0.024	0.196	0.548
80	19.75	0.0896	0.724	0.529
80	26.25	0.0759	0.614	0.467
80	39.25	0.0468	0.378	0.458
80	46	0.0366	0.296	0.412
80	59.25	0.0234	0.19	0.366
80	79	0.0112	0.091	0.359
80	98.75	0.0064	0.052	0.351
80	118.5	0.0035	0.028	0.318
80	128.5	0.0033	0.027	0.308

115

APPENDIX D

PROCESS MODELING

In the RTM process, the three interrelated phases, resin flow, heat transfer and cure reaction, can be modeled by Darcy's law, an energy balance equation, and cure kinetics equations, respectively. These equations can be solved by various numerical techniques which incorporate the coupling between the different phases of the RTM process.

D.1 Resin Flow

The basic physics of the fill phase of RTM is flow through porous media which has traditionally been described by Darcy's law, which relates the fluid flow to the pressure gradient using the fluid viscosity and the permeability of the porous medium. This relationship is defined by:

$$u = -\frac{K}{\eta}\nabla P, \tag{D.1}$$

in which u is the superficial velocity, or average velocity in local volumes, h is the viscosity of the fluid, ∇P is the pressure gradient, and K is the permeability tensor of the porous medium which is a function of the porous medium structure and porosity. For two dimensional problems, the permeability has the following form:

$$K = \begin{pmatrix} k_{xx} & k_{xy} \\ k_{yx} & k_{yy} \end{pmatrix} \tag{D.2}$$

116

In a homogeneous porous medium, the permeability is orthotropic; thus, it is always possible to find an orthogonal coordinate system which diagonalizes the permeability tensor. Solving Darcy's law in the principal directions can simplify the problems, as all the cross-terms of permeability vanish. After applying the continuity condition to Darcy's law, the governing equation for the pressure distribution becomes:

$$k_{xx} \frac{\partial^2 P}{\partial x^2} + k_{yy} \frac{\partial^2 P}{\partial y^2} = 0$$ (D.3)

where

P: resin pressure, Pa.

k_{xx}: permeability in the direction of flow, m^{-2}.

k_{yy}: permeability perpendicular to the direction of flow, m^{-2}.

k_{xy}: in-plane cross-permeability of preform, m^{-2}.

The modeling of the filling process is a quasi-steady problem. The boundary conditions can be stated as:

At flow front: $P=0$.

At injection ports: $P=P_0$.

At mold wall: $\nabla P \bullet \vec{n} = 0$.

Although Darcy's law has been widely used and accepted as a model for RTM flow, this equation is used under the assumption that the resin behaves as a Newtonian fluid. By definition, a Newtonian fluid is one in which the friction behavior is adequately described by a linear relation between the extra-stresses and the rate of strain, or

$$\tau = \eta \dot{\gamma}$$ (D.4)

117

where τ is the shear stress, η represents the shear viscosity and $\dot{\gamma}$ is the shear rate.

On the other hand, liquids, such as polymers, behave differently from a Newtonian fluid and are referred to as non-Newtonian fluids. The following summarizes the hypotheses regarding the frictional behavior of non-Newtonian fluids:

• The extra-stresses acting on a fluid particle at a particular time depend on the motion of the fluid in the past; i.e., the fluid has memory. The future movement, however, does not influence the present time.

• The extra-stresses acting on the fluid particle depend only on the deformation history of the particle under observation and, more precisely, on the history of its relative deformation gradient.

The general relationship for the shear stress is written as:

$$\tau = f(\gamma) \tag{D.5}$$

A more accurate representation of the resin flow stage occurs when the behavior of the flow is modeled as a non-Newtonian liquid; this requires that the shear rate be considered.

D.2 Heat Transfer

In the RTM process, the mold filling does not take place under isothermal conditions. In general, the mold is heated and resin is injected into the mold. As the resin flows through the fiber preform, heat transfer between the mold walls, the fiber preform and the resin will occur. Therefore, the resin temperature will vary throughout the mold. As the fluid viscosity is strongly dependent on the temperature increases, cure will initiate after a threshold temperature is reached. Resin cure is often a strongly exothermic reaction, which substantially influences the overall heat transfer.

118

Heat transfer in flow through porous media has been analyzed by different methods. Basically, they can be grouped into two categories: equilibrium models, and two phase models. For the equilibrium approach, the assumption is that the fluid and fiber have the same temperature at the same point, implying that heat transfer between the resin and the fiber is instantaneous. If the in-plane conduction and out of plane convection are ignored, the energy balance equation can be written as:

$$(\phi \rho_r c_{pr} + (1 - \phi) \rho_f c_{pf}) \frac{\partial T}{\partial t} + \phi \rho_r c_{pr} (u_x \frac{\partial T}{\partial x} + u_y \frac{\partial T}{\partial y}) = k \frac{\partial^2 T}{\partial z^2} + \phi s \quad \text{(D.6)}$$

where T is temperature and t is time; ρ_r, c_{pr}, ρ_f and c_{pf} are the density and heat capacity of resin and fiber preform, respectively; and f is the porosity. The first term on the left-hand side of Equation (D.6) represents the change in internal energy of both the fluid and the fiber preform. The second term represents the contribution due to convection of fluid. Conduction through the thickness is taken into account by the first term of right hand side. The energy generated in the resin due to curing is represented as the source term s. The effective through-thickness thermal conductivity of the fluid and fiber medium is denoted by k.

To solve Equation (D.6), boundary conditions are applied, which are the temperature of the top and bottom of the mold, the temperature of the flow front, and the temperature at all the injection gates.

D.3 Cure Reaction

To model the source term in Equation (D.6), the following equation presented by Kamal et al. [1973] is widely used:

$$s = R_\alpha E_\alpha \quad \text{(D.7)}$$

119

where R_α is the rate of reaction, E_α is the heat of reaction and α is the degree of cure. The reaction rate itself is a function of temperature and the degree of cure reaction. Since the resin flows through the mold, an expression for the convection of the degree of cure is necessary. A conservation of species equation provides the cure α as a function of time and position, and may be expressed by the continuity equation as:

$$\frac{\partial \alpha}{\partial t} + u_x \frac{\partial \alpha}{\partial x} + u_y \frac{\partial \alpha}{\partial y} = R_\alpha \qquad (D.8)$$

The left -hand side of this equation represents the change in the degree of cure at a point in space as well as the convection of the degree of cure through space by the flowing fluid. The right-hand side is the rate of reaction, and acts as a source term in this continuity equation.

120

APPENDIX E

VOLUMETRIC AND WEIGHT MEASUREMENTS

Table E.1. Volumetric measurements for experiment 1

Specimen	1	2	3	4	5	6	7	8	9	10	11	12
1	9.19	9.18	9.23	9.20	9.22	9.25	69.03	69.01	69.01	68.97	9.23	9.22
2	9.18	9.18	9.22	9.24	9.24	9.26	69.04	69.03	69.03	69.05	9.24	9.24
3	9.20	9.19	9.20	9.23	9.25	9.23	69.05	69.05	69.05	69.05	9.25	9.24
4	9.19	9.20	9.22	9.24	9.25	9.23	69.04	69.04	69.04	69.06	9.25	9.23
5	9.19	9.20	9.23	9.23	9.25	9.22	69.04	69.04	69.04	69.05	9.23	9.24
6	9.18	9.18	9.22	9.24	9.23	9.25	69.04	69.04	69.04	69.04	9.25	9.26
7	9.17	9.17	9.2	9.21	9.23	9.27	69.02	69.05	69.05	69.06	9.25	9.24
8	9.18	9.19	9.2	9.22	9.26	9.22	69.03	69.04	69.04	69.05	9.24	9.22
9	9.16	9.17	9.2	9.2	9.25	9.22	69.04	69.05	69.05	69.05	9.23	9.22
10	9.15	9.16	9.17	9.18	9.23	9.24	69.03	69.04	69.04	69.05	9.21	9.23
11	9.16	9.15	9.18	9.18	9.23	9.25	69.03	69.05	69.05	69.04	9.20	9.23
12	9.15	9.15	9.20	9.18	9.24	9.26	69.02	69.04	69.04	69.04	9.19	9.22
A1	9.19	9.19	9.17	9.20	9.19	9.27	26.10	26.15	26.15	26.14	9.26	9.26
A2	9.17	9.20	9.17	9.18	9.18	9.25	26.10	26.12	26.12	26.10	9.21	9.26
A3	9.19	9.18	9.19	9.18	9.15	9.27	26.11	26.10	26.10	26.12	9.22	9.26
A4	9.19	9.16	9.17	9.17	9.14	9.23	26.17	26.25	26.25	26.12	9.22	9.24
A5	9.20	9.19	9.18	9.18	9.14	9.23	26.23	26.30	26.30	26.19	9.21	9.22
A6	9.18	9.19	9.15	9.17	9.08	9.22	26.28	26.33	26.33	26.27	9.17	9.25
A7	9.19	9.19	9.18	9.20	9.15	9.24	26.33	26.37	26.37	26.30	9.22	9.26
A8	9.18	9.16	9.18	9.18	9.16	9.26	26.40	26.42	26.42	26.35	9.22	9.24
A9	9.16	9.15	9.15	9.16	9.17	9.25	26.45	26.49	26.49	26.43	9.22	9.24
A10	9.15	9.16	9.11	9.17	9.17	9.26	26.51	26.52	26.52	26.47	9.21	9.25
A11	9.14	9.19	9.14	9.15	9.18	9.24	26.58	26.58	26.58	26.54	9.22	9.24
A12	9.17	9.17	9.09	9.15	9.11	9.23	26.63	26.63	26.63	26.59	9.21	9.23
B1	9.20	9.22	9.21	9.23	9.20	9.21	24.74	24.67	24.67	24.57	8.94	9.14
B2	9.19	9.23	9.21	9.21	9.23	9.22	24.94	24.79	24.79	24.75	8.87	9.14
B3	9.20	9.20	9.21	9.24	9.22	9.24	25.09	24.94	24.94	24.97	8.97	9.15
B4	9.16	9.20	9.21	9.20	9.22	9.24	25.15	24.91	24.91	25.10	8.90	9.15
B5	9.16	9.20	9.18	9.23	9.21	9.22	25.24	25.07	25.07	25.19	8.91	9.14

121

Table E.1—continued

B6	9.21	9.16	9.15	9.18	9.20	9.21	25.34	25.24	25.24	25.22	8.91	9.17
B7	9.19	9.20	9.19	9.20	9.22	9.24	25.47	25.36	25.36	25.35	8.92	9.10
B8	9.19	9.20	9.17	9.17	9.20	9.24	25.62	25.56	25.56	25.51	8.93	9.16
B9	9.17	9.20	9.21	9.22	9.21	9.24	25.77	25.64	25.64	25.60	8.90	9.15
B10	9.17	9.16	9.16	9.21	9.19	9.22	25.87	25.77	25.62	25.75	8.90	9.14
B11	9.17	9.19	9.17	9.19	9.22	9.23	26.07	25.95	25.77	25.93	8.89	9.14
B12	9.16	9.17	9.22	9.18	9.23	9.26	26.30	26.18	25.94	26.12	9.00	9.20

Table E.2. Volumetric measurements for experiment 2

Specimen	1	2	3	4	5	6	7	8	9	10	11	12
1	9.59	9.61	9.59	9.59	9.23	9.23	68.91	68.94	68.89	68.90	9.23	9.23
2	9.56	9.59	9.59	9.60	9.22	9.25	68.96	68.96	68.95	68.94	9.21	9.23
3	9.58	9.59	9.60	9.61	9.22	9.23	68.97	68.98	68.97	68.98	9.20	9.23
4	9.59	9.57	9.58	9.61	9.23	9.22	68.96	68.97	68.98	68.97	9.23	9.21
5	9.59	9.59	9.60	9.61	9.22	9.21	68.98	68.98	68.98	68.98	9.21	9.22
6	9.58	9.57	9.59	9.61	9.20	9.23	68.97	68.98	68.97	68.98	9.19	9.20
7	9.57	9.60	9.58	9.62	9.22	9.24	68.97	68.98	68.98	68.98	9.19	9.22
8	9.58	9.57	9.58	9.60	9.22	9.25	68.98	68.98	68.98	68.98	9.22	9.23
9	9.58	9.60	9.58	9.59	9.22	9.25	68.99	69.00	68.99	68.99	9.20	9.24
10	9.56	9.58	9.56	9.58	9.21	9.23	68.99	68.98	68.98	68.99	9.20	9.21
11	9.56	9.54	9.55	9.56	9.22	9.23	68.99	68.99	68.98	69.00	9.21	9.22
12	9.53	9.55	9.58	9.57	9.22	9.24	68.98	69.00	68.99	68.99	9.17	9.24
A1	9.59	9.58	9.57	9.58	9.16	9.23	26.05	26.08	26.02	26.04	9.23	9.24
A2	9.59	9.60	9.57	9.57	9.16	9.24	26.08	26.10	26.08	26.09	9.25	9.24
A3	9.60	9.60	9.59	9.60	9.20	9.22	26.12	26.10	26.09	26.10	9.22	9.23
A4	9.64	9.60	9.60	9.60	9.15	9.24	26.12	26.12	26.11	26.13	9.23	9.26
A5	9.59	9.54	9.57	9.60	9.14	9.22	26.11	26.13	26.10	26.15	9.22	9.23
A6	9.55	9.51	9.59	9.61	9.15	9.21	26.09	26.16	26.15	26.15	9.22	9.24
A7	9.51	9.53	9.59	9.59	9.19	9.24	26.11	26.19	26.15	26.11	9.22	9.26
A8	9.52	9.51	9.57	9.60	9.15	9.23	26.12	26.20	26.18	26.12	9.24	9.25
A9	9.50	9.48	9.56	9.60	9.16	9.23	26.15	26.17	26.18	26.15	9.22	9.25
A10	9.49	9.57	9.56	9.59	9.17	9.23	26.13	26.16	26.16	26.16	9.21	9.24
A11	9.55	9.56	9.55	9.59	9.16	9.22	26.11	26.16	26.16	26.15	9.22	9.23
A12	9.55	9.54	9.54	9.56	9.18	9.23	26.06	26.15	26.15	26.10	9.24	9.26
B1	9.57	9.59	9.61	9.64	9.23	9.26	21.35	21.27	21.31	21.42	9.08	9.17
B2	9.59	9.60	9.59	9.62	9.24	9.24	21.21	21.17	21.25	21.32	9.08	9.18

122

B3	9.61	9.60	9.60	9.62	9.21	9.24	21.12	21.06	21.15	21.21	9.09	9.15
B4	9.63	9.63	9.64	9.63	9.22	9.25	21.03	20.89	21.01	21.08	9.09	9.16
B5	9.63	9.61	9.62	9.61	9.22	9.21	20.94	20.78	20.83	21.01	9.12	9.16
B6	9.59	9.59	9.64	9.66	9.22	9.23	20.93	20.71	20.75	20.93	9.09	9.16
B7	9.60	9.59	9.65	9.64	9.22	9.24	20.91	20.70	20.69	20.92	9.07	9.15
B8	9.61	9.59	9.64	9.63	9.23	9.25	20.87	20.73	20.69	20.90	9.09	9.18
B9	9.57	9.57	9.61	9.64	9.23	9.24	20.86	20.71	20.71	20.87	9.08	9.15
B10	9.56	9.57	9.59	9.60	9.23	9.23	20.87	20.74	20.72	20.86	9.08	9.17
B11	9.58	9.59	9.57	9.59	9.25	9.25	20.86	20.81	20.73	20.9	9.11	9.17
B12	9.57	9.63	9.59	9.59	9.23	9.33	20.94	20.85	20.79	20.86	9.16	9.31

Table E.3. Volumetric measurements for experiment 3

Specimen	1	2	3	4	5	6	7	8	9	10	11	12
1	9.75	9.77	9.77	9.78	9.23	9.24	68.89	68.89	68.89	68.89	9.23	9.24
2	9.75	9.77	9.78	9.78	9.20	9.22	68.89	68.89	68.89	68.89	9.23	9.24
3	9.76	9.78	9.80	9.79	9.23	9.23	68.88	68.89	68.89	68.89	9.24	9.22
4	9.78	9.75	9.80	9.81	9.23	9.23	68.89	68.88	68.88	68.88	9.23	9.25
5	9.77	9.79	9.83	9.85	9.24	9.21	68.90	68.88	68.88	68.88	9.25	9.25
6	9.78	9.80	9.81	9.83	9.23	9.21	68.88	68.89	68.87	68.87	9.25	9.23
7	9.79	9.79	9.84	9.88	9.22	9.22	68.87	68.87	68.87	68.88	9.25	9.24
8	9.83	9.83	9.84	9.83	9.22	9.20	68.86	68.87	68.87	68.88	9.23	9.23
9	9.82	9.81	9.85	9.84	9.22	9.23	68.87	68.87	68.87	68.87	9.25	9.25
10	9.83	9.82	9.84	9.84	9.22	9.22	68.86	68.88	68.86	68.86	9.24	9.24
11	9.83	9.80	9.85	9.85	9.20	9.22	68.85	68.86	68.87	68.86	9.24	9.23
12	9.82	9.83	9.82	9.81	9.25	9.23	68.82	68.81	68.82	68.84	9.25	9.25
A1	9.80	9.76	9.77	9.78	9.23	9.23	27.79	28.06	27.76	28.03	9.24	9.23
A2	9.78	9.79	9.78	9.81	9.22	9.22	27.93	28.20	27.81	28.11	9.26	9.23
A3	9.78	9.79	9.79	9.76	9.25	9.23	28.18	28.33	28.03	28.20	9.23	9.25
A4	9.80	9.81	9.70	9.79	9.25	9.22	28.40	28.53	28.21	28.41	9.27	9.24
A5	9.79	9.82	9.80	9.78	9.23	9.22	28.62	28.80	28.41	28.56	9.24	9.25
A6	9.77	9.80	9.77	9.80	9.25	9.24	28.92	29.04	28.66	28.87	9.24	9.24
A7	9.83	9.84	9.80	9.79	9.23	9.23	29.20	29.35	28.95	29.10	9.24	9.25
A8	9.84	9.82	9.79	9.83	9.27	9.25	29.57	29.65	29.25	29.39	9.25	9.25
A9	9.83	9.86	9.84	9.81	9.27	9.26	29.89	30.02	29.60	29.69	9.28	9.24
A10	9.84	9.84	9.83	9.83	9.25	9.25	30.32	30.40	29.97	30.05	9.27	9.27
A11	9.77	9.68	9.81	9.82	9.27	9.26	30.68	30.79	30.37	30.44	9.26	9.25

123

A12	9.55	9.63	9.80	9.81	9.26	9.23	31.04	31.17	30.70	30.82	9.29	9.24
B1	9.80	9.80	9.83	9.84	9.27	9.11	26.58	26.58	26.62	26.61	9.24	9.23
B2	9.81	9.81	9.84	9.83	9.26	9.11	26.55	26.54	26.57	26.57	9.27	9.19
B3	9.84	9.83	9.84	9.84	9.27	9.13	26.51	26.48	26.57	26.53	9.26	9.19
B4	9.84	9.82	9.84	9.83	9.24	9.12	26.46	26.47	26.46	26.48	9.25	9.23
B5	9.83	9.85	9.82	9.85	9.27	9.14	26.36	26.40	26.41	26.42	9.28	9.20
B6	9.81	9.82	9.83	9.82	9.23	9.08	26.36	26.37	26.34	26.39	9.24	9.18
B7	9.84	9.82	9.83	9.83	9.24	9.09	26.33	26.37	26.33	26.37	9.25	9.14
B8	9.82	9.84	9.85	9.83	9.24	9.07	26.34	26.36	26.34	26.38	9.25	9.15
B9	9.86	9.85	9.85	9.84	9.26	9.11	26.41	26.39	26.34	26.36	9.26	9.17
B10	9.85	9.84	9.84	9.85	9.24	9.10	26.39	26.40	26.38	26.35	9.26	9.14
B11	9.86	9.87	9.87	9.85	9.25	9.14	26.40	26.38	26.33	26.39	9.24	9.18
B12	9.84	9.83	9.86	9.87	9.31	9.21	26.42	26.43	26.39	26.40	9.28	9.24

Table E.4. Volumetric measurements for experiment 4

Specimen	1	2	3	4	5	6	7	8	9	10	11	12
1	9.69	9.70	9.69	9.66	9.21	9.23	68.92	68.92	68.88	68.89	9.21	9.21
2	9.71	9.73	9.70	9.71	9.21	9.22	68.96	68.95	68.93	68.93	9.21	9.24
3	9.72	9.75	9.71	9.77	9.22	9.22	68.96	68.97	68.96	68.97	9.21	9.20
4	9.75	9.80	9.71	9.73	9.21	9.23	68.97	68.96	68.96	68.98	9.20	9.23
5	9.76	9.78	9.68	9.77	9.22	9.24	69.00	68.99	68.99	68.98	9.22	9.23
6	9.73	9.76	9.72	9.74	9.23	9.25	68.99	68.99	68.99	68.99	9.21	9.24
7	9.72	9.77	9.70	9.74	9.24	9.24	68.99	68.98	69.00	68.99	9.22	9.25
8	9.77	9.77	9.73	9.73	9.20	9.22	68.98	68.99	68.99	69.00	9.21	9.22
9	9.75	9.77	9.71	9.76	9.22	9.22	69.00	68.98	68.99	68.99	9.20	9.24
10	9.75	9.79	9.71	9.77	9.24	9.25	68.98	68.98	68.99	68.98	9.22	9.24
11	9.78	9.78	9.71	9.75	9.23	9.24	68.98	68.98	69.00	68.98	9.20	9.22
12	9.76	9.77	9.74	9.73	9.24	9.25	68.99	68.98	68.98	69.03	9.21	9.24
A1	9.78	9.82	9.72	9.71	9.20	9.24	26.25	26.16	26.14	26.27	9.23	9.25
A2	9.77	9.79	9.72	9.74	9.18	9.24	26.25	26.18	26.14	26.25	9.23	9.23
A3	9.77	9.80	9.76	9.75	9.19	9.23	26.28	26.21	26.20	26.24	9.24	9.25
A4	9.78	9.83	9.78	9.75	9.18	9.25	26.33	26.32	26.27	26.29	9.23	9.24
A5	9.76	9.77	9.74	9.77	9.16	9.24	26.42	26.36	26.33	26.35	9.23	9.26
A6	9.74	9.81	9.74	9.75	9.18	9.24	26.49	26.43	26.36	26.44	9.22	9.24
A7	9.73	9.78	9.76	9.80	9.20	9.24	26.56	26.57	26.43	26.51	9.23	9.27
A8	9.73	9.80	9.77	9.77	9.19	9.22	26.67	26.72	26.56	26.56	9.21	9.23

Table E.4—continued

A9	9.76	9.79	9.76	9.77	9.17	9.21	26.84	26.85	26.73	26.70	9.23	9.23
A10	9.77	9.74	9.77	9.78	9.16	9.24	26.93	26.99	26.86	26.85	9.24	9.24
A11	9.78	9.78	9.76	9.77	9.17	9.24	27.03	27.04	27.00	26.96	9.23	9.23
A12	9.78	9.77	9.74	9.76	9.17	9.23	27.14	27.17	27.04	27.05	9.22	9.24
B1	9.69	9.74	9.77	9.82	9.22	9.24	22.94	22.81	22.88	23.04	9.07	9.15
B2	9.71	9.74	9.70	9.82	9.24	9.26	22.79	22.70	22.82	23.89	9.08	9.15
B3	9.74	9.79	9.73	9.75	9.22	9.22	22.63	22.56	22.66	23.77	9.08	9.14
B4	9.72	9.76	9.74	9.76	9.22	9.24	22.49	22.41	22.53	23.6	9.06	9.15
B5	9.73	9.72	9.74	9.78	9.23	9.23	22.38	22.24	22.38	23.48	9.06	9.14
B6	9.73	9.74	9.73	9.75	9.21	9.23	22.26	22.11	22.22	23.36	9.05	9.15
B7	9.72	9.73	9.73	9.76	9.24	9.27	22.20	22.03	22.10	23.25	9.06	9.19
B8	9.73	9.78	9.73	9.74	9.22	9.24	22.14	21.94	22.01	23.17	9.07	9.17
B9	9.74	9.72	9.76	9.76	9.22	9.24	22.12	21.94	21.92	23.12	9.06	9.17
B10	9.73	9.73	9.74	9.76	9.24	9.25	22.07	21.90	21.91	22.10	9.09	9.19
B11	9.72	9.76	9.78	9.76	9.24	9.23	22.02	21.91	21.88	22.06	9.08	9.18
B12	9.73	9.74	9.74	9.82	9.23	9.25	21.99	21.89	21.89	22.02	9.10	9.22

Table E.5. Volumetric measurements for experiment 5

Specimen	1	2	3	4	5	6	7	8	9	10	11	12
1	9.07	9.11	9.17	9.18	9.22	9.25	68.99	68.97	68.88	68.94	9.20	9.23
2	9.08	9.12	9.18	9.20	9.21	9.23	68.99	68.98	68.97	68.97	9.22	9.23
3	9.09	9.09	9.21	9.20	9.24	9.23	69.00	69.00	68.98	69.00	9.23	9.21
4	9.10	9.10	9.21	9.23	9.21	9.22	68.99	69.00	68.99	68.99	9.20	9.21
5	9.10	9.13	9.22	9.23	9.24	9.25	68.99	69.00	68.99	69.01	9.21	9.24
6	9.11	9.13	9.21	9.22	9.24	9.23	69.01	68.99	68.99	69.00	9.21	9.23
7	9.11	9.13	9.22	9.26	9.21	9.24	68.98	68.98	69.00	68.98	9.19	9.22
8	9.12	9.13	9.24	9.26	9.21	9.24	68.99	68.98	68.98	69.00	9.21	9.22
9	9.15	9.16	9.23	9.27	9.22	9.25	68.99	69.00	68.98	69.00	9.22	9.22
10	9.12	9.16	9.27	9.27	9.22	9.23	68.99	68.99	68.98	69.00	9.20	9.21
11	9.16	9.16	9.25	9.26	9.21	9.24	68.99	68.97	68.98	69.00	9.18	9.22
12	9.18	9.19	9.27	9.26	9.21	9.25	68.99	68.97	68.97	68.99	9.17	9.20
A1	9.05	9.06	9.04	9.07	9.15	9.23	25.93	25.88	25.92	26.00	9.22	9.22
A2	9.05	9.11	9.07	9.07	9.16	9.23	25.87	25.86	25.88	25.91	9.24	9.23
A3	9.05	9.09	9.09	9.11	9.16	9.22	25.86	25.78	25.85	25.87	9.21	9.22
A4	9.07	9.08	9.09	9.09	9.16	9.22	25.86	25.86	25.78	25.88	9.22	9.24
A5	9.06	9.10	9.10	9.09	9.15	9.23	25.87	25.86	25.85	25.87	9.22	9.24

125

A6	9.07	9.09	9.13	9.12	9.15	9.25	25.89	25.90	25.85	25.89	9.21	9.23
A7	9.08	9.10	9.12	9.11	9.13	9.23	25.92	25.94	25.89	25.89	9.20	9.23
A8	9.08	9.12	9.12	9.13	9.17	9.22	25.98	26.01	25.96	25.95	9.22	9.21
A9	9.10	9.14	9.14	9.14	9.15	9.23	26.00	26.04	26.00	26.00	9.21	9.24
A10	9.12	9.14	9.16	9.16	9.15	9.24	26.03	26.06	26.04	26.03	9.21	9.25
A11	9.12	9.13	9.16	9.17	9.15	9.24	26.12	26.11	26.06	26.05	9.21	9.26
A12	9.15	9.17	9.20	9.21	9.15	9.24	26.19	26.14	26.09	26.12	9.21	9.23
B1	9.18	9.23	9.20	9.22	9.20	9.25	20.94	20.93	20.58	20.69	9.11	9.17
B2	9.16	9.21	9.23	9.23	9.21	9.22	21.25	21.22	20.96	20.97	9.11	9.20
B3	9.19	9.23	9.23	9.24	9.20	9.21	21.53	21.47	21.24	21.29	9.08	9.16
B4	9.21	9.24	9.24	9.27	9.21	9.21	21.79	21.75	21.51	21.57	9.07	9.15
B5	9.20	9.24	9.24	9.24	9.21	9.23	22.04	21.95	21.74	21.83	9.09	9.14
B6	9.23	9.23	9.28	9.30	9.23	9.24	22.27	22.26	21.98	22.08	9.12	9.15
B7	9.23	9.25	9.31	9.39	9.21	9.22	22.57	22.55	22.29	22.30	9.12	9.17
B8	9.25	9.26	9.30	9.31	9.20	9.22	22.86	22.84	22.57	22.60	9.10	9.16
B9	9.22	9.27	9.30	9.32	9.21	9.24	23.15	23.12	22.85	22.90	9.13	9.17
B10	9.25	9.28	9.30	9.27	9.21	9.24	23.43	23.45	23.17	23.19	9.12	9.17
B11	9.26	9.31	9.30	9.31	9.22	9.22	23.72	23.72	23.46	23.46	9.08	9.18
B12	9.26	9.30	9.31	9.30	9.23	9.24	24.01	23.98	23.75	23.76	9.13	9.19

Table E.6. Volumetric measurements for experiment 6

Specimen	1	2	3	4	5	6	7	8	9	10	11	12
1	9.79	9.79	9.80	9.83	9.23	9.24	68.92	68.93	68.88	68.89	9.21	9.19
2	9.78	9.78	9.78	9.80	9.23	9.23	68.94	68.94	68.94	68.92	9.20	9.20
3	9.78	9.80	9.78	9.79	9.24	9.23	68.95	68.95	68.96	68.95	9.22	9.23
4	9.78	9.79	9.78	9.80	9.23	9.23	68.97	68.98	68.97	68.97	9.22	9.23
5	9.78	9.79	9.79	9.79	9.23	9.24	68.96	68.97	68.98	68.97	9.22	9.23
6	9.77	9.80	9.77	9.79	9.22	9.25	68.97	68.97	68.98	68.97	9.20	9.22
7	9.75	9.80	9.78	9.79	9.24	9.23	68.98	68.98	68.98	68.97	9.21	9.23
8	9.75	9.73	9.72	9.75	9.24	9.24	68.98	68.97	68.98	68.98	9.20	9.23
9	9.73	9.74	9.73	9.75	9.22	9.24	68.98	68.99	68.98	68.99	9.19	9.21
10	9.72	9.76	9.73	9.76	9.22	9.23	68.98	68.99	68.98	68.99	9.19	9.25
11	9.72	9.73	9.73	9.74	9.24	9.24	68.98	68.98	68.98	68.99	9.21	9.27
12	9.72	9.76	9.74	9.74	9.23	9.25	68.98	68.97	68.97	68.98	9.16	9.22
A1	9.82	9.80	9.78	9.81	9.19	9.21	26.26	26.29	26.31	26.27	9.23	9.21
A2	9.80	9.81	9.80	9.78	9.17	9.23	26.27	26.30	26.29	26.27	9.23	9.23

126

Table E.6—continued

A3	9.81	9.82	9.79	9.82	9.17	9.22	26.26	26.31	26.28	26.27	9.22	9.23
A4	9.81	9.81	9.79	9.81	9.16	9.23	26.26	26.28	26.31	26.28	9.22	9.24
A5	9.77	9.79	9.77	9.80	9.17	9.24	26.27	26.31	26.30	26.29	9.23	9.25
A6	9.79	9.76	9.76	9.79	9.17	9.21	26.27	26.31	26.30	26.29	9.23	9.25
A7	9.78	9.78	9.75	9.76	9.0	9.23	26.31	26.31	26.30	26.28	9.23	9.24
A8	9.78	9.76	9.73	9.77	9.18	9.23	26.28	26.31	26.31	26.30	9.23	9.24
A9	9.76	9.77	9.74	9.74	9.18	9.22	26.32	26.33	26.31	26.30	9.22	9.23
A10	9.75	9.74	9.74	9.74	9.19	9.22	26.30	26.32	26.32	26.32	9.23	9.25
A11	9.73	9.75	9.74	9.77	9.19	9.22	26.32	26.34	26.32	26.32	9.24	9.24
A12	9.75	9.77	9.77	9.76	9.20	9.24	26.32	26.34	26.33	26.32	9.23	9.25
B1	9.82	9.81	9.85	9.86	9.23	9.24	22.02	22.02	21.80	21.86	9.11	9.20
B2	9.82	9.84	9.84	9.84	9.21	9.23	22.23	22.19	22.05	22.05	9.09	9.15
B3	9.80	9.81	9.82	9.84	9.23	9.23	22.41	22.34	22.21	22.25	9.08	9.17
B4	9.79	9.80	9.82	9.82	9.23	9.24	22.55	22.50	22.40	22.42	9.11	9.19
B5	9.82	9.80	9.79	9.82	9.26	9.22	22.69	22.65	22.52	22.58	9.11	9.18
B6	9.78	9.79	9.78	9.80	9.23	9.25	22.82	22.77	22.67	22.71	9.11	9.17
B7	9.77	9.78	9.81	9.79	9.22	9.26	22.96	22.94	22.79	22.83	9.10	9.20
B8	9.78	9.76	9.80	9.79	9.21	9.22	23.11	23.07	22.95	22.98	9.09	9.17
B9	9.74	9.76	9.77	9.80	9.23	9.22	23.25	23.21	23.09	23.12	9.10	9.15
B10	9.74	9.76	9.74	9.75	9.24	9.23	23.38	23.35	23.22	23.25	9.10	9.17
B11	9.73	9.75	9.75	9.74	9.27	9.27	23.53	23.59	23.41	23.40	9.20	9.21
B12	9.72	9.76	9.75	9.75	9.23	9.40	23.67	23.65	23.61	23.54	9.06	9.28

Table E7. Volumetric measurements for experiment 7

Specimen	1	2	3	4	5	6	7	8	9	10	11	12
1	9.21	9.21	9.17	9.18	9.23	9.19	68.86	68.85	68.85	68.87	9.24	9.24
2	9.22	9.25	9.19	9.19	9.21	9.22	68.86	68.84	68.88	68.85	9.22	9.23
3	9.23	9.24	9.17	9.18	9.21	9.21	68.89	68.84	68.84	68.85	9.25	9.21
4	9.25	9.25	9.18	9.19	9.22	9.19	68.83	68.84	68.83	68.84	9.22	9.22
5	9.24	9.24	9.18	9.21	9.24	9.20	68.85	68.84	68.83	68.84	9.24	9.23
6	9.22	9.23	9.18	9.17	9.21	9.20	68.85	68.82	68.83	68.84	9.22	9.23
7	9.24	9.24	9.17	9.15	9.23	9.21	68.82	68.81	68.82	68.83	9.24	9.23
8	9.20	9.20	9.16	9.19	9.21	9.19	68.85	68.84	68.83	68.82	9.23	9.22
9	9.20	9.22	9.16	9.15	9.24	9.21	68.84	68.83	68.85	68.82	9.22	9.23
10	9.18	9.21	9.15	9.14	9.24	9.21	68.82	68.83	68.83	68.83	9.24	9.23
11	9.16	9.18	9.14	9.14	9.21	9.22	68.83	68.81	68.83	68.83	9.25	9.21

127

12	9.15	9.17	9.14	9.15	9.24	9.20	68.81	68.79	68.80	68.82	9.23	9.23
A1	9.22	9.25	9.22	9.21	9.22	9.24	25.64	25.79	25.66	25.79	9.25	9.24
A2	9.25	9.24	9.23	9.22	9.20	9.23	25.67	25.82	25.63	25.79	9.22	9.27
A3	9.22	9.25	9.22	9.22	9.22	9.23	25.72	25.82	25.67	25.81	9.24	9.23
A4	9.24	9.24	9.22	9.22	9.23	9.23	25.79	25.86	25.72	25.83	9.24	9.25
A5	9.24	9.25	9.24	9.23	9.21	9.24	25.82	26.00	25.77	25.91	9.25	9.24
A6	9.24	9.25	9.22	9.22	9.22	9.24	25.91	26.07	25.85	26.03	9.27	9.26
A7	9.25	9.26	9.21	9.22	9.22	9.23	26.09	26.24	25.93	26.11	9.26	9.26
A8	9.24	9.24	9.24	9.24	9.22	9.22	26.28	26.38	26.08	26.24	9.23	9.24
A9	9.24	9.22	9.19	9.21	9.23	9.21	26.43	26.59	26.25	26.39	9.24	9.25
A10	9.22	9.22	9.18	9.19	9.24	9.23	26.62	26.77	26.44	26.59	9.23	9.25
A11	9.21	9.20	9.16	9.17	9.23	9.23	26.83	26.95	26.63	26.86	9.25	9.26
A12	9.20	9.18	9.19	9.15	9.22	9.22	26.99	27.09	26.80	26.92	9.20	9.21
B1	9.19	9.20	9.20	9.18	9.22	9.07	26.83	26.80	26.81	26.73	9.23	9.14
B2	9.18	9.19	9.20	9.20	9.20	9.01	26.80	26.82	26.80	26.80	9.19	9.14
B3	9.20	9.21	9.21	9.22	9.22	9.03	26.80	26.80	26.82	26.83	9.22	9.20
B4	9.20	9.19	9.22	9.21	9.21	9.06	26.87	26.83	26.86	26.79	9.25	9.15
B5	9.20	9.18	9.23	9.20	9.20	9.05	26.85	26.81	26.83	26.83	9.23	9.19
B6	9.22	9.17	9.19	9.19	9.20	9.06	26.83	26.80	26.81	26.80	9.22	9.15
B7	9.18	9.16	9.22	9.18	9.23	9.04	26.82	26.76	26.80	26.80	9.28	9.17
B8	9.17	9.18	9.20	9.23	9.22	9.03	26.75	26.77	26.81	26.77	9.24	9.12
B9	9.18	9.15	9.18	9.17	9.21	9.06	26.81	26.77	26.80	26.77	9.26	9.13
B10	9.13	9.15	9.18	9.19	9.23	9.04	26.71	26.71	26.76	26.76	9.25	9.15
B11	9.15	9.14	9.17	9.18	9.22	9.06	26.67	26.67	26.57	26.71	9.23	9.14
B12	9.15	9.15	9.16	9.17	9.25	9.08	26.70	26.65	26.65	26.65	9.26	9.17

Table E8. Volumetric measurements for experiment 8

Specimen	1	2	3	4	5	6	7	8	9	10	11	12
1	9.20	9.20	9.20	9.20	9.23	9.25	68.98	68.98	68.85	68.94	9.23	9.25
2	9.19	9.20	9.20	9.21	9.23	9.24	69.00	69.00	68.98	69.01	9.26	9.25
3	9.20	9.20	9.21	9.21	9.23	9.25	69.00	69.00	69.00	69.02	9.25	9.25
4	9.20	9.21	9.19	9.22	9.23	9.24	69.00	69.00	69.00	69.01	9.24	9.24
5	9.18	9.20	9.19	9.19	9.23	9.22	68.99	69.01	69.01	69.01	9.25	9.25
6	9.19	9.19	9.18	9.20	9.22	9.25	68.99	69.00	69.00	69.02	9.23	9.23
7	9.19	9.18	9.16	9.18	9.22	9.26	68.98	68.99	68.99	69.01	9.23	9.22
8	9.17	9.16	9.17	9.18	9.22	9.23	68.99	68.99	68.99	69.00	9.22	9.24

9	9.16	9.17	9.13	9.16	9.21	9.25	68.99	69.00	68.99	69.02	9.24	9.23
10	9.15	9.16	9.13	9.15	9.22	9.24	68.99	69.00	68.99	69.01	9.21	9.23
11	9.12	9.13	9.12	9.12	9.23	9.24	68.99	69.01	68.99	69.02	9.23	9.22
12	9.12	9.13	9.14	9.14	9.23	9.25	68.99	69.02	69.00	69.02	9.20	9.22
A1	9.25	9.24	9.19	9.19	9.18	9.23	26.24	26.11	26.21	26.09	9.24	9.24
A2	9.24	9.24	9.19	9.19	9.21	9.24	26.3	26.16	26.25	26.11	9.22	9.24
A3	9.25	9.26	9.17	9.19	9.22	9.23	26.33	26.21	26.29	26.19	9.23	9.24
A4	9.23	9.24	9.20	9.18	9.22	9.23	26.34	26.23	26.32	26.20	9.23	9.24
A5	9.21	9.22	9.21	9.21	9.21	9.23	26.39	26.27	26.39	26.25	9.23	9.23
A6	9.18	9.20	9.19	9.19	9.20	9.24	26.40	26.37	26.35	26.31	9.23	9.23
A7	9.17	9.20	9.18	9.19	9.20	9.24	26.44	26.38	26.38	26.33	9.23	9.24
A8	9.15	9.16	9.14	9.15	9.15	9.23	26.44	26.40	26.41	26.37	9.20	9.26
A9	9.16	9.15	9.14	9.16	9.11	9.21	26.46	26.40	26.44	26.43	9.20	9.22
A10	9.14	9.12	9.14	9.13	9.13	9.23	26.49	26.36	26.45	26.41	9.22	9.24
A11	9.12	9.11	9.11	9.13	9.14	9.24	26.46	26.28	26.46	26.37	9.20	9.24
A12	9.10	9.10	9.10	9.13	9.13	9.23	26.30	26.22	26.40	26.28	9.21	9.25
B1	9.21	9.21	9.21	9.22	9.22	9.23	20.83	20.93	20.46	20.68	8.90	9.16
B2	9.21	9.21	9.22	9.23	9.17	9.25	21.21	21.10	20.84	20.98	8.93	9.19
B3	9.20	9.21	9.21	9.22	9.22	9.24	21.43	21.32	21.10	21.22	8.89	9.15
B4	9.16	9.21	9.18	9.21	9.21	9.23	21.62	21.54	21.28	21.41	8.87	9.17
B5	9.19	9.19	9.19	9.20	9.18	9.24	21.82	21.77	21.54	21.62	8.93	9.14
B6	9.21	9.20	9.16	9.20	9.22	9.25	21.99	21.93	21.81	21.88	8.91	9.16
B7	9.18	9.20	9.11	9.16	9.18	9.23	22.21	22.11	21.97	22.02	8.88	9.16
B8	9.16	9.18	9.12	9.11	9.22	9.25	22.42	22.35	22.14	22.26	8.89	9.18
B9	9.15	9.16	9.15	9.18	9.20	9.26	22.66	22.58	22.41	22.47	8.95	9.16
B10	9.17	9.14	9.07	9.16	9.20	9.26	22.85	22.79	22.57	22.69	8.96	9.21
B11	9.11	9.15	9.08	9.13	9.24	9.28	23.05	23.01	22.82	22.86	9.03	9.21
B12	9.17	9.18	9.14	9.11	9.24	9.29	23.25	23.23	23.00	23.08	9.12	9.25

Table E.9. Volumetric measurements for experiment 9

Specimen	1	2	3	4	5	6	7	8	9	10	11	12
1	9.63	9.61	9.61	9.66	9.19	9.23	68.88	68.90	68.84	68.87	9.21	9.24
2	9.60	9.65	9.63	9.65	9.22	9.22	68.95	68.94	68.92	68.92	9.20	9.21
3	9.60	9.63	9.64	9.66	9.21	9.23	68.96	68.96	68.94	68.96	9.19	9.22
4	9.62	9.63	9.65	9.64	9.21	9.23	68.97	68.98	68.97	68.97	9.20	9.24
5	9.64	9.63	9.66	9.66	9.19	9.23	68.98	68.98	68.98	68.99	9.19	9.23

Table E.9—continued

6	9.65	9.65	9.65	9.67	9.20	9.25	68.98	69.00	68.99	68.99	9.20	9.24
7	9.66	9.66	9.68	9.68	9.20	9.25	68.99	68.99	68.98	68.99	9.20	9.21
8	9.67	9.67	9.67	9.68	9.21	9.24	69.00	69.00	68.99	69.00	9.20	9.22
9	9.68	9.68	9.69	9.70	9.21	9.25	69.00	69.00	69.00	69.01	9.21	9.24
10	9.68	9.69	9.70	9.70	9.21	9.24	69.00	69.00	69.00	69.00	9.21	9.23
11	9.69	9.70	9.68	9.69	9.22	9.24	69.00	68.99	69.01	69.00	9.20	9.21
12	9.69	9.69	9.68	9.70	9.21	9.24	69.00	68.98	68.99	69.00	9.19	9.23
A1	9.62	9.63	9.60	9.63	9.17	9.21	26.01	25.88	25.90	25.94	9.23	9.25
A2	9.63	9.64	9.62	9.61	9.19	9.21	26.05	26.05	25.90	26.04	9.22	9.22
A3	9.63	9.64	9.63	9.62	9.19	9.21	26.08	26.08	26.06	26.06	9.24	9.23
A4	9.63	9.65	9.65	9.64	9.20	9.24	26.09	26.13	26.08	26.10	9.24	9.23
A5	9.65	9.65	9.65	9.70	9.19	9.20	26.12	26.12	26.13	26.13	9.24	9.24
A6	9.66	9.66	9.64	9.68	9.21	9.21	26.06	26.05	26.08	26.13	9.23	9.26
A7	9.68	9.67	9.67	9.68	9.20	9.21	26.05	26.01	26.02	26.07	9.22	9.24
A8	9.67	9.69	9.69	9.68	9.20	9.22	26.05	25.98	26.01	26.03	9.23	9.25
A9	9.68	9.67	9.68	9.71	9.19	9.24	26.11	26.05	25.98	26.07	9.25	9.26
A10	9.71	9.70	9.70	9.68	9.21	9.23	26.13	26.11	26.02	26.11	9.22	9.23
A11	9.69	9.72	9.66	9.71	9.18	9.22	26.20	26.16	26.09	26.18	9.22	9.24
A12	9.70	9.72	9.68	9.69	9.19	9.22	26.27	26.21	26.16	26.22	9.24	9.23
B1	9.67	9.71	9.64	9.65	9.25	9.27	27.80	27.69	27.72	27.90	9.07	9.18
B2	9.65	9.68	9.65	9.64	9.24	9.21	27.65	27.55	27.66	27.77	9.00	9.13
B3	9.64	9.64	9.66	9.60	9.22	9.23	27.54	27.32	27.52	27.63	9.02	9.13
B4	9.65	9.68	9.70	9.67	9.23	9.24	27.40	27.20	27.22	27.52	9.01	9.14
B5	9.67	9.67	9.69	9.70	9.23	9.23	27.27	27.17	27.19	27.73	9.08	9.13
B6	9.68	9.67	9.72	9.69	9.24	9.28	27.19	27.12	27.14	27.23	9.06	9.21
B7	9.67	9.69	9.71	9.71	9.23	9.25	27.15	27.01	27.12	27.19	9.04	9.17
B8	9.68	9.70	9.73	9.71	9.22	9.23	27.10	26.95	26.97	27.13	9.02	9.14
B9	9.70	9.72	9.73	9.73	9.22	9.24	27.09	26.98	26.93	27.09	9.06	9.15
B10	9.71	9.74	9.72	9.73	9.24	9.25	27.06	26.90	26.91	27.05	9.05	9.18
B11	9.70	9.69	9.73	9.73	9.23	9.25	27.07	26.93	26.88	27.04	9.04	9.15
B12	9.71	9.71	9.72	9.74	9.25	9.25	27.08	26.95	26.91	27.06	9.08	9.21

130

Table E.10. Volumetric measurements for experiment 10

Specimen	1	2	3	4	5	6	7	8	9	10	11	12
1	9.66	9.68	9.67	9.70	9.23	9.25	68.92	68.90	68.86	68.88	9.25	9.25
2	9.66	9.65	9.67	9.67	9.21	9.23	68.94	68.93	68.93	68.92	9.22	9.22
3	9.67	9.66	9.67	9.65	9.22	9.25	68.96	68.97	68.94	68.94	9.22	9.23
4	9.66	9.65	9.66	9.67	9.21	9.22	68.95	68.96	68.94	68.96	9.22	9.23
5	9.67	9.67	9.68	9.68	9.22	9.23	68.96	68.96	68.94	68.95	9.23	9.25
6	9.66	9.66	9.67	9.68	9.21	9.24	68.98	68.97	68.97	68.96	9.22	9.23
7	9.66	9.68	9.67	9.68	9.21	9.22	68.97	68.98	68.97	68.96	9.21	9.24
8	9.63	9.65	9.63	9.61	9.20	9.21	68.98	68.97	68.97	68.98	9.22	9.23
9	9.64	9.63	9.65	9.68	9.22	9.25	68.97	68.98	68.98	68.99	9.22	9.23
10	9.62	9.63	9.63	9.65	9.22	9.24	68.99	68.98	68.97	68.99	9.19	9.19
11	9.62	9.64	9.68	9.66	9.22	9.25	68.99	68.99	68.97	68.98	9.22	9.24
12	9.62	9.65	9.64	9.65	9.22	9.24	68.97	68.97	68.97	68.98	9.20	9.22
A1	9.68	9.68	9.67	9.67	9.18	9.23	26.12	26.14	26.20	26.15	9.24	9.26
A2	9.67	9.67	9.66	9.67	9.18	9.22	26.06	26.07	26.13	26.11	9.23	9.25
A3	9.68	9.68	9.66	9.66	9.16	9.22	26.02	26.14	26.04	26.06	9.21	9.23
A4	9.68	9.68	9.66	9.66	9.15	9.24	26.03	26.14	26.14	26.02	9.23	9.25
A5	9.68	9.68	9.67	9.66	9.18	9.21	26.04	26.13	26.12	26.03	9.22	9.24
A6	9.66	9.68	9.66	9.67	9.17	9.21	26.03	26.14	26.14	26.05	9.23	9.25
A7	9.67	9.68	9.67	9.67	9.17	9.21	26.07	26.12	26.13	26.06	9.22	9.22
A8	9.57	9.67	9.67	9.65	9.17	9.20	26.04	26.20	26.12	26.09	9.20	9.21
A9	9.68	9.67	9.65	9.67	9.16	9.22	26.07	26.17	26.22	26.06	9.22	9.23
A10	9.68	9.65	9.64	9.65	9.17	9.22	26.09	26.18	26.18	26.09	9.23	9.23
A11	9.66	9.66	9.64	9.67	9.18	9.23	26.09	26.20	26.19	26.10	9.21	9.23
A12	9.65	9.64	9.64	9.67	9.17	9.20	26.11	26.23	26.22	26.11	9.21	9.24
B1	9.69	9.69	9.67	9.70	9.26	9.26	27.19	27.12	26.93	27.03	9.06	9.18
B2	9.67	9.70	9.68	9.71	9.22	9.23	27.39	27.30	27.13	27.20	9.07	9.14
B3	9.68	9.70	9.66	9.71	9.23	9.25	27.56	27.49	27.32	27.40	9.04	9.16
B4	9.68	9.68	9.66	9.67	9.23	9.24	27.72	27.67	27.51	27.56	9.03	9.17
B5	9.68	9.68	9.67	9.66	9.24	9.27	27.87	27.85	27.69	27.72	9.06	9.17
B6	9.69	9.68	9.67	9.68	9.23	9.24	28.06	28.01	27.85	27.90	9.06	9.20
B7	9.70	9.70	9.59	9.69	9.24	9.25	28.21	28.19	28.05	28.06	9.03	9.14
B8	9.65	9.68	9.66	9.44	9.22	9.24	28.39	28.38	28.22	28.23	9.06	9.21
B9	9.66	9.66	9.68	9.68	9.23	9.22	28.55	28.54	28.39	28.40	9.07	9.17
B10	9.66	9.68	9.67	9.68	9.21	9.21	28.74	28.68	28.54	28.55	9.05	9.16
B11	9.65	9.67	9.66	9.69	9.24	9.28	28.92	28.89	28.70	28.78	9.06	9.16
B12	9.66	9.70	9.64	9.67	9.23	9.25	29.10	29.06	28.88	28.95	9.09	9.26

131

Table E.11. Volumetric measurements for experiment 11

Specimen	1	2	3	4	5	6	7	8	9	10	11	12
1	9.77	9.77	9.76	9.76	9.24	9.26	68.94	68.94	68.86	68.90	9.25	9.24
2	9.76	9.75	9.77	9.77	9.22	9.24	68.95	68.96	68.94	68.95	9.25	9.24
3	9.75	9.77	9.77	9.76	9.24	9.24	68.95	68.96	68.97	68.97	9.23	9.22
4	9.74	9.76	9.75	9.77	9.24	9.22	68.95	68.96	68.97	68.97	9.22	9.23
5	9.74	9.75	9.76	9.75	9.23	9.22	68.97	68.97	68.96	68.97	9.21	9.22
6	9.75	9.75	9.77	9.75	9.23	9.23	68.96	68.97	68.97	68.98	9.23	9.22
7	9.74	9.75	9.74	9.76	9.23	9.23	68.98	68.99	68.97	68.97	9.22	9.24
8	9.74	9.76	9.72	9.77	9.21	9.23	68.97	68.99	68.97	68.98	9.22	9.23
9	9.73	9.74	9.74	9.77	9.21	9.24	68.98	68.99	68.98	68.99	9.19	9.21
10	9.73	9.74	9.76	9.77	9.21	9.23	68.99	69.00	69.00	69.00	9.20	9.21
11	9.71	9.72	9.75	9.76	9.22	9.25	68.98	69.02	68.98	69.01	9.20	9.21
12	9.71	9.72	9.78	9.77	9.23	9.24	68.99	69.01	68.99	69.00	9.19	9.21
A1	9.74	9.79	9.76	9.75	9.16	9.25	26.10	26.15	26.13	26.14	9.21	9.25
A2	9.80	9.79	9.76	9.76	9.16	9.24	26.09	26.18	26.16	26.10	9.21	9.25
A3	9.79	9.79	9.75	9.76	9.13	9.27	26.11	26.15	26.18	26.12	9.20	9.25
A4	9.78	9.78	9.74	9.75	9.15	9.24	26.16	26.16	26.14	26.14	9.22	9.24
A5	9.78	9.77	9.75	9.74	9.14	9.24	26.18	26.22	26.17	26.15	9.22	9.24
A6	9.77	9.73	9.75	9.74	9.14	9.23	26.18	26.25	26.22	26.17	9.20	9.22
A7	9.72	9.76	9.71	9.76	9.16	9.24	26.19	26.30	26.24	26.21	9.19	9.22
A8	9.72	9.75	9.71	9.75	9.18	9.26	26.26	26.32	26.30	26.28	9.22	9.26
A9	9.73	9.77	9.72	9.78	9.19	9.24	26.30	26.34	26.29	26.30	9.20	9.23
A10	9.72	9.72	9.71	9.73	9.16	9.23	26.26	26.40	26.33	26.34	9.21	9.24
A11	9.71	9.71	9.71	9.74	9.15	9.25	26.36	26.43	26.38	26.34	9.21	9.24
A12	9.69	9.73	9.72	9.73	9.15	9.25	26.41	26.47	26.41	26.41	9.20	9.24
B1	9.77	9.75	9.79	9.82	9.21	9.23	31.71	31.62	31.35	31.61	8.87	9.17
B2	9.75	9.76	9.75	9.83	9.24	9.30	31.74	31.66	31.63	31.67	9.02	9.16
B3	9.76	9.79	9.78	9.82	9.23	9.30	31.75	31.66	31.61	31.65	8.96	9.17
B4	9.77	9.76	9.79	9.79	9.21	9.27	31.65	31.60	31.66	31.74	8.88	9.15
B5	9.78	9.79	9.80	9.81	9.21	9.25	31.68	31.61	31.55	31.70	8.92	9.14
B6	9.76	9.77	9.78	9.82	9.22	9.25	31.66	31.58	31.61	31.67	8.92	9.14
B7	9.76	9.79	9.77	9.82	9.23	9.26	31.59	31.55	31.57	31.66	8.90	9.15
B8	9.77	9.73	9.78	9.83	9.23	9.25	31.57	31.55	31.55	31.63	8.96	9.17
B9	9.79	9.77	9.74	9.77	9.23	9.25	31.61	31.52	31.53	31.60	8.87	9.15
B10	9.72	9.75	9.71	9.77	9.23	9.22	31.51	31.52	31.51	31.60	8.95	9.18
B11	9.74	9.80	9.74	9.77	9.24	9.24	31.49	31.49	31.51	31.55	8.96	9.14
B12	9.75	9.82	9.77	9.78	9.25	9.30	31.49	31.47	31.49	31.48	9.08	9.25

132

Table E.12. Volumetric measurements for experiment 12

Specimen	1	2	3	4	5	6	7	8	9	10	11	12
1	9.50	9.51	9.46	9.48	9.23	9.24	68.91	68.93	68.89	68.91	9.23	9.26
2	9.49	9.53	9.51	9.46	9.22	9.23	68.93	68.94	68.93	68.92	9.21	9.24
3	9.50	9.51	9.48	9.53	9.21	9.25	68.93	68.95	68.94	68.94	9.19	9.24
4	9.51	9.54	9.50	9.50	9.20	9.23	68.94	68.96	68.96	68.94	9.20	9.23
5	9.50	9.50	9.48	9.48	9.20	9.20	68.94	68.95	68.93	68.94	9.18	9.21
6	9.49	9.50	9.49	9.47	9.19	9.20	68.95	68.95	68.94	68.94	9.19	9.22
7	9.51	9.53	9.47	9.52	9.21	9.24	68.96	68.96	68.96	68.96	9.21	9.23
8	9.52	9.52	9.49	9.50	9.22	9.23	68.95	68.96	68.97	68.97	9.20	9.23
9	9.49	9.51	9.49	9.49	9.22	9.22	68.97	68.97	68.97	68.97	9.20	9.25
10	9.52	9.51	9.52	9.52	9.22	9.22	68.97	68.97	68.96	68.99	9.19	9.24
11	9.50	9.50	9.51	9.51	9.22	9.26	68.97	68.97	68.97	68.98	9.20	9.24
12	9.51	9.50	9.46	9.50	9.22	9.26	68.98	68.98	68.98	68.98	9.21	9.24
A1	9.54	9.54	9.50	9.51	9.15	9.25	26.04	26.07	26.07	26.04	9.23	9.26
A2	9.54	9.55	9.52	9.50	9.18	9.24	26.04	26.04	26.07	26.04	9.24	9.23
A3	9.52	9.47	9.53	9.55	9.15	9.23	26.01	26.00	26.03	26.04	9.24	9.25
A4	9.51	9.56	9.51	9.53	9.16	9.23	26.01	25.97	25.99	26.02	9.22	9.23
A5	9.54	9.53	9.48	9.53	9.16	9.22	25.95	25.94	25.94	26.00	9.23	9.25
A6	9.51	9.55	9.51	9.52	9.17	9.22	25.97	25.91	25.93	25.97	9.23	9.24
A7	9.51	9.52	9.51	9.52	9.14	9.23	26.01	25.91	25.94	25.98	9.22	9.24
A8	9.53	9.51	9.49	9.50	9.13	9.24	26.03	25.96	25.91	25.98	9.22	9.24
A9	9.52	9.52	9.50	9.48	9.12	9.24	26.04	25.98	25.93	25.99	9.21	9.24
A10	9.50	9.47	9.49	9.51	9.13	9.25	26.12	26.05	25.99	26.07	9.23	9.26
A11	9.44	9.52	9.50	9.50	9.12	9.24	26.22	26.15	26.07	26.14	9.21	9.27
A12	9.52	9.40	9.52	9.44	9.14	9.24	26.30	26.23	26.15	26.23	9.20	9.25
B1	9.48	9.48	9.49	9.45	9.22	9.26	28.15	28.12	28.24	28.24	9.05	9.20
B2	9.46	9.50	9.48	9.51	9.22	9.22	27.94	27.91	28.08	28.12	9.06	9.16
B3	9.45	9.49	9.45	9.47	9.19	9.23	27.76	27.67	27.87	27.92	9.08	9.14
B4	9.50	9.51	9.46	9.44	9.21	9.21	27.53	27.45	27.67	27.72	9.06	9.13
B5	9.49	9.49	9.46	9.49	9.21	9.22	27.28	27.24	27.40	27.48	9.06	9.13
B6	9.47	9.50	9.43	9.50	9.24	9.23	27.07	27.05	27.19	27.24	9.06	9.15
B7	9.47	9.50	9.48	9.44	9.21	9.20	26.83	26.84	27.00	27.05	9.07	9.14
B8	9.47	9.47	9.45	9.50	9.22	9.22	26.65	26.61	26.81	26.82	9.06	9.14
B9	9.48	9.48	9.44	9.50	9.20	9.21	26.46	26.35	26.60	26.64	9.07	9.13
B10	9.48	9.49	9.48	9.48	9.19	9.22	26.27	26.23	26.32	26.45	9.06	9.14
B11	9.46	9.51	9.49	9.48	9.21	9.23	26.14	26.06	26.18	26.25	9.06	9.15
B12	9.48	9.49	9.41	9.43	9.23	9.28	26.01	25.86	26.02	26.13	9.10	9.19

133

Table E.13. Volumetric measurements for experiment 13

Specimen	1	2	3	4	5	6	7	8	9	10	11	12
1	9.25	9.27	9.28	9.26	9.08	9.15	68.87	68.91	68.90	68.92	9.11	9.14
2	9.24	9.24	9.27	9.25	9.04	9.17	68.90	68.94	68.90	68.92	9.08	9.13
3	9.28	9.29	9.26	9.27	9.04	9.12	68.90	68.92	68.92	68.93	9.05	9.15
4	9.28	9.27	9.27	9.26	9.04	9.16	68.90	68.92	68.92	68.92	9.11	9.14
5	9.28	9.26	9.24	9.24	9.06	9.13	68.89	68.91	68.89	68.90	9.08	9.15
6	9.26	9.25	9.25	9.24	9.05	9.15	68.89	68.91	68.90	68.90	9.12	9.16
7	9.24	9.24	9.24	9.21	9.07	9.14	68.88	68.89	68.90	68.89	9.08	9.16
8	9.26	9.24	9.25	9.23	9.06	9.18	68.88	68.89	68.88	68.89	9.09	9.19
9	9.28	9.29	9.25	9.22	9.09	9.13	68.88	68.90	68.88	68.89	9.09	9.15
10	9.25	9.25	9.21	9.22	9.05	9.14	68.92	68.90	68.91	68.90	9.04	9.15
11	9.26	9.25	9.20	9.23	9.05	9.12	68.87	68.89	68.88	68.89	9.05	9.15
12	9.25	9.26	9.25	9.24	9.05	9.11	68.84	68.87	68.87	68.87	9.07	9.12
A1	9.24	9.25	9.25	9.25	9.05	9.04	25.23	25.25	25.20	25.23	9.06	9.02
A2	9.23	9.25	9.25	9.25	9.04	9.04	25.24	25.28	25.29	25.24	9.04	9.03
A3	9.24	9.25	9.25	9.25	9.04	9.05	25.28	25.29	25.25	25.26	9.04	9.06
A4	9.22	9.27	9.28	9.24	9.04	9.06	25.29	25.32	25.29	25.30	9.07	9.06
A5	9.28	9.25	9.24	9.24	9.02	9.07	25.33	25.36	25.31	25.34	9.06	9.11
A6	9.25	9.26	9.25	9.25	9.06	9.07	25.36	25.39	25.35	25.35	9.06	9.06
A7	9.23	9.26	9.24	9.25	9.05	9.08	25.42	25.42	25.38	25.40	9.07	9.07
A8	9.25	9.24	9.24	9.25	9.07	9.08	25.43	25.48	25.42	25.45	9.06	9.07
A9	9.23	9.23	9.25	9.25	9.05	9.05	25.49	25.51	25.45	25.49	9.06	9.06
A10	9.23	9.24	9.24	9.23	9.06	9.07	25.49	25.54	25.48	25.52	9.08	9.08
A11	9.24	9.26	9.24	9.23	9.06	9.05	25.52	25.57	25.49	25.55	9.07	9.06
A12	9.25	9.24	9.27	9.26	9.04	9.06	25.54	25.50	25.51	25.56	9.05	9.05
B1	9.23	9.25	9.18	9.14	9.11	9.16	26.71	26.69	26.66	26.63	9.11	9.14
B2	9.23	9.22	9.18	9.15	9.13	9.11	26.72	26.73	26.69	26.69	9.14	9.16
B3	9.22	9.24	9.19	9.16	9.14	9.16	26.67	26.70	26.70	26.71	9.12	9.17
B4	9.24	9.25	9.20	9.17	9.12	9.12	26.65	26.66	26.70	26.68	9.13	9.18
B5	9.23	9.23	9.18	9.20	9.13	9.13	26.69	26.64	26.62	26.63	9.18	9.17
B6	9.24	9.26	9.19	9.19	9.16	9.11	26.63	26.64	26.67	26.62	9.15	9.19
B7	9.23	9.24	9.20	9.19	9.16	9.11	26.64	26.63	26.62	26.61	9.16	9.16
B8	9.24	9.25	9.17	9.18	9.17	9.10	26.63	26.59	26.59	26.63	9.18	9.18
B9	9.26	9.27	9.16	9.18	9.17	9.12	26.60	26.60	26.62	26.59	9.16	9.18
B10	9.25	9.25	9.19	9.17	9.14	9.12	26.63	26.61	26.63	26.59	9.14	9.19
B11	9.25	9.27	9.14	9.17	9.11	9.13	26.57	26.60	26.59	26.57	9.13	9.18
B12	9.27	9.29	9.14	9.16	9.11	9.16	26.54	26.54	26.54	26.54	9.13	9.21

134

Table E.14. Volumetric measurements for experiment 14

Specimen	1	2	3	4	5	6	7	8	9	10	11	12
1	9.53	9.55	9.55	9.58	9.23	9.28	68.94	68.94	68.89	68.92	9.25	9.27
2	9.54	9.55	9.53	9.55	9.20	9.24	68.93	68.95	68.96	68.95	9.18	9.24
3	9.53	9.55	9.54	9.52	9.25	9.24	68.95	68.98	68.91	68.97	9.28	9.23
4	9.52	9.54	9.57	9.54	9.22	9.23	68.97	68.96	68.93	68.90	9.25	9.23
5	9.53	9.53	9.53	9.56	9.22	9.24	68.94	68.96	68.95	68.99	9.22	9.24
6	9.55	9.56	9.53	9.54	9.26	9.26	68.96	68.95	68.94	68.96	9.28	9.29
7	9.56	9.58	9.55	9.53	9.22	9.21	68.94	68.94	68.95	68.95	9.23	9.23
8	9.55	9.55	9.56	9.56	9.20	9.25	68.92	68.93	68.92	68.94	9.22	9.23
9	9.55	9.58	9.55	9.58	9.21	9.24	68.92	68.93	68.94	68.92	9.21	9.25
10	9.58	9.55	9.54	9.54	9.25	9.23	68.94	68.93	68.93	68.94	9.24	9.22
11	9.54	9.55	9.54	9.57	9.23	9.24	68.92	68.93	68.93	68.95	9.19	9.22
12	9.56	9.58	9.56	9.54	9.21	9.25	68.90	68.92	68.92	68.95	9.25	9.25
A1	9.52	9.56	9.53	9.53	9.10	9.28	26.66	26.54	26.59	26.54	9.22	9.3
A2	9.54	9.55	9.54	9.57	9.03	9.20	26.63	26.56	26.61	26.52	9.16	9.23
A3	9.55	9.53	9.54	9.53	9.03	9.23	26.69	26.57	26.64	26.54	9.18	9.23
A4	9.53	9.58	9.55	9.57	9.00	9.20	26.63	26.71	26.69	26.63	9.18	9.22
A5	9.54	9.54	9.60	9.56	9.05	9.22	26.73	26.69	26.71	26.63	9.14	9.25
A6	9.56	9.55	9.57	9.57	9.02	9.27	26.75	26.77	26.76	26.71	9.22	9.28
A7	9.56	9.55	9.58	9.57	8.98	9.19	26.79	26.72	26.78	26.76	9.19	9.22
A8	9.58	9.57	9.57	9.56	8.95	9.21	26.82	26.8	26.82	26.71	9.13	9.21
A9	9.57	9.56	9.55	9.57	9.01	9.26	26.84	26.79	26.82	26.78	9.18	9.25
A10	9.57	9.58	9.57	9.58	9.01	9.23	26.88	25.85	26.86	26.8	9.15	9.23
A11	9.57	9.59	9.56	9.57	8.94	9.21	26.89	26.87	26.87	26.86	9.11	9.21
A12	9.57	9.57	9.55	9.56	8.94	9.19	26.93	26.89	26.90	26.93	9.15	9.21
B1	9.56	9.56	9.51	9.54	9.24	9.26	26.67	27.50	27.67	27.92	9.24	9.28
B2	9.52	9.51	9.52	9.54	9.23	9.21	26.24	27.40	27.10	27.52	9.24	9.24
B3	9.52	9.52	9.53	9.52	9.24	9.22	26.74	27.85	27.01	27.12	9.24	9.25
B4	9.52	9.51	9.52	9.54	9.23	9.24	26.33	27.49	27.65	27.76	9.24	9.24
B5	9.54	9.56	9.52	9.50	9.27	9.24	26.12	27.91	27.24	27.40	9.22	9.23
B6	9.53	9.52	9.58	9.55	9.25	9.21	25.73	25.66	25.84	26.00	9.26	9.25
B7	9.56	9.58	9.56	9.60	9.25	9.28	25.43	25.35	25.57	25.61	9.26	9.29
B8	9.54	9.56	9.55	9.57	9.25	9.24	25.01	25.14	25.24	25.36	9.26	9.29
B9	9.55	9.56	9.54	9.59	9.25	9.21	24.81	24.87	24.92	25.07	9.24	9.24
B10	9.57	9.55	9.54	9.56	9.23	9.25	24.49	24.59	24.63	24.87	9.25	9.27
B11	9.56	9.58	9.55	9.53	9.23	9.23	24.27	24.35	24.43	24.56	9.27	9.26
B12	9.54	9.57	9.56	9.57	9.24	9.27	24.04	24.16	24.18	24.29	9.26	9.25

135

Table E.15. Volumetric measurements for experiment 15

Specimen	1	2	3	4	5	6	7	8	9	10	11	12
1	9.57	9.56	9.56	9.55	9.08	9.08	68.84	68.83	68.81	68.93	9.15	9.15
2	9.58	9.56	9.59	9.55	9.15	9.17	68.81	68.82	68.82	68.83	9.15	9.15
3	9.58	9.57	9.56	9.56	9.18	9.16	68.82	68.81	68.80	68.82	9.16	9.16
4	9.58	9.57	9.57	9.56	9.16	9.16	68.82	68.83	68.81	68.82	9.18	9.14
5	9.58	9.59	9.57	9.56	9.20	9.19	68.84	68.82	68.82	68.82	9.20	9.19
6	9.58	9.57	9.55	9.54	9.23	9.23	68.84	68.82	68.82	68.83	9.23	9.23
7	9.58	9.56	9.55	9.53	9.22	9.23	68.85	68.84	68.83	68.83	9.21	9.21
8	9.58	9.55	9.55	9.52	9.16	9.16	68.85	68.84	68.84	68.83	9.15	9.12
9	9.58	9.57	9.54	9.56	9.18	9.20	68.85	68.86	68.85	68.85	9.18	9.19
10	9.56	9.57	9.54	9.55	9.14	9.15	68.86	68.85	68.85	68.86	9.11	9.16
11	9.56	9.52	9.54	9.53	9.13	9.15	68.83	68.83	68.85	68.84	9.15	9.15
12	9.54	9.56	9.57	9.56	9.11	9.05	68.8	68.82	68.85	68.83	9.08	9.12
A1	9.57	9.57	9.54	9.54	9.24	9.22	28.25	28.25	28.20	28.22	9.24	9.23
A2	9.56	9.57	9.56	9.55	9.23	9.23	28.33	28.32	28.26	28.28	9.22	9.22
A3	9.60	9.58	9.56	9.55	9.23	9.24	28.38	28.34	28.33	28.34	9.22	9.23
A4	9.58	9.59	9.57	9.55	9.24	9.23	28.42	28.40	28.34	28.37	9.22	9.23
A5	9.57	9.57	9.57	9.54	9.24	9.22	28.48	28.43	28.39	28.42	9.21	9.22
A6	9.58	9.56	9.54	9.54	9.23	9.22	28.52	28.48	28.46	28.47	9.21	9.23
A7	9.58	9.58	9.55	9.55	9.21	9.21	28.57	28.55	28.53	28.55	9.21	9.20
A8	9.58	9.56	9.54	9.53	9.21	9.24	28.60	28.56	28.54	28.58	9.20	9.21
A9	9.57	9.59	9.55	9.54	9.24	9.24	28.64	28.62	28.58	28.62	9.23	9.25
A10	9.57	9.56	9.53	9.56	9.22	9.21	28.69	28.64	28.65	28.67	9.21	9.23
A11	9.55	9.55	9.55	9.39	9.24	9.24	28.73	28.68	28.67	28.74	9.22	9.23
A12	9.54	9.53	9.55	9.53	9.25	9.19	28.73	28.67	28.70	28.74	9.21	9.24
B1	9.52	9.54	9.56	9.56	9.23	9.15	26.78	26.82	26.79	26.66	9.21	9.16
B2	9.54	9.54	9.55	9.55	9.22	9.17	26.80	26.86	26.84	26.78	9.22	9.16
B3	9.55	9.54	9.55	9.55	9.21	9.14	26.81	26.86	26.85	26.83	9.23	9.13
B4	9.54	9.53	9.54	9.55	9.22	9.12	26.84	26.85	26.86	26.83	9.21	9.15
B5	9.55	9.53	9.54	9.55	9.21	9.12	26.83	26.83	26.87	26.83	9.22	9.15
B6	9.53	9.54	9.54	9.55	9.23	9.16	26.80	26.83	26.83	26.83	9.22	9.14
B7	9.53	9.53	9.55	9.52	9.21	9.17	26.80	26.85	26.81	26.84	9.20	9.12
B8	9.55	9.53	9.57	9.56	9.25	9.17	26.79	26.81	26.82	26.80	9.22	9.14
B9	9.53	9.52	9.53	9.56	9.27	9.17	26.79	26.80	26.86	26.78	9.23	9.12
B10	9.53	9.53	9.55	9.55	9.22	9.12	26.77	26.80	26.80	26.79	9.22	9.14
B11	9.53	9.54	9.54	9.54	9.22	9.14	26.77	26.78	26.78	26.78	9.22	9.15
B12	9.55	9.55	9.56	9.52	9.27	9.25	26.72	26.70	26.77	26.74	9.26	9.19

136

Table E.16. Volumetric measurements for experiment 16

Specimen	1	2	3	4	5	6	7	8	9	10	11	12
1	9.51	9.48	9.51	9.54	9.22	9.24	68.96	68.97	68.82	68.95	9.22	9.22
2	9.52	9.52	9.49	9.51	9.23	9.22	68.99	68.99	68.97	68.99	9.22	9.22
3	9.51	9.51	9.51	9.52	9.23	9.23	69.00	69.01	68.99	69.01	9.23	9.24
4	9.52	9.50	9.51	9.52	9.22	9.23	68.99	69.01	68.99	69.02	9.22	9.22
5	9.52	9.52	9.51	9.52	9.23	9.24	69.00	69.01	68.99	69.01	9.22	9.22
6	9.53	9.52	9.53	9.52	9.22	9.25	69.01	69.02	69.02	69.03	9.23	9.23
7	9.54	9.54	9.52	9.53	9.23	9.26	69.00	69.02	69.01	69.03	9.23	9.23
8	9.53	9.55	9.52	9.53	9.24	9.22	69.01	69.02	69.00	69.02	9.23	9.22
9	9.54	9.54	9.51	9.52	9.23	9.24	69.00	69.02	69.00	69.04	9.21	9.23
10	9.54	9.55	9.52	9.55	9.23	9.24	69.01	69.02	69.00	69.03	9.22	9.22
11	9.55	9.55	9.51	9.52	9.24	9.24	69.00	69.04	69.02	69.03	9.19	9.21
12	9.53	9.54	9.50	9.51	9.25	9.27	69.00	69.02	69.03	69.04	9.20	9.23
A1	9.52	9.54	9.49	9.48	9.14	9.22	25.91	26.03	25.99	25.92	9.22	9.23
A2	9.51	9.55	9.47	9.52	9.14	9.22	25.98	26.04	25.99	25.95	9.18	9.21
A3	9.54	9.54	9.50	9.51	9.12	9.25	25.96	26.07	26.01	26.00	9.22	9.24
A4	9.52	9.55	9.46	9.49	9.14	9.27	26.02	26.10	26.01	26.00	9.18	9.22
A5	9.54	9.54	9.48	9.49	9.15	9.23	26.06	26.15	26.11	26.04	9.17	9.23
A6	9.55	9.56	9.50	9.52	9.19	9.23	26.06	26.18	26.14	26.07	9.15	9.25
A7	9.52	9.52	9.50	9.51	9.14	9.21	26.10	26.20	26.13	26.13	9.18	9.26
A8	9.54	9.52	9.53	9.52	9.15	9.22	26.17	26.22	26.14	26.11	9.18	9.22
A9	9.52	9.54	9.55	9.53	9.09	9.23	26.17	26.24	26.21	26.15	9.21	9.23
A10	9.54	9.53	9.54	9.54	9.15	9.23	26.19	26.25	26.18	26.17	9.16	9.25
A11	9.53	9.54	9.53	9.54	9.14	9.23	26.22	26.24	26.25	26.25	9.20	9.24
A12	9.54	9.54	9.53	9.54	9.18	9.26	26.21	26.26	26.18	26.21	9.20	9.27
B1	9.54	9.55	9.52	9.55	9.20	9.27	28.27	28.22	27.84	28.11	8.86	9.14
B2	9.50	9.52	9.53	9.55	9.22	9.24	28.47	28.33	28.23	28.31	8.85	9.14
B3	9.49	9.53	9.53	9.55	9.22	9.24	28.56	28.41	28.34	28.48	8.86	9.15
B4	9.47	9.52	9.55	9.57	9.22	9.25	28.61	28.46	28.41	28.56	8.83	9.11
B5	9.50	9.53	9.56	9.55	9.21	9.25	28.68	28.52	28.46	28.61	8.85	9.12
B6	9.52	9.55	9.54	9.61	9.22	9.27	28.75	28.61	28.51	28.67	8.92	9.16
B7	9.53	9.54	9.54	9.58	9.25	9.24	28.82	28.69	28.62	28.76	8.88	9.16
B8	9.56	9.53	9.53	9.55	9.23	9.25	28.93	28.81	28.69	28.85	8.87	9.15
B9	9.54	9.55	9.52	9.54	9.22	9.26	29.01	28.84	28.82	28.90	8.89	9.15
B10	9.55	9.54	9.52	9.50	9.23	9.29	29.12	29.06	28.96	29.02	8.94	9.16
B11	9.54	9.51	9.52	9.51	9.23	9.30	29.21	29.12	29.05	29.15	8.98	9.19
B12	9.53	9.52	9.52	9.53	9.27	9.31	29.38	29.27	29.14	29.27	9.07	9.35

Table E.17. Volumetric measurements for experiment 17

Specimen	1	2	3	4	5	6	7	8	9	10	11	12
1	9.56	9.57	9.54	9.54	9.23	9.21	68.88	68.87	68.85	68.88	9.23	9.24
2	9.58	9.57	9.56	9.56	9.25	9.18	68.87	68.87	68.86	68.88	9.22	9.20
3	9.57	9.55	9.56	9.56	9.23	9.25	68.88	68.87	68.88	68.87	9.23	9.23
4	9.54	9.57	9.57	9.58	9.22	9.21	68.87	68.88	68.87	68.91	9.24	9.24
5	9.55	9.55	9.58	9.57	9.23	9.23	68.88	68.87	68.88	68.87	9.24	9.22
6	9.57	9.55	9.56	9.58	9.22	9.26	68.86	68.86	68.86	68.87	9.27	9.28
7	9.53	9.56	9.58	9.57	9.23	9.21	68.85	68.87	68.86	68.86	9.25	9.25
8	9.55	9.55	9.59	9.57	9.25	9.20	68.85	68.86	68.86	68.85	9.23	9.25
9	9.55	9.57	9.58	9.57	9.22	9.23	68.85	68.86	68.86	68.87	9.23	9.24
10	9.54	9.55	9.59	9.58	9.23	9.22	68.85	68.86	68.85	68.86	9.28	9.23
11	9.53	9.56	9.58	9.6	9.23	9.21	68.86	68.87	68.85	68.86	9.23	9.23
A1	9.53	9.57	9.54	9.53	9.19	9.22	27.97	27.95	27.91	27.93	9.22	9.24
A2	9.55	9.55	9.54	9.54	9.21	9.21	27.91	27.92	27.93	27.93	9.22	9.25
A3	9.53	9.57	9.57	9.55	9.22	9.22	27.90	27.90	27.90	27.91	9.20	9.22
A4	9.53	9.56	9.55	9.55	9.21	9.22	27.86	27.88	27.91	27.92	9.21	9.25
A5	9.54	9.56	9.54	9.57	9.19	9.22	27.93	27.91	27.86	27.88	9.22	9.25
A6	9.55	9.57	9.52	9.55	9.22	9.23	27.89	27.83	27.84	27.86	9.24	9.23
A7	9.54	9.55	9.56	9.59	9.23	9.22	27.80	27.79	27.83	27.85	9.23	9.23
A8	9.55	9.51	9.55	9.57	9.21	9.13	27.85	27.78	27.80	27.80	9.21	9.23
A9	9.53	9.53	9.53	9.56	9.19	9.25	27.74	27.75	27.76	27.78	9.22	9.22
A10	9.52	9.54	9.52	9.52	9.21	9.23	27.71	27.72	27.75	27.75	9.22	9.25
A11	9.54	9.52	9.55	9.56	9.19	9.20	27.68	27.68	27.71	27.72	9.20	9.20
B1	9.56	9.57	9.57	9.58	9.21	9.12	26.26	26.25	26.22	26.22	9.24	9.13
B2	9.54	9.56	9.58	9.59	9.18	9.14	26.24	26.23	26.26	26.24	9.21	9.17
B3	9.56	9.57	9.57	9.59	9.20	9.12	26.25	26.23	26.24	26.23	9.23	9.15
B4	9.54	9.58	9.59	9.59	9.17	9.16	26.26	26.24	26.25	26.25	9.23	9.14
B5	9.55	9.58	9.58	9.58	9.19	9.13	26.24	26.22	26.23	26.24	9.21	9.13
B6	9.57	9.56	9.57	9.58	9.24	9.14	26.24	26.24	26.26	26.24	9.25	9.18
B7	9.56	9.59	9.59	9.56	9.22	9.14	26.24	26.25	26.24	26.23	9.24	9.15
B8	9.55	9.58	9.57	9.59	9.20	9.10	26.22	26.26	26.23	26.24	9.21	9.12
B9	9.58	9.57	9.57	9.57	9.23	9.10	26.24	26.23	26.23	26.24	9.23	9.13
B10	9.57	9.55	9.59	9.56	9.21	9.15	26.21	26.22	26.22	26.23	9.23	9.16
B11	9.59	9.59	9.59	9.57	9.21	9.16	26.22	26.24	26.24	26.23	9.23	9.15

138

Table E.18. Volumetric measurements for experiment 18

Specimen	1	2	3	4	5	6	7	8	9	10	11	12
1	9.61	9.60	9.58	9.59	9.26	9.26	68.87	68.89	68.88	68.89	9.27	9.31
2	9.54	9.61	9.55	9.56	9.32	9.25	68.88	68.96	68.92	68.91	9.32	9.25
3	9.63	9.63	9.63	9.59	9.29	9.29	68.88	68.90	68.89	68.88	9.29	9.30
4	9.64	9.66	9.59	9.62	9.24	9.26	68.89	68.90	68.90	68.90	9.26	9.26
5	9.60	9.59	9.64	9.67	9.30	9.25	68.90	68.91	68.89	68.91	9.33	9.26
6	9.63	9.63	9.66	9.68	9.29	9.26	68.91	68.94	68.90	68.93	9.27	9.28
7	9.59	9.57	9.56	9.25	9.26	9.29	68.91	68.93	68.93	68.94	9.27	9.29
8	9.59	9.60	9.58	9.58	9.23	9.26	68.96	68.94	68.92	68.91	9.24	9.23
9	9.62	9.63	9.58	9.56	9.27	9.22	68.93	68.93	68.94	68.92	9.27	9.23
10	9.56	9.58	9.59	9.57	9.28	9.27	68.99	68.97	68.93	68.93	9.27	9.28
11	9.59	9.58	9.56	9.58	9.27	9.26	68.95	68.98	68.92	68.93	9.26	9.25
12	9.58	9.55	9.59	9.59	9.24	9.26	68.92	68.92	68.91	68.92	9.26	9.26
A1	9.59	9.6	9.59	9.57	9.24	9.25	26.79	26.82	26.82	26.83	9.26	9.26
A2	9.60	9.59	9.57	9.59	9.23	9.26	26.71	26.74	26.75	26.80	9.26	9.27
A3	9.59	9.59	9.60	9.57	9.24	9.28	26.66	26.64	26.69	26.73	9.27	9.25
A4	9.60	9.61	9.55	9.57	9.26	9.23	26.63	26.63	26.67	26.68	9.23	9.24
A5	9.64	9.63	9.57	9.55	9.25	9.25	26.62	26.59	26.59	26.62	9.27	9.25
A6	9.60	9.60	9.60	9.59	9.23	9.23	26.56	26.50	26.55	26.56	9.24	9.25
A7	9.61	9.62	9.60	9.55	9.21	9.25	26.51	26.54	26.56	26.51	9.24	9.24
A8	9.57	9.59	9.61	9.59	9.24	9.24	26.39	26.39	26.42	26.44	9.25	9.25
A9	9.60	9.60	9.56	9.58	9.25	9.26	26.33	26.31	26.32	26.35	9.24	9.26
A10	9.55	9.58	9.58	9.57	9.24	9.25	26.30	26.31	26.33	26.30	9.24	9.24
A11	9.59	9.59	9.56	9.55	9.23	9.22	26.08	26.11	26.18	26.20	9.22	9.23
A12	9.55	9.54	9.56	9.54	9.27	9.26	26.03	26.01	26.07	26.08	9.29	9.27
B1	9.56	9.55	9.61	9.58	9.24	9.19	26.80	26.78	26.80	26.81	9.27	9.21
B2	9.59	9.57	9.61	9.60	9.26	9.22	26.79	26.80	26.82	26.78	9.23	9.21
B3	9.54	9.57	9.62	9.57	9.25	9.17	26.78	26.77	26.79	26.79	9.24	9.18
B4	9.56	9.60	9.63	9.62	9.29	9.16	26.77	26.75	26.81	26.77	9.24	9.17
B5	9.58	9.60	9.62	9.61	9.23	9.17	26.75	26.72	26.75	26.73	9.24	9.21
B6	9.59	9.57	9.59	9.60	9.28	9.16	26.77	26.72	26.74	26.71	9.29	9.20
B7	9.56	9.59	9.61	9.63	9.28	9.19	26.70	26.69	26.73	26.71	9.26	9.20
B8	9.61	9.57	9.56	9.60	9.24	9.17	26.73	26.66	26.72	26.72	9.26	9.18
B9	9.55	9.58	9.59	9.59	9.27	9.19	26.74	26.68	26.71	26.67	9.28	9.21
B10	9.60	9.59	9.59	9.57	9.27	9.17	26.63	26.59	26.66	26.61	9.26	9.19
B11	9.56	9.55	9.55	9.55	9.26	9.24	26.60	26.57	26.62	26.60	9.28	9.21
B12	9.56	9.59	9.59	9.50	9.24	9.19	26.67	26.63	26.56	26.58	9.26	9.21

139

Table E.19. Volumetric measurements for experiment 19

Specimen	1	2	3	4	5	6	7	8	9	10	11	12
1	9.58	9.55	9.61	9.6	9.25	9.23	68.96	68.95	68.91	68.93	9.21	9.24
2	9.57	9.58	9.59	9.61	9.29	9.31	68.99	68.99	68.98	68.97	9.24	9.25
3	9.58	9.57	9.59	9.57	9.22	9.22	68.99	68.99	68.99	69.01	9.20	9.22
4	9.57	9.59	9.61	9.59	9.20	9.21	68.99	68.99	69.00	68.99	9.22	9.23
5	9.58	9.59	9.57	9.59	9.20	9.22	68.99	68.99	68.99	69.00	9.20	9.21
6	9.59	9.59	9.59	9.59	9.21	9.21	69.00	68.99	68.99	68.99	9.20	9.20
7	9.59	9.60	9.59	9.60	9.22	9.20	68.99	69.00	68.99	68.99	9.14	9.13
8	9.58	9.61	9.59	9.60	9.25	9.23	68.99	69.00	68.99	69.00	9.25	9.23
9	9.58	9.58	9.59	9.59	9.19	9.20	68.99	68.98	68.98	68.99	9.19	9.18
10	9.58	9.58	9.59	9.59	9.26	9.29	68.99	69.00	68.98	68.99	9.24	9.25
11	9.58	9.58	9.58	9.58	9.22	9.23	68.98	68.98	68.99	68.99	9.20	9.21
12	9.57	9.58	9.58	9.57	9.24	9.25	68.99	68.99	69.00	68.98	9.20	9.23
A2	9.57	9.55	9.57	9.56	9.18	9.23	25.82	25.90	25.87	25.79	9.24	9.26
A3	9.56	9.57	9.57	9.58	9.19	9.22	25.88	25.92	25.91	25.84	9.22	9.25
A4	9.59	9.59	9.59	9.60	9.17	9.22	25.91	25.95	25.91	25.91	9.21	9.22
A5	9.59	9.65	9.59	9.59	9.18	9.22	25.96	25.99	25.95	25.92	9.22	9.23
A6	9.63	9.65	9.57	9.59	9.19	9.22	25.98	26.00	26.00	25.98	9.22	9.24
A7	9.63	9.64	9.58	9.58	9.18	9.21	26.03	26.05	26.01	26.05	9.20	9.21
A8	9.65	9.65	9.59	9.56	9.19	9.22	26.07	26.08	26.05	26.05	9.23	9.24
A9	9.65	9.64	9.57	9.57	9.16	9.17	26.10	26.12	26.07	26.07	9.20	9.18
A10	9.61	9.62	9.59	9.61	9.20	9.28	26.12	26.16	26.11	26.15	9.26	9.28
A11	9.60	9.59	9.58	9.58	9.19	9.23	26.17	26.19	26.15	26.16	9.23	9.24
A12	9.57	9.60	9.56	9.57	9.18	9.23	26.19	26.20	26.16	26.19	9.22	9.23
B1	9.61	9.60	9.64	9.65	9.23	9.24	26.60	26.71	26.37	26.40	9.06	9.19
B2	9.58	9.58	9.63	9.65	9.28	9.32	26.82	26.84	26.69	26.62	9.15	9.27
B3	9.57	9.60	9.66	9.65	9.21	9.23	26.97	26.94	26.85	26.90	9.13	9.20
B4	9.59	9.61	9.65	9.66	9.20	9.24	27.05	27.01	26.95	26.98	9.14	9.20
B5	9.58	9.61	9.67	9.71	9.21	9.25	27.12	27.07	26.99	27.06	9.14	9.19
B6	9.60	9.61	9.68	9.70	9.23	9.23	27.17	27.11	27.05	27.16	9.14	9.17
B7	9.60	9.62	9.65	9.72	9.16	9.12	27.15	27.13	27.10	27.19	9.03	9.07
B8	9.58	9.60	9.61	9.66	9.24	9.24	27.26	27.20	27.14	27.17	9.06	9.15
B9	9.60	9.60	9.64	9.63	9.20	9.20	27.29	27.27	27.18	27.26	9.05	9.12
B10	9.59	9.59	9.61	9.64	9.25	9.26	27.35	27.32	27.26	27.29	9.07	9.17
B11	9.58	9.57	9.60	9.62	9.23	9.24	27.42	27.36	27.31	27.37	9.08	9.16
B12	9.57	9.59	9.62	9.64	9.25	9.26	27.44	27.41	27.36	27.44	9.10	9.26

140

Table E.20. Weight measurements for experiments 1-7

Specimen	Expmt 1	Expmt 2	Expmt 3	Expmt 4	Expmt 5	Expmt 6	Expmt 7
1	11.5293	12.2844	11.3506	12.018	11.8306	12.1747	11.3963
2	11.5702	12.2919	11.35	12.0862	11.8418	12.1499	11.3214
3	11.5517	12.2857	11.3523	12.0509	11.8761	12.1288	11.3549
4	11.4974	12.2895	11.3149	12.046	11.9049	12.1149	11.3683
5	11.5101	12.2462	11.3242	12.0655	11.9259	12.0905	11.3881
6	11.4963	12.2009	11.2618	12.0256	11.9162	12.0841	11.3928
7	11.4866	12.1557	11.2798	11.9042	11.9083	11.9799	11.3944
8	11.4598	12.1965	11.2252	11.9881	11.8953	12.068	11.4876
9	11.4531	12.168	11.2144	12.0029	11.8813	12.0123	11.6811
10	11.4013	12.1459	11.2361	11.9944	11.8083	12.0809	11.8065
11	11.4061	12.1412	11.1797	11.9939	11.6993	12.1111	11.6864
12	11.4095	12.1729	11.2123	11.9935	11.5999	12.149	11.4934
A1	4.3688	4.6512	4.2583	4.6183	4.4464	4.648	4.6469
A2	4.3617	4.6399	4.2635	4.6005	4.414	4.6399	4.6503
A3	4.3532	4.6435	4.2563	4.6118	4.4176	4.6318	4.6857
A4	4.3535	4.6514	4.2564	4.623	4.4336	4.6107	4.7189
A5	4.3748	4.6382	4.2713	4.6474	4.4486	4.5917	4.7672
A6	4.3787	4.6184	4.2699	4.6257	4.4543	4.5812	4.77
A7	4.3833	4.6062	4.3133	4.5931	4.4552	4.5612	4.8503
A8	4.3779	4.6188	4.3165	4.6698	4.4597	4.5879	4.9147
A9	4.3671	4.6098	4.3487	4.6792	4.457	4.5774	5.0389
A10	4.3706	4.5899	4.3796	4.689	4.4361	4.581	5.1103
A11	4.3742	4.5903	4.3919	4.6963	4.4212	4.5814	5.1103
A12	4.3863	4.5944	4.4271	4.6863	4.3942	4.608	5.0903
B1	4.0892	3.7785	4.3953	4.0105	3.5663	3.8718	4.4135
B2	4.1387	3.7603	4.39	3.9699	3.6176	3.8657	4.3802
B3	4.1545	3.74	4.3858	3.9381	3.6692	3.8837	4.3929
B4	4.1338	3.7201	4.3763	3.8925	3.7313	3.9072	4.3561
B5	4.152	3.689	4.3727	3.8679	3.7882	3.9346	4.3497
B6	4.1732	3.6698	4.3574	3.8356	3.8287	3.934	4.3541
B7	4.1958	3.6536	4.3731	3.7913	3.8921	3.9615	4.3683
B8	4.2098	3.667	4.3566	3.8113	3.9401	3.9931	4.4051
B9	4.2312	3.6477	4.3554	3.8081	3.9769	4.0057	4.444
B10	4.2331	3.6455	4.3617	3.7982	4.0158	4.048	4.4563
B11	4.2738	3.6541	4.3183	3.7929	3.9811	4.0995	4.4674
B12	4.3291	3.6805	4.3458	3.7978	4.021	4.1045	4.4167

141

Table E.21. Weight measurements for experiments 8-14

Specimen	Expmt 8	Expmt 9	Expmt 10	Expmt 11	Expmt 12	Expmt 13	Expmt 14
1	11.5788	11.7700	12.0059	12.0136	11.1980	11.0642	11.6363
2	11.6103	11.7189	12.0441	12.0378	11.3277	11.0774	11.5758
3	11.5677	11.7096	12.0450	12.0316	11.5799	11.0864	11.5458
4	11.5652	11.6766	12.0311	11.9681	11.4122	11.0412	11.4488
5	11.6060	11.7239	12.0201	11.9886	11.3635	11.0665	11.3105
6	11.6525	11.6996	12.0429	12.0172	11.3789	11.0906	11.268
7	11.6023	11.7153	12.0690	11.9209	11.3521	11.0913	11.1816
8	11.5412	11.7552	11.9221	12.0201	11.4329	11.0862	11.1338
9	11.5593	11.7762	11.9603	11.9892	11.4452	11.068	11.139
10	11.4871	11.7943	11.8303	11.886	11.4802	11.0532	11.0907
11	11.4612	11.8639	11.8164	11.8675	11.5143	11.0689	11.0298
12	11.4762	11.8647	11.806	11.8439	11.5096	11.0857	11.0184
A1	4.4646	4.4121	4.5554	4.6137	4.3223	4.0727	4.4372
A2	4.4708	4.4244	4.5485	4.6050	4.3803	4.0766	4.4114
A3	4.4733	4.4167	4.5388	4.5736	4.3208	4.0830	4.4073
A4	4.4803	4.4255	4.5269	4.5301	4.3098	4.0867	4.3985
A5	4.5109	4.4357	4.5217	4.5486	4.2927	4.0857	4.3687
A6	4.5160	4.4097	4.545	4.5523	4.2929	4.1019	4.3642
A7	4.4974	4.4077	4.5547	4.5176	4.2805	4.0778	4.3477
A8	4.4893	4.4011	4.3911	4.5688	4.2941	4.0810	4.3131
A9	4.4801	4.4101	4.5266	4.5690	4.2991	4.0981	4.2939
A10	4.4427	4.4260	4.4868	4.5557	4.3134	4.0982	4.2928
A11	4.4283	4.4759	4.4732	4.5690	4.3233	4.1239	4.2662
A12	4.4188	4.4928	4.4868	4.5866	4.332	4.1250	4.2814
B1	3.5093	4.7524	4.7015	5.5050	4.6493	4.3078	4.6291
B2	3.5538	4.7073	4.7387	5.5120	4.6769	4.3025	4.5525
B3	3.5873	4.6608	4.7694	5.5046	4.6008	4.299	4.4788
B4	3.6188	4.6308	4.7808	5.4997	4.5447	4.2977	4.4168
B5	3.6737	4.6169	4.8054	5.5148	4.4954	4.2923	4.3483
B6	3.7273	4.5853	4.8440	5.4923	4.4723	4.3088	4.2909
B7	3.7212	4.5920	4.8676	5.4858	4.4281	4.3034	4.2034
B8	3.7418	4.5878	4.8301	5.5002	4.4073	4.3046	4.1001
B9	3.7853	4.6066	4.9028	5.4586	4.3645	4.3049	4.0273
B10	3.7957	4.6261	4.9041	5.4373	4.3386	4.2778	3.9395
B11	3.8289	4.6478	4.9529	5.4417	4.3254	4.2856	3.8838
B12	3.8861	4.6692	4.9872	5.4437	4.3113	4.2978	3.8670

142

Table E.22. Weight measurements for experiments 15-19

Specimen	Expmt 15	Expmt 16	Exmpt 17	Expmt 18	Expmt 19
1	11.7385	11.0782	11.7725	11.7498	11.198
2	11.8424	11.1025	11.8051	11.7126	11.3277
3	11.8437	11.1005	11.8363	11.7233	11.5799
4	11.8438	11.0699	11.7857	11.739	11.4122
5	11.8261	11.1288	11.8131	11.7159	11.3635
6	11.8405	11.1519	11.8151	11.7507	11.3789
7	11.7762	11.1586	11.803	11.6668	11.3521
8	11.7881	11.1488	11.7993	11.7186	11.4329
9	11.8584	11.1729	11.8329	11.7568	11.4452
10	11.8359	11.2093	11.8249	11.8396	11.4802
11	11.8440	11.1540	11.7280	11.8515	11.5143
12	11.771	11.1652	----	11.7390	11.5096
A1	4.8973	4.1971	4.7879	4.6069	4.3223
A2	4.9113	4.1948	4.8006	4.5697	4.3803
A3	4.9188	4.1856	4.8028	4.5532	4.3208
A4	4.9244	4.2027	4.7826	4.5446	4.3098
A5	4.9185	4.2248	4.7853	4.5299	4.2927
A6	4.8811	4.2236	4.7618	4.5149	4.2929
A7	4.9029	4.2120	4.7597	4.4664	4.2805
A8	4.9137	4.2196	4.7407	4.4848	4.2941
A9	4.9384	4.2377	4.7388	4.4614	4.2991
A10	4.9344	4.2615	4.7224	4.4799	4.3134
A11	4.9451	4.2477	4.7026	4.4493	4.3233
A12	4.9457	4.2538	----	4.4499	4.3320
B1	4.6157	4.5328	4.4858	4.5813	4.6493
B2	4.6238	4.5576	4.4778	4.5510	4.6769
B3	4.5897	4.5650	4.4738	4.5663	4.6008
B4	4.5791	4.579	4.4453	4.5693	4.5447
B5	4.5567	4.5934	4.4558	4.5500	4.4954
B6	4.5643	4.6297	4.4474	4.5376	4.4723
B7	4.5415	4.6116	4.4568	4.5142	4.4281
B8	4.5673	4.6274	4.4529	4.5139	4.4073
B9	4.5834	4.6571	4.4616	4.5244	4.3645
B10	4.5728	5.6902	4.4854	4.5264	4.3386
B11	4.5785	5.6968	4.4712	4.5256	4.3254
B12	4.5965	5.7401	---	4.5062	4.3113

APPENDIX F
STRENGTH MEASUREMENTS

Table F.1. Strength measurements for experiments 1-7

Specimen	Expmt 1	Expmt 2	Expmt 3	Expmt 4	Expmt 5	Expmt 6	Expmt 7
1	781.250	937.500	825.195	991.211	727.539	869.141	864.258
2	771.484	922.852	834.961	966.797	703.125	844.727	903.320
3	820.313	908.203	825.195	1000.980	722.656	883.789	913.086
4	791.016	947.266	834.961	986.328	703.125	874.023	913.086
5	800.781	893.555	834.961	986.328	693.359	854.492	898.438
7	805.664	981.445	844.727	971.680	693.359	878.906	888.672
8	786.133	971.680	844.727	961.914	698.242	839.844	869.141
9	805.664	966.797	810.547	961.914	688.477	869.141	874.023
10	756.836	981.445	810.547	952.148	668.945	849.609	859.375
11	805.664	957.031	800.781	971.680	639.648	849.609	864.258
12	791.016	—	820.313	966.797	615.234	849.609	869.141

Table F.2. Strength measurements for experiments 8-14

Specimen	Expmt 8	Expmt 9	Expmt 10	Expmt 11	Expmt 12	Expmt 13	Expmt 14
1	791.016	898.438	859.375	800.781	791.016	791.016	849.609
2	820.313	908.203	849.609	800.781	820.313	820.313	834.961
3	786.133	874.023	878.906	800.781	815.430	815.430	869.141
4	795.898	898.438	893.555	795.898	805.664	805.664	854.492
5	786.133	878.906	864.258	786.133	795.898	795.898	815.430
7	795.898	888.672	893.555	830.078	830.078	830.078	839.844
8	791.016	903.320	849.609	800.781	805.664	805.664	844.727
9	791.016	898.438	834.961	776.367	786.133	786.133	849.609
10	805.664	898.438	830.078	776.367	810.547	810.547	844.727
11	771.484	893.555	800.781	756.836	771.484	771.484	834.961
12	—	—	810.547	756.836	747.070	747.070	878.906

144

Table F.3. Strength measurements for experiments 15-19

Specimen	Expmt 15	Expmt 16	Exmpt 17	Expmt 18	Expmt 19
1	908.203	751.953	810.547	937.500	864.258
2	922.852	771.484	849.609	922.852	844.727
3	922.852	756.836	854.492	942.383	869.141
4	927.734	751.953	878.906	922.852	849.609
5	922.852	756.836	844.727	976.563	795.898
7	937.500	737.305	878.906	966.797	815.430
8	927.734	751.953	883.789	942.383	830.078
9	908.203	756.836	888.672	991.211	830.078
10	903.320	751.953	839.844	966.797	810.547
11	869.141	751.953	844.727	991.211	791.016
12	917.969	766.602	----	981.445	795.898
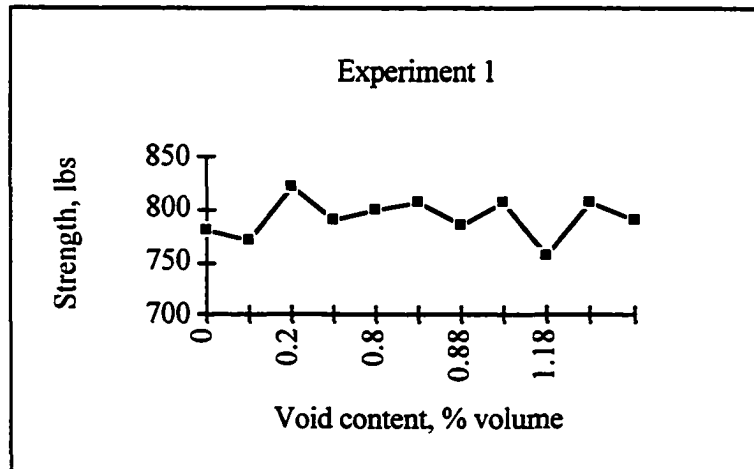
Figure F.1. Strength versus void content for experiment 1

145
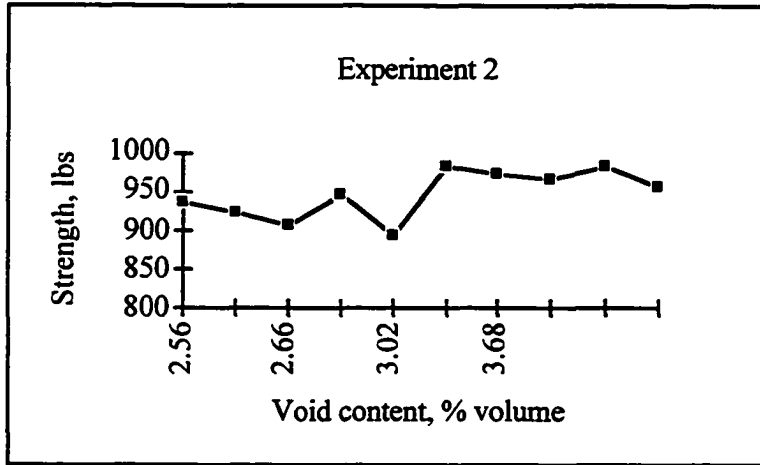
Figure F.2. Strength versus void content for experiment 2
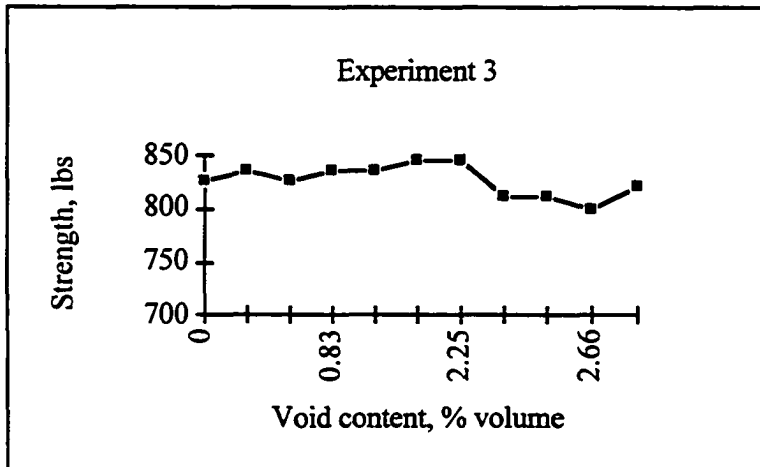
Figure F.3. Strength versus void content for experiment 3

146
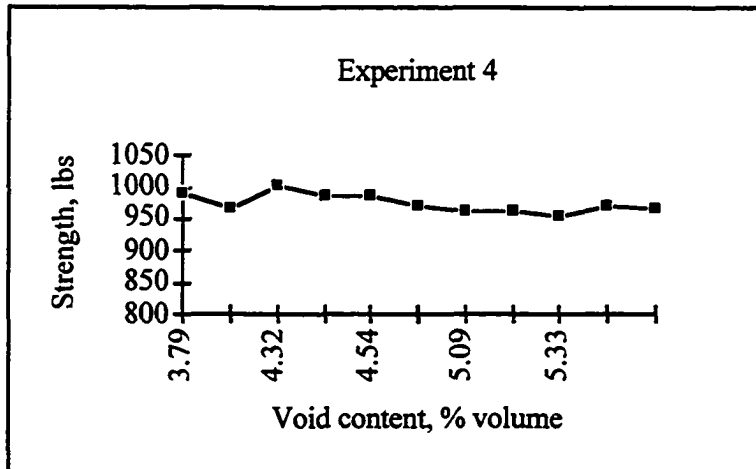
Figure F.4. Strength versus void content for experiment 4
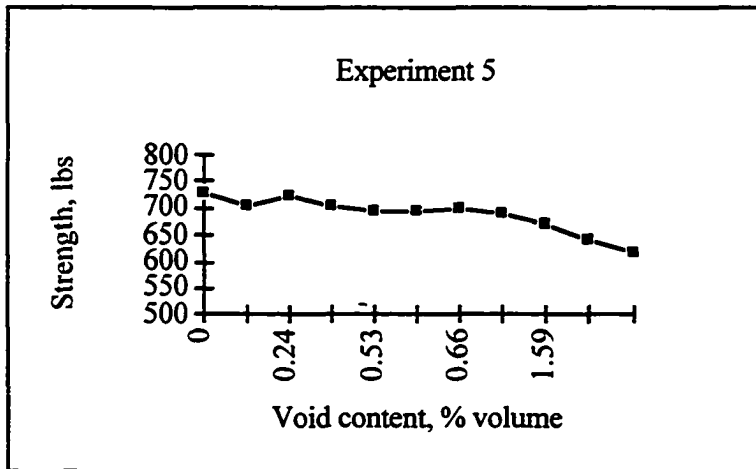
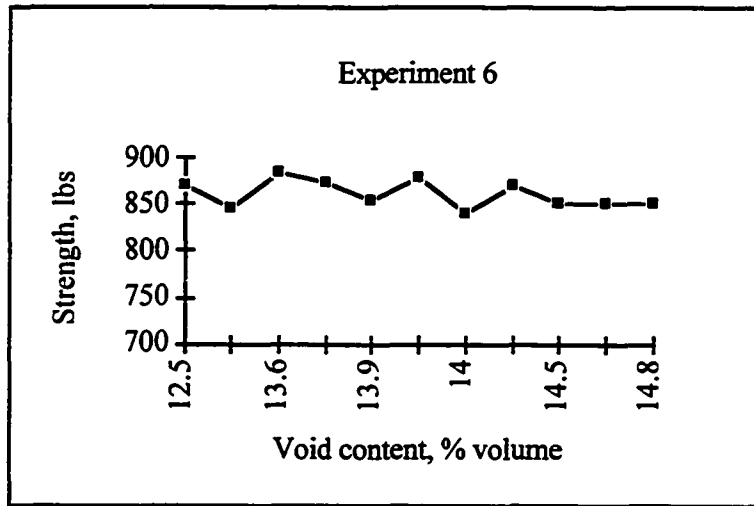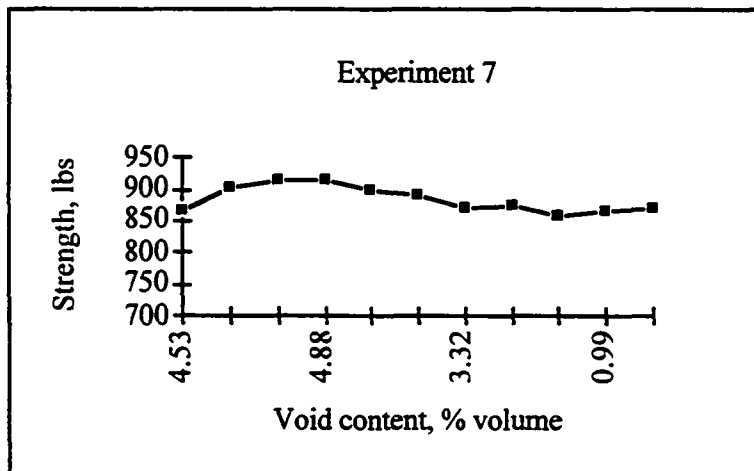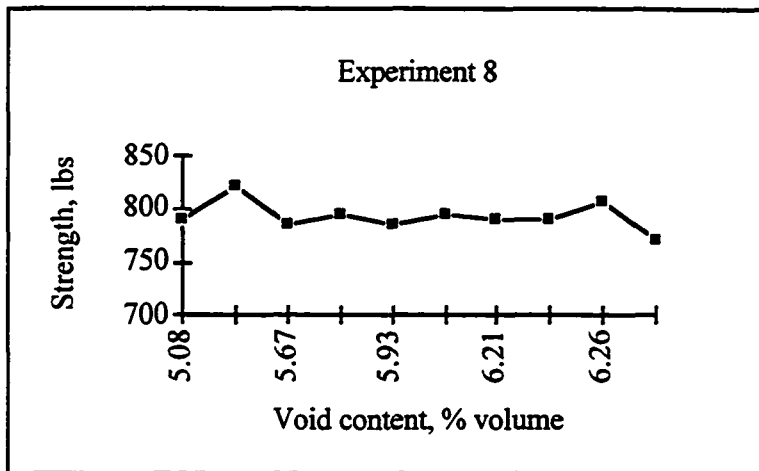Figure F.5. Strength versus void content for experiment 5

147

Figure F.6. Strength versus void content for experiment 6

Figure F.7. Strength versus void content for experiment 7

148

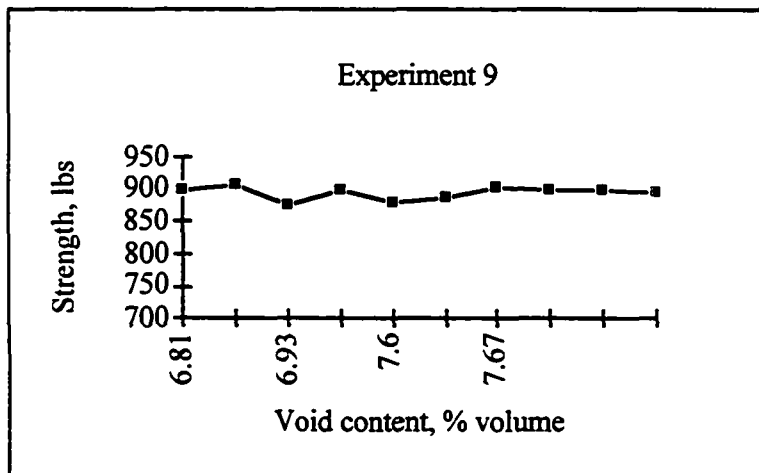Figure F.8. Strength versus void content for experiment 8

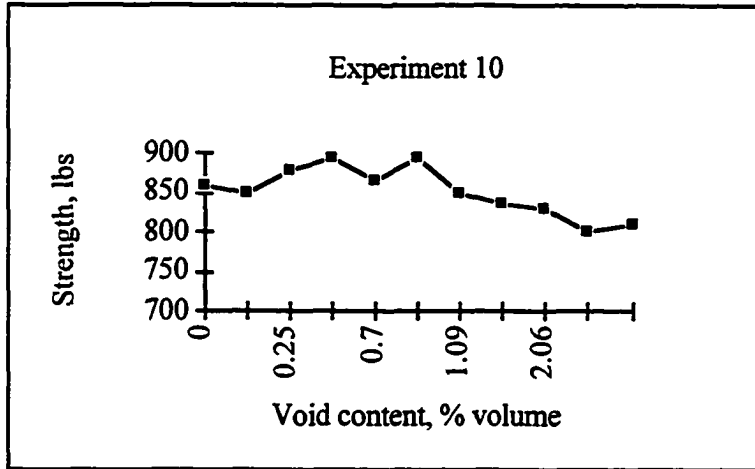Figure F.9. Strength versus void content for experiment 9

149

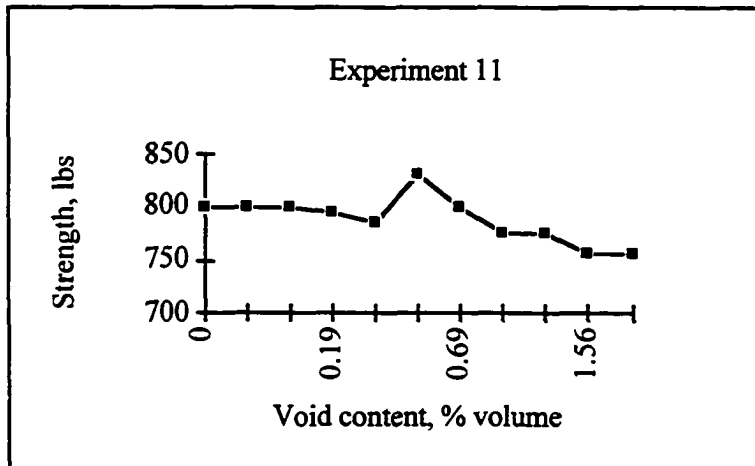Figure F.10. Strength versus void content for experiment 10

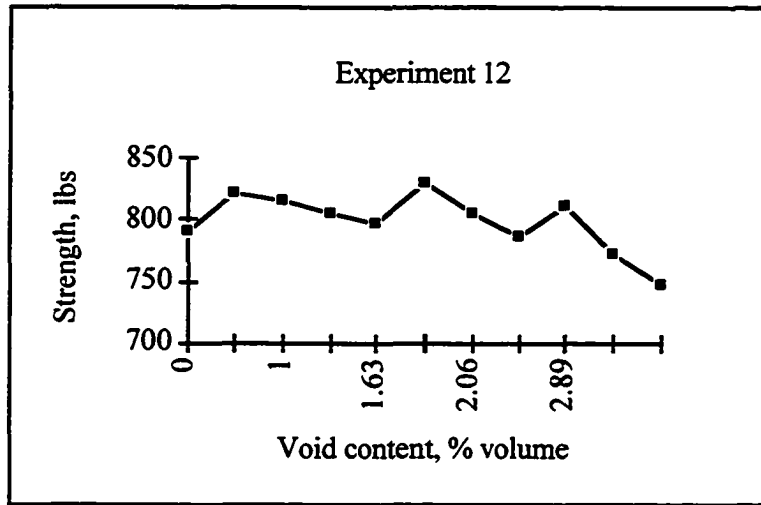Figure F.11. Strength versus void content for experiment 11

150

Figure F.12. Strength versus void content for experiment 12

Figure F.13. Strength versus void content for experiment 13

151

Figure F.14. Strength versus void content for experiment 14

Figure F.15. Strength versus void content for experiment 15

152

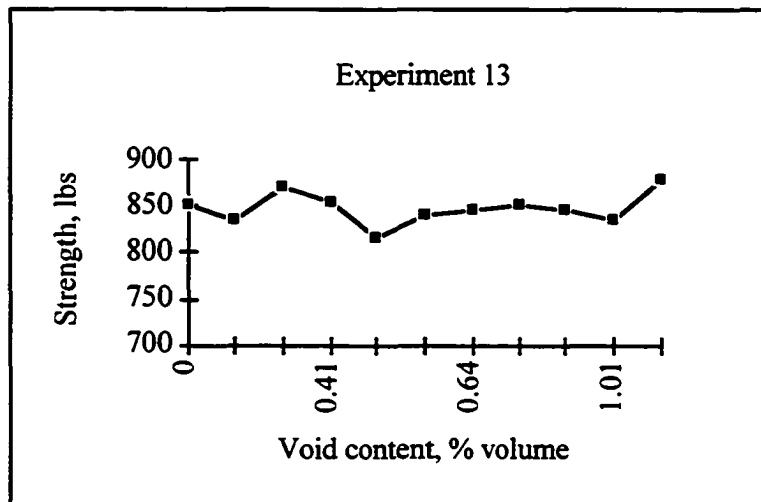Figure F.16. Strength versus void content for experiment 16

Figure F.17. Strength versus void content for experiment 17

153

Figure F.18. Strength versus void content for experiment 18

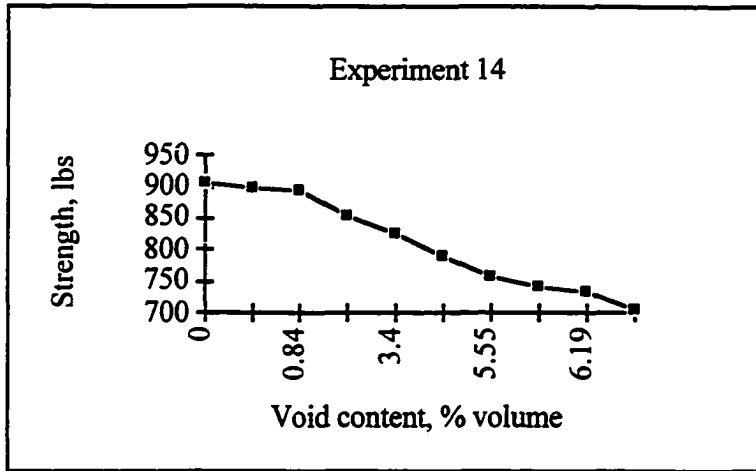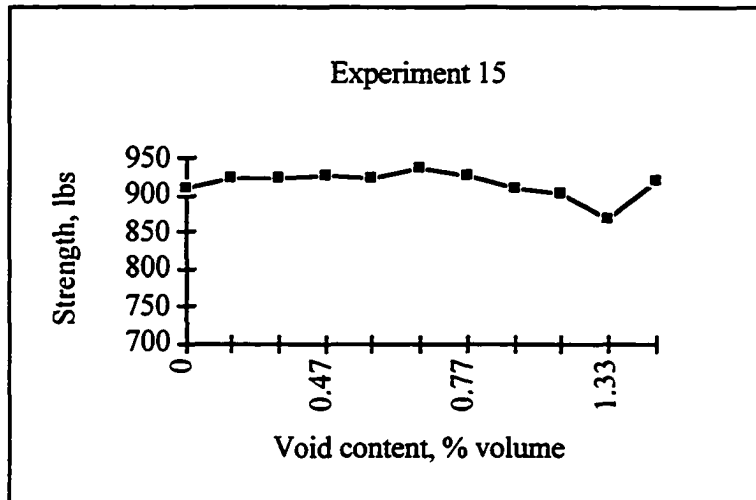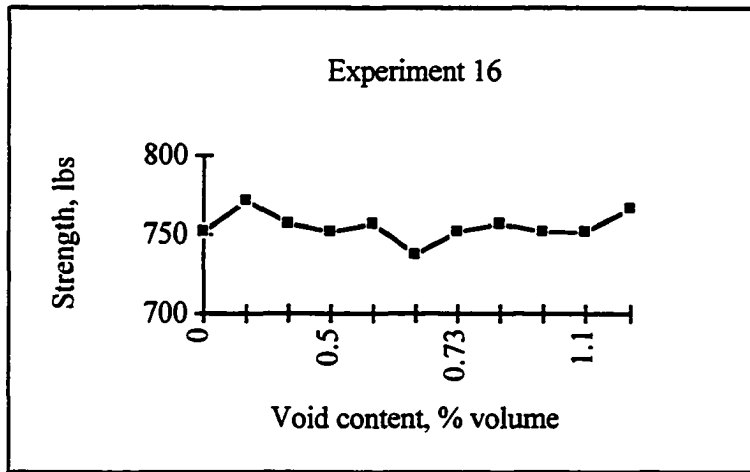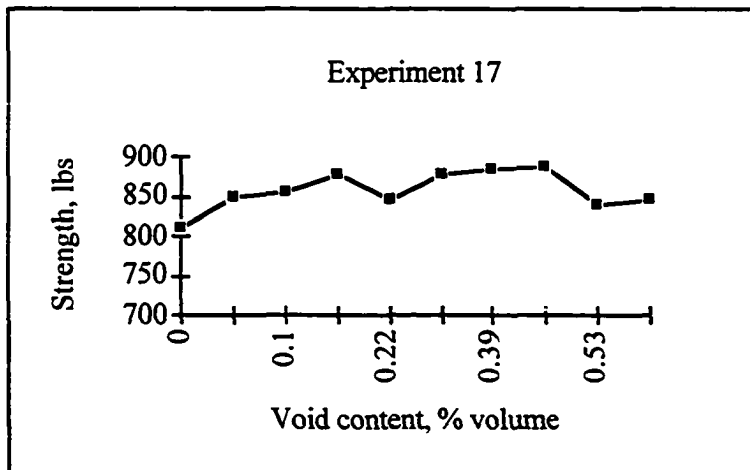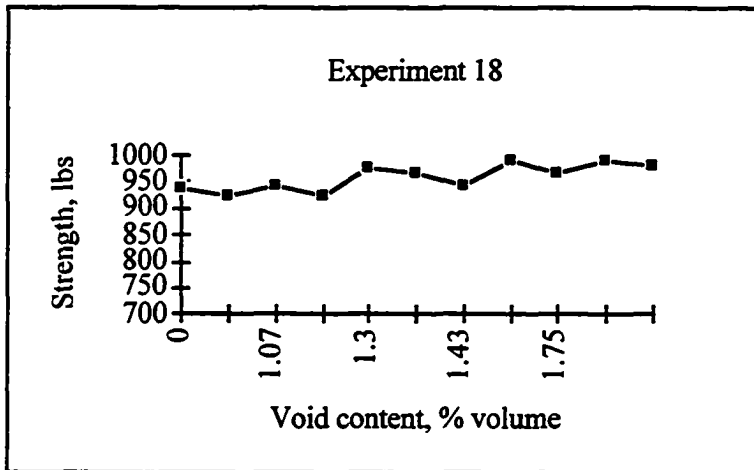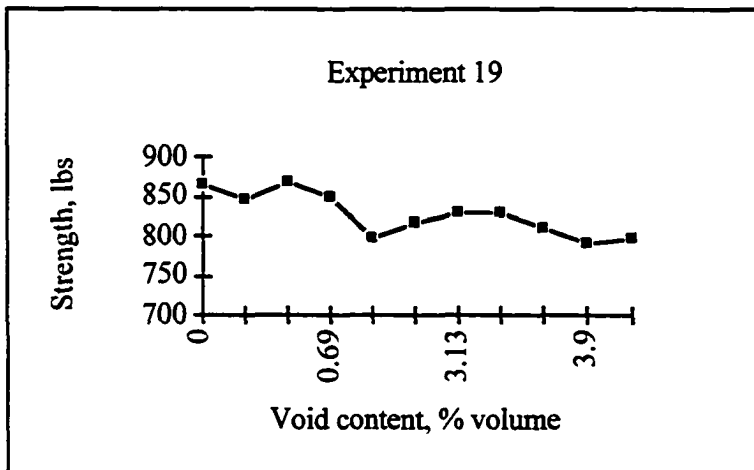Figure F.19. Strength versus void content for experiment 19

154

BIBLIOGRAPHY

"A Model for Moulding." *Engineering*, Vol. 232, April 1992, pp. ACE11-12.

Andersen, K., Cook, G.E., Karsai, G. and Ramaswamy, K., "Artificial Neural Networks Applied to Arc Welding Process Modeling and Control," *IEEE Transactions on Industry Applications*, Vol. 26, No. 5, September/October 1990, pp. 824-830.

Advani, S.G., Bruschke, M.V. and Parnas, R.S., "Resin Transfer Molding Flow Phenomena in Polymeric Composites," in: *Flow and Rheology in Polymer Composites Manufacturing*, Elsevier Science, 1994.

Astrom, B.T., Pipes, R.B. and Advani, S.G., "On Flow Through Aligned Fiber Beds and it Application to Composite Processing," *Journal of Composite Materials*, Vol. 26, No. 9, 1992, pp. 1351-1373.

Blankenship, G.L., Lebow, L.G., Hassim, A. and Dutoya, A., "COMPO: A System for CAD of Composite Materials," in: Proceedings of the American Society of Composites 7th Technical Conference, 1992, pp. 330-344.

Bowles, K.J. and Frimpong, S., "Void Effects on the Interlaminar Shear Strength of Unidirectional Graphite-Fiber-Reinforced Composites," *Journal of Composite Materials*, Vol. 26, No. 10, 1992, pp. 1487-1509.

Bruschke, M. and Advani, S. "A Finite Element/Control Volume Approach to Mold Filling in Anisotropic Porous Media," *Polymer Composites*, Vol. 11, No. 6, 1990, pp.

Bruschke, M.V., Luce, T.L. and Advani, S.G., "Effective In-plane Permeability of Multi-layered RTM Preforms", in: Proceedings of the American Society for Composites 7th Technical Conference, 1992, pp. 103-112.

155

Cai, Z., "Analysis of Mold Filling in RTM Process," *Journal of Composite Materials*, Vol. 26, No. 9, 1992, pp. 1310-1338.

Cai, Zhong, "Simplified Mold Filling Simulation in Resin Transfer Molding," *Journal of Composite Materials*, Vol. 26, No. 17, 1992, pp. 2606-2630.

Chan, A.W. and Hwang, S.-T., "Modeling of the Impregnation Process during Resin Transfer Molding," *Polymer Engineering and Science*, Mid-Aug., Vol. 31, 1991, pp. 1149-1156.

Chan, A. and Hwang, S.-T., "Modeling Nonisothermal Impregnation of Fibrous Media with Reactive Polymer Resin," *Polymer Engineering and Science*, Vol. 32, 1992, pp. 310-318.

Chan, A.W. and Hwang, S.-T., "Modeling Resin Transfer Molding of Polyimide (PRM-15)/Fiber Composites," *Polymer Composites*, Vol. 14, No. 6, December, 1993, pp. 524-528.

Chan, A.W. and Morgan, R.J., "Modeling Preform Impregnation and Void Formation in Resin Transfer Molding of Unidirectional Composites," *SAMPE Quarterly*, Vol. 23, No. 3, April 1992, pp. 48-52.

Chan, A.W. and Morgan, R.J., "Sequential Multiple Port Injection for Resin Transfer Molding of Polymer Composites," *SAMPE Quarterly*, Vol. 24, No. 1, October, 1992, pp. 45-53.

Chan, A.W. and Morgan, R.J., "Tow Impregnation during Resin Transfer Molding of Bi-Directional Nonwoven Fabrics," *Polymer Composites*, Vol. 14, No. 4, August, 1993, pp. 335-340.

Chan, A.W., Larive, D.E. and Morgan, R.J., "Anisotropic Permeability of Fiber Preforms: Constant Flow Rate Measurement," *Journal of Composite Materials*, Vol. 27, No. 10, 1993, pp. 996-1008.

Chan, C.Y., Beris, A.N. and Advani, S.G., "3-D Simulation of Fiber-Fluid Interactions During Composite Manufacturing Using the Galerkin Boundary Element Method," in: 3rd International Conference on Computer Aided Design Composite Material Technology CADCOMP '92, published by Computational Mechanics Publishing, Shouthampton, England, 1992, pp. 385-403.

Ciriscioli, P.R., Springer, G.S. and Lee, W.I., "An Expert System for Autoclave Curing of Composites," *Journal of Composite Materials*, Vol. 25, December, 1991, pp. 1542-1562.

Colton, J.S. and Suh, N.P., "Nucleation of Microcellular Foams: Theory and Practice," *Polymer Engineering and Science*, Vol. 27, 1987, pp. 493-500.

Dementyev, V., Kostritskiy, S., Petuhov, M. and Torkunov, A., "On the Optimization of the Fiber Reinforced Composites Manufacturing Process with Two Pressure Steps," in : 3rd International Conference on Computer Aided Design Composite Material Technology CADCOMP '92, published by Computational Mechanics Publishing, Shouthampton, England, 1992, pp. 37-47.

Fahlman, S., "The Recurrent Cascade-Correlation Architecture," in R.P. Lippmann *et al.* (eds.), *Advances in Neural Information Processing Systems*, Morgan Kaufmann, Los Altos, CA, 1991, pp. 190-196.

Fahlman, S. and Lebiere, C., "The Cascade-Correlation Learning Architecture," in D.S. Touretzky *et al.* (eds.), *Advances in Neural Information Processing Systems*, Morgan Kaufmann, Los Altos, CA, Vol. 2, 1990, pp. 524-532.

Frean, M., "The Upstart Algorithm" A Method for Constructing and Training Feedforward Neural Networks," *Neural Computation*, 2, 1990, pp. 198-209.

Gauvin, R. and Trochu, F., "Comparison between Numerical and Experimental Results for Mold Filling in Resin Transfer Molding," *Plastics, Rubber and Composites Processing and Application*, Vol. 19, No. 3, 1993, pp. 151-157.

Goldberg, D.E., *Genetic Algorithm in Search, Optimization, and Machine Learning*, Addison Wesley, Reading, MA, 1989.

Gonzalez-Romero, V. and Macosko, C., "Process Parameters Estimation for Structural Reaction Injection Molding and Resin Transfer Molding," *Polymer Engineering and Science*, Vol. 30, Mid-Feb 1990, pp. 142-146.

Han, K., Trevino, L., Lee, J. and Liou, M., "Fiber Mat Deformation in Liquid Composite Molding. I: Experimental Analysis," *Polymer Composites*, Vol. 14, No. 2, April 1993, pp. 144-150.

Han, K., Lee, J. and Liou, M., "Fiber Mat Deformation in Liquid Composite Molding. II: Modeling," *Polymer Composites*, Vol. 14, No. 2, April 1993, pp. 151-160.

Hanover, V. and Uhr, L., "Generative Learning Structures and Processes for Generalized Connectionist Networks," *Technical Report #91-2, Department of Computer Science, Iowa State University*, Ames, IA.

Hayes, R.E., Dannelongue, H.H. and Tanguy, P.A., "Numerical Simulation of Mold Filling in Reaction Injection Molding," *Polymer Engineering and Science*, Vol. 31, No. 11, Mid-June, 1991, pp. 842-848.

Hayward, J. and Harris, B., "Effect of Process Variables on the Quality of RTM Mouldings," *SAMPE Journal*, Vol. 26, No. 3, May/June 1990, pp. 39-46.

Jang, B.Z., Boxwell, R., Liu, Y.M. and Tai, H.J., "Computer-Assisted Cure Cycle Design, Monitoring, Control and Post-Fabrication Damage Assessment in Thermoset Composites," in: 3rd International Conference on Computer Aided Design Composite Material Technology CADCOMP '92, published by Computational Mechanics Publishing, Shouthampton, England, 1992, pp. 49-62.

Jang, B.Z. and Zhu, G.H., Applied Polymer Science, Vol. 31, 1986 p. 2627.

Johnson, C.F., "Resin Transfer Molding," in: Engineered Materials Handbook: Composites, Vol. 1, ASM International, 1987.

Joseph, B. and Hanratty, F., "Predictive Control of Quality in a Batch Manufacturing Process Using Artificial Neural Network Models," *Industrial and Engineering Chemistry Research*, Vol. 32, 1993, pp. 1951-1961.

158

Kamal, M.R., Sourour, S. and Ryan, M. "Integrated Thermo-Rheological Analysis of the Cure of Thermosets," *SPE Technical Paper*, 18, 1973, pp. 187-191.

Karbhari, V.M., "The Role of Expert and Decision Support Systems in Composites Design and Manufacturing," 3rd International Conference on Computer Aided Design Composite Material Technology CADCOMP '92, published by Computational Mechanics Publishing, Shouthampton, England, 1992, pp. 359-370.

Kataja, M., Rybin, A. and Timonen, J., "Permeability of Highly Compressible Porous Medium," *Journal of Applied Physics*, Vol. 72, No. 4, August 15, 1992, pp. 1271-1274.

Kenny, J.M., "Integration of Processing Models with Control and Optimization of Polymer Composites Fabrication," in: 3rd International Conference on Computer Aided Design Composite Material Technology CADCOMP '92, published by Computational Mechanics Publishing, Shouthampton, England, 1992, pp. 529-544.

Kranbuehl, D., Eichinger, D., Hamilton, T., and Clark, R., "In-situ Monitoring of the Resin Transfer Molding Impregnation and Cure Process," *Polymer Engineering and Science*, Vol. 31, Mid-Jan 1991, pp. 56-60.

Kranbuehl, D.E., Kingsley, P., Hart, S., Hasko, G., Dexter, B. and Loos, A.C., "In Situ Sensor Monitoring and Intelligent Control of the Resin Transfer Molding Process," *Polymer Composites*, Vol. 15, No. 4, August 1994, pp. 299-305.

Lam, R.C. and Kardos, J.L., "The Permeability and Compressibility of Aligned and Cross-Plied Carbon Fiber Beds during Processing of Composites," *Polymer Engineering and Science*, Vol. 31, No. 14, July, 1991, pp. 1064-1069.

Lan, X.K. and Khodadadi, J.M., "Fluid Flow and Heat Transfer Through a Porous Medium Channel with Permeable Walls," *International Journal of Heat Mass Transfer*, Vol. 36, No. 8, 1993, pp. 2242-2245.

Lin, S.-S., "Integrated Mechanical Tolerancing for Design and Manufacturing," Ph.D. Dissertation, Florida State University, August 1994.

159

Lundstrom, T.S. and Gebart, B.R., "Influence from Process Parameters on Void Formation in Resin Transfer Molding," *Polymer Composites*, Vol. 15, No. 1, February 1994, pp. 25-33.

Manzione, L.T., Osinski, J.S., Poelzing, G.W., Crouthamel, D.L. and Thierfelder, W.G., "A Semi-Empirical Algorithm for Flow Balancing in Multi-Cavity Transfer Molding," *Polymer Engineering and Science*, Vol. 29, No. 11, Mid-June, 1989, pp. 749-761.

Mezard, M and Nadal, J.-P., "Learning in Feedforward Neural Networks: The Tiling Algorithm," *J. Phys. A: Math.Gen.*, 22, 1989, pp. 2191-2203.
Montgomery, D.C., *Design and Analysis of Experiments*, John Wiley & Sons, Inc., 1984.

Montgomery, D.C. and Runger, G.C., *Applied Statistics and Probability for Engineers*, John Wiley & Sons, Inc., 1994.

Osakada, K., Yang, G.-B., Nakamura, T., Mori, K., "Expert System for Cold-Forging Process Based on FEM Simulation," *Annals of the CIRP*, Vol. 37, No. 1, 1990, pp. 249-252.

Osswald, T. and Tucker, C., "A Boundary Element Simulation of Compression Mold Filling," *Polymer Engineering and Science*, Vol. 28, No. 7, Mid-April, 1988, pp. 413-420.

Owen, M.J., Rice, E.V., Rudd, C.D. and Middleton, V., "Resin Transfer Moulding for Automobile Manufacture: Reality and Simulation," 3rd International Conference on Computer Aided Design Composite Material Technology CADCOMP '92, published by Computational Mechanics Publishing, Shouthampton, England, 1992, pp. 120-142.

Parnas, R.S. and Phelan, F.R., Jr., "The Effect of Heterogeneous Porous Media on Mold Filling in Resin Transfer Molding," *SAMPE Quarterly*, January 1991, pp. 53-60.

Parnas, R.S. and Salem, A.J., "A Comparison of the Unidirectional and Radial In-Plane Flow of Fluids Through Woven Composite Reinforcements," *Polymer Composites*, Vol. 14, No. 5, October 1993, pp. 383-394.

160

Roychowdhury, S., Gillespie, J.W., Jr. and Advani, S.G., "Void Formation and Growth in Thermoplastic Processing," in: 3rd International Conference on Computer Aided Design Composite Material Technology CADCOMP '92, published by Computational Mechanics Publishing, Shouthampton, England, 1992, pp. 89-97.

Rudd, C., Owen, M., and Middleton, V., "Effects of Process Variables on Cycle Time during Resin Transfer Moulding for High Volume Manufacture," *Materials Science and Technology*, Vol. 6, July 1990, pp. 656-65.

Rudd, C.D., Rice, E.V., Bulmer, L.J., and Long, A.C. "Process Modelling and Design for Resin Transfer Molding," *Plastics, Rubber and Composites Processing and Applications*, Vol. 20, No. 2, 1993, pp. 67-76.

Rummelhart, D.E., Hinton, G.E. and Williams, R.J., "Learning Internal Representations by Error Propagation," in: Rummelhart, D.E. and McClelland, J.L., *Parallel Distributed Processing: Explorations in the Microstructure of Cognition*, MIT Press.

Skartsis, L., Kardos, J.L. and Khomami, B., "Resin Flow through Fiber Beds during Composite Manufacturing Processes. Part I: Review of Newtonian Flow through Fiber Beds," *Polymer Engineering and Science*, Vol. 32, No. 4, February, 1992, pp. 221-229.

Smith, G.D. and Poursartip, A., "A Comparison of Two Resin Flow Models for Laminate Processing," *Journal of Composite Materials*, Vol. 27, No. 17, 1993, pp. 1695-1711.

Stark, E.B. and Breitigam, W.V., "Resin Transfer Molding Materials," in: Engineered Materials Handbook: Composites, Vol. 1, ASM International, 1987, pp.168-171.

Swain, J.J., "Nonlinear Regression," in: Wadsworth, H.M., *Handbook of Statistical Methods for Engineers and Scientists*, McGraw-Hill, Inc., 1990, pp. 17.1-17.27.

Trochu, R., Gavin, R. and Gao, D.-M., "Numerical Analysis of the Resin Transfer Molding Process by the Finite Element Method," *Advances in Polymer Technology*, Vol. 12, No. 4, 1993, pp. 329-342.

161

Trochu, F., Gauvin, R. and Zhang, Z., "Simulation of Mold Filling in Resin Transfer Molding by Non-Conforming Finite Elements," 3rd International Conference on Computer Aided Design Composite Material Technology CADCOMP '92, published by Computational Mechanics Publishing, Shouthampton, England, 1992, pp. 109-117.

Tucker, C.L., III and Dessenberger, R.B., "Governing Equations for Flow and Heat Transfer in Stationary Fiber Beds," in: *Flow and Rheology in Polymer Composites Manufacturing*, Elsevier Science, 1994, pp. 257-321.

Ulrych, T.J. and Ooe, M., "Autoregressive and Mixed ARMA Models and Spectra," in: Haykin, S., ed., *Nonlinear Methods of Spectral Analysis*, 2nd ed., Springer-Verlag, New York, 1983.

Um, M.-K., and Lee, W., "A Study on the Mold Filling Process in Resin Transfer Molding," *Polymer Engineering and Science*, Vol. 31, No. 11, Mid-June, 1991, pp. 765-771.

Wadworth, H.M., *Handbook of Statistical Methods for Engineers and Scientists*, McGraw-Hill, Inc., 1990.

Warner, J. and O'Connor, J., "Molding Process is Improved by Using the Taguchi Method," *Modern Plastics*, Vol. 66, July 1989, pp. 65-68.

Weisberg, S., *Applied Linear Regression*, John Wiley & Sons, Inc., 1985.

Wheeler, A.B., Jones, R.S. and Phillips, T.N., "Numerical Simulation of Fibre Reorientation in a Squeezing Flow and other Flow Geometries Using an Explicit Projection Method," 3rd International Conference on Computer Aided Design Composite Material Technology CADCOMP '92, published by Computational Mechanics Publishing, Shouthampton, England, 1992, pp. 177-188.

Wymer, S.A. and Engel, R.S., "A Numerical Study of Nonisothermal Resin Flow in RTM with Heated Uniaxial Fibers," *Journal of Composite Materials*, Vol. 28, No. 1, 1994, pp. 53-65.

BIOGRAPHICAL SKETCH

The author was born on June 10, 1968 in Cedar Falls, Iowa. She has two sisters and one brother. Her educational experience began at North Iowa Area Community College, near her home town. An A.A. degree was awarded in May 1988. Completion of the B.S. degree was achieved at the University of Iowa in August 1991, followed by an M.S. degree in May 1992 at the same university. She transferred to Florida State University in the summer of 1993 and remained there until completion of the doctoral degree in August 1995. In her spare time, the author enjoys reading novels, especially mysteries. She likes to keep physically fit by running, biking or swimming. Some day, she would like to have her own workshop and take up wood carving as a hobby.